2017

Creating a Scaling Relationship between Peak Discharge and Drainage Area To Identify Tile Drainage Inputs into an Agricultural Stream

Ryan Plath
Illinois State University, ryanplath11@augustana.edu

CREATING A SCALING RELATIONSHIP BETWEEN PEAK DISCHARGE AND DRAINAGE AREA TO IDENTIFY TILE DRAINAGE INPUTS INTO AN AGRICULTURAL STREAM

Ryan Plath

102 Pages

Tile drains have been shown to contribute to high levels of nitrate in agricultural streams. Locations of tile drains on a watershed scale, however, are often unknown due to tile drains being located on many separate parcels of private property. This study evaluates the ability of a methodology, using scaling relationships between discharge and drainage area, for locating areas of large tile drainage contribution to Money Creek, in McLean County, Illinois. Additionally, this study examines the difference in scaling relationships and physical stream hydrology between tileflow and no-tileflow conditions. Eight stream sites were created in the watershed, that recorded stage every 15 minutes. The drainage area of each stream site was calculated in ArcGIS. Hydrographs were created from rating curves that were developed for each site, and used to create scaling relationships between peak discharge and drainage area for 21 storms throughout the study period.

Overall, this method was not effective for detecting tile drain input into Money Creek, because there were no major differences in the outliers of the scaling relationships between the tileflow and no-tileflow periods. The scaling exponent means between the tileflow and no-tileflow period were statistically different. This is likely due to, factors that other studies have shown to cause regional differences in scaling exponents (evapotranspiration, soil moisture

storage, and sunshine) are causing seasonal differences in the scaling exponent within the Money Creek watershed. Additionally, this study observed double peaks in storm hydrographs, which were interpreted as being caused from the difference in runoff generation timing between overland flow and tile drainage.

KEYWORDS: Agricultural Hydrology, Scaling Relationship, Tile Drains, Scaling Exponent, Double Peaks

CREATING A SCALING RELATIONSHIP BETWEEN PEAK DISCHARGE AND DRAINAGE AREA TO IDENTIFY TILE DRAINAGE INPUTS INTO AN AGRICULTURAL STREAM

RYAN PLATH

A Thesis Submitted in Partial
Fulfillment of the Requirements
for the Degree of

MASTER OF SCIENCE

Department of Geography-Geology

ILLINOIS STATE UNIVERSITY

2017

CREATING A SCALING RELATIONSHIP BETWEEN PEAK DISCHARGE AND DRAINAGE AREA TO IDENTIFY TILE DRAINAGE INPUTS INTO AN AGRICULTURAL STREAM

RYAN PLATH

COMMITTEE MEMBERS:

Catherine O’Reilly, Chair

Eric Peterson

Bill Perry

Rex Rowley

ACKNOWLEDGMENTS

I would like to thank my committee members, Catherine O'Reilly, Eric Peterson, RJ Rowley, and Bill Perry for their guidance and support throughout my thesis project. I thank Rick Twait and the City of Bloomington for providing the inspiration and the stream site equipment needed for this thesis. Additionally, I appreciate Chad Carey and help from other Bloomington water department staff with creating and installing the stream sites for this thesis. I thank Jackie Kraft and Ross Fogle from the McLean County Soil and Water Conservation District for their help with identifying and contacting landowners in the watershed. I thank the Geological Society of America for its graduate research grant and Illinois State University's Graduate School for the 2016 and 2017 graduate student grants. Without this funding my thesis would not have been possible. I would like to thank Johnathan Thayn and Wondwosen Seyoum for their help with R. Finally, I would like to thank Jeremy Neundorff, Eric Deck, Romeo Akara, Audrey Happel, Carolyn Plath, Luke Lampo, and Ben Bruening for help with fieldwork and other aspects of this thesis.

R. P.

CONTENTS

TABLES

FIGURES

CHAPTER I: INTRODUCTION

Framing the Problem

The Midwestern United States is a region of intense agricultural production, and nonpoint source pollution of waterbodies is a continual problem. Non-point source pollution comes from many diffuse sources, while point source pollution comes from a known discrete entity. The relative lack of nonpoint source reduction, as compared to point source reduction, has put much focus on water quality improvement in agricultural areas (Brown and Froemke, 2012). The application of nitrogen fertilizer has greatly increased yields; an estimated 40-60% of United States crop yield is attributed to fertilizer application (Stewart et al, 2005). Unfortunately, this fertilizer is the major supplier of nonpoint source pollution to water bodies in these same agricultural areas (David et al, 1997).

Nitrate

In particular, nitrogen, in the form of nitrate (NO3-), is a major environmental concern (Ikenberry et al., 2014; Kladivko et al., 2004). High nitrate concentrations in an agricultural stream degrades overall stream quality (Randall et al., 2008). Agricultural streams often flow into reservoirs or larger streams that supply drinking water to local communities. These communities struggle to provide water to their citizens that measures below the EPA nitrate standard of 10 mg/L nitrate nitrogen or NO3- N (Hatfield and Follett, 2008; Ikenberry et al., 2014). Excess levels of nitrate can lead to methemoglobinemia (blue baby syndrome), which leads to newborns not having enough oxygen circulating through their blood streams (Powlson et al., 2008). High nitrate levels in Midwestern streams also drain through the Mississippi River system and contribute to the hypoxic zone in the Gulf of Mexico (Williams et al., 2015). The hypoxic zone is the result of increased nitrate concentrations, which cause algal blooms. The

decomposition of these massive algal blooms, in turn, leads to anoxic conditions in large sections of the Gulf of Mexico (David et al., 2010). The hypoxic zone is detrimental to the ecology and fishing industry in the Gulf of Mexico (Breitburg, 2002). Indeed, Ocean hypoxic zones are not limited to the Gulf of Mexico, and exist in many parts of the world where major river systems enter an ocean (Tiemeyer et al., 2010). In short, high concentrations of nitrate in agricultural streams have negative effects on local, regional and international scales.

Tile Drains

Although tile drains have improved the drainage of naturally poorly drained soils and allow for the exemplary crop growth, they exacerbate the problem of poor water quality in agricultural streams (Skaggs et al. 1994; Ikenberry et al., 2014). Nitrate dissolves into water on fields, infiltrates into tile drains and rapidly shuttles to streams. The swift removal of nitrate from fields allow biogeochemical processes that aid in denitrification to be largely bypassed. Biogeochemical processes are bypassed due to short water residence times in artificially drained soils and the inert biochemical nature of enclosed drainage pipes (Billy et al. 2011). Many best management practices (BMPs), such as riparian buffer zones, have been implemented in agricultural regions to reduce nitrate pollution in waterways. Unfortunately, tile drains often override these BMPs. In the Mackinaw River watershed in Illinois, for example, riparian buffer zones and strip-tillage were bypassed due to tile drainage (Lemke et al., 2011). Conservation practices that intercept and increase residence times of water need to be implemented to reduce nitrate loads (Lemke et al., 2011).

Locating Tile Drains

The first step in implementing conservation practices that intercept and increase residence times of tile drainage water is locating tile drains. Unfortunately, little is known of

their location. In Illinois, tile drains are located on private property and cannot be publically accessed or accounted for. Indeed, many farmers do not know specifically where tile drains are located on their property because the drains were installed decades ago and their location was not recorded during installation. Currently, aerial photography is used for broad surveys, but this method is often unsuccessful because high-resolution images during proper tile viewing conditions are commonly unavailable (Sugg, 2007). The objective of this study is to locate areas in a stream that might have large tile drainage contributions and that would be potentially good areas to implement effective conservation practices. The capability of a new methodology for locating areas of large tile drainage contributions, using scaling relationships, will be evaluated. Additionally, this study aims to observe the effects of tile drains on physical stream hydrology.

Scaling Relationships

A scaling relationship is the dependence of a catchment hydrologic property on catchment area. Scaling relationships can be used to examine how catchment area effects physical properties of streams (Powlson et al., 2008). Discharge is fundamental variable used in hydrology because it tells us how much water flows through a stream. Specifically, peak is often used because large loads of nitrate often move through streams during these high flow events (Christianson and Harmel, 2015; Billy et al., 2008). Creating a rating curve is a common procedure used to identify peak discharge (Ogden and Dawdy, 2003). Once peak discharges throughout a stream are calculated, they can be compared to each respective drainage area to create a scaling relationship.

When peak discharge vs. drainage area scaling relationships are graphed, the regressed exponent known as the scaling exponent (θ) can be calculated (Fig. 1). Simple, or linear, scaling relationships are represented by the equation: $Qp=\alpha A\theta$ where Qp is the peak discharge, A is the

drainage area, θ is the scaling exponent (slope of the best fit line), and α is the y-intercept of the best fit line (Furey and Gupta, 2005; Lee et al., 2008). θ and α can be thought of as measures that exhibit the extent that a basin prevents runoff from entering its stream (Goodrich et al, 1997). Scaling exponent values typically lie between 0.5 and 1, with a value of 1 representing surface area increasing evenly with discharge throughout the stream (Alexander, 1972). Most streams have a scaling exponent near 0.8 (Medhi and Tripathi, 2015).

Galster (2007) analyzed five major rivers throughout the United States and found that the scaling exponent can vary for different rivers systems. The scaling exponent is below 1 when a river has proportionally less water being added in the downstream section than the upstream area. Greater slope and elevation in the headwaters of a watershed generally result in more runoff being delivered to a river than in the downstream section of the river, causing the scaling exponent to typically be less than one (Galster, 2007).

Rivers in areas subject to glacial drift have been observed to have lower scaling exponents. For example, the Wabash river, which drains Indiana and eastern Illinois, has a scaling exponent of only 0.65 (Galster, 2007). While the mechanism for this is not fully understood, it is speculated that poorly integrated channel networks are responsible (Gupta and Waymire, 1998). Goodwin Creek in Northern Mississippi was found to obey a simple, or linear, scaling relationship because there was relatively uniform precipitation across the small 21.2 km2 basin (Ogden and Dawdy, 2003). On the contrary, Walnut Gulch, in southeastern Arizona (1480 km2), was found to become less linear with increasing area (Goodrich et al., 1997). This is consistent with the literature, which shows that linearity and the scaling exponent decrease with increasing drainage area and aridity (Alexander, 1972). No research has focused on an examination of small tile-drained watersheds in the Midwest. As highlighted by the previously

mentioned studies, there is abundant research pertaining to the controls on variance in the scaling exponent as a whole, while there is limited research on why particular gauging stations may plot above or below the scaling exponent.

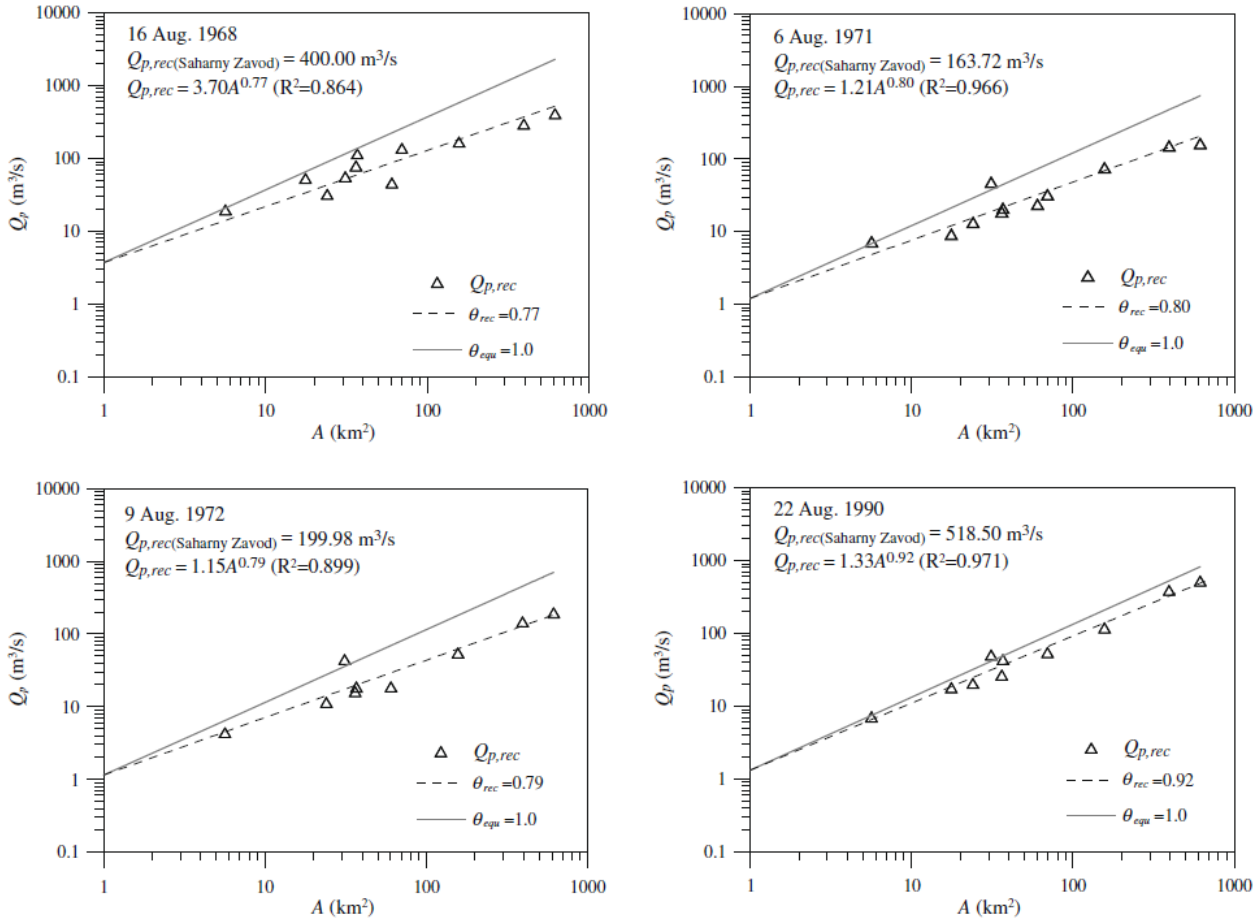

Figure 1. Four different rain events in the Komarovka River represented by peak discharge vs. drainage area scaling relationships. Θ_{rec} represents the scaling exponent (θ). Taken from Lee et al., 2008.

Although individual gauging points in a stream can vary with regard to where they plot within the scaling relationship, the scaling exponent remains invariant with changes in drainage areas (Lee et al., 2008). Lee et. al. (2008) used a kinematic wave-geomorphologic instantaneous unit hydrograph (KW-GIUH) modeling to create a continuous set of discharge data throughout

the Komarovka River, in southern Russia. They found that sudden fluxes of water, such as tributaries, will cause a transition break that deviates from the scaling exponent (Lee et al 2008). In agricultural watersheds, many first and second orders streams have been replaced by tile drainage, which often cuts across natural drainage divisions (Blann et al., 2009). This study will examine if points plot above the scaling exponent in agricultural streams, and if these points represent areas of large tile drain influx into the main steam.

Double Peaks

A number of studies have investigated the phenomenon of double peaks storms events within hydrographs. The geography of the streams that display double peaks and the cause of the double peaks vary. The Slapton Woods Catchment in Devon, UK displayed a double peak due to differences in timing between overland flow and subsurface flow (Birkinshaw, 2008). Subsurface flow only produced double peaks during the wet season, when the basin was "wetted up". The study interpreted subsurface flow to be moving horizontally between the soil and bedrock interface.

An additional study developed a hydrologic model that could simulate double peaks in streams (Yang et al., 2015). The model focused on two watersheds. The first watershed was the Onondaga Creek watershed in Syracuse, NY, a 285 km2 watershed that displayed double peaks due to an urban downstream area that produced an initial hydrograph peak from overland flow over impervious surfaces and a forested upper watershed that produced a slower secondary peak through subsurface flow. The second watershed was the Williams Creek watershed in Missouri. This watershed was a 19.7 km2 forested watershed, which only displayed double peaks during extreme rainfall events when the soil became over-saturated. This created a large component of overland flow and a large component of subsurface flow with corresponding double peaks.

Other studies have found subsurface flow through fractured bedrock (Onda et al., 2001), and conduit-driven flow through karst watersheds (Hirose et al., 1994; Lakey and Krothe, 1996) can produce storm event hydrographs with double peaks. Though the mechanism for double peaks vary by watershed, the common denominator is an initial fast peak through overland flow and a slower secondary peak through subsurface flow. No studies have specifically focused on double peaks in regions with a high prevalence of tile drainage, but the literature suggests that tile drainage, through the concept of subsurface flow, is a viable mechanism for double peaks in hydrographs.

Study Area

This study is located in the upper watershed of Money Creek, in central Illinois. The surface is covered in Wisconsin age glacial till (Patterson et al., 2003). The upstream section of the study area is the Batestown Till Member of the Wedron Formation, a gray silty till that oxidizes to olive brown. The downstream area of the study area is the Snider Till Member of the Wedron Formation, a gray silty clayey till with a coarse blocky structure. One small locality is a kame and is part of the Wasco Member of the Henry Formation, unevenly sorted sand and gravel with irregularly bedded lenses of silt and till. Land cover is dominated by corn and soybean agriculture. The study area focuses on the upper 55% of the watershed and encompasses a drainage area of 77.2 km2 (Fig. 2).

Money Creek is the tributary of Lake Bloomington, which serves as the water supply for the City of Bloomington, Illinois. Due to high loads of nitrate from Money Creek, Lake Bloomington periodically has nitrate concentrations above the EPA limit. During these times, the City of Bloomington dilutes Lake Bloomington's water with water piped in from nearby Lake Evergreen. This adds an extra cost and burden to water purification for the City. Due to

the extra costs associated with high nitrate levels, the city is interested in understanding where large fluxes of water or nitrate enter the watershed. The City of Bloomington has limited resources for implementing best management practices, which can reduce nitrate levels in Lake Bloomington. If large fluxes of water or nitrate entering Money Creek can be identified, then the city can more efficiently use their resources to target these important areas and reduce nitrate loads entering Lake Bloomington. This same methodology could be applied to other areas throughout the Midwest to locate target zones for best management practices in nutrient reduction.

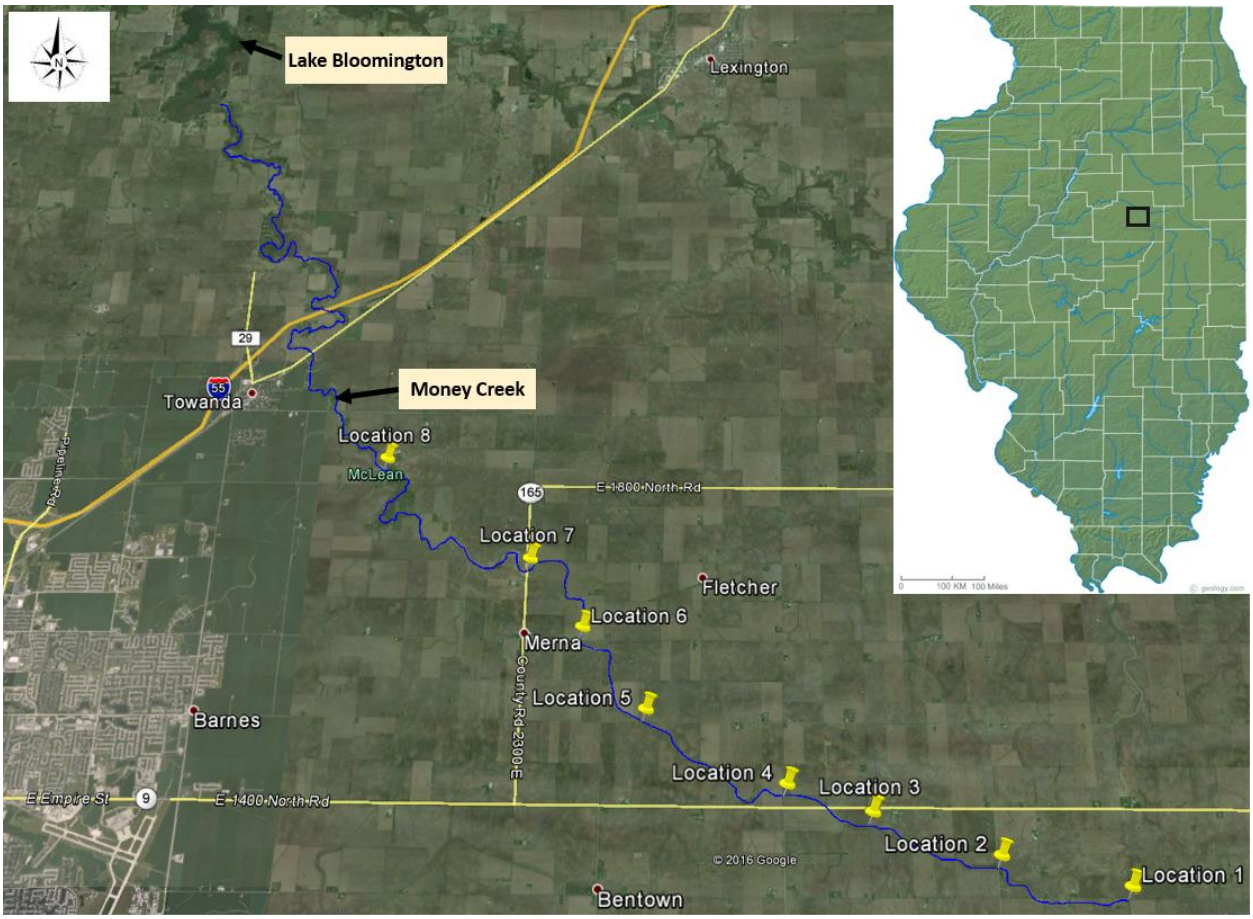

Figure 2. Study region with the eight sampling site locations.

Research Questions:

Primary Question: Is there a difference in scaling relationships between tileflow and no-tileflow conditions?

There will likely be differences in the scaling relationships between tileflow and no-tileflow conditions. The peak discharge for each sampling location will likely be less due to the increased evapotranspiration that occurs during no-tileflow conditions. Well-established field crops allow for greater transpiration, and greater temperatures allow for greater evaporation later in the season during no-tileflow conditions. Decreased precipitation during the later summer and fall then the late spring and early summer also leads to decreased peak discharge during no-tileflow conditions. There is also a possibility for the scaling exponent to change between tileflow and no-tileflow conditions. Outliers in the tileflow scaling relationship could disappear when large sections of tile drain input cease during no-tileflow conditions.

Secondary Question: Is there a difference in hydrologic characteristics between tileflow and no-tileflow conditions?

Hydrographs in agricultural streams could potentially exhibit dual or extended peaks due to differences in timing between when overland flow and tile drainage enters the creek. These characteristics could be present during tileflow conditions, but would be expected to disappear during no-tileflow conditions.

CHAPTER II: METHODOLOGY

Site Selection

I selected eight sites for this study. This number provides a balance between producing adequate data and spatial resolution for the study, while still being a manageable number of sites to monitor in one sampling trip. All of the sites selected were in the upper watershed of Money Creek, east of Bloomington, Illinois. This section of creek has lower discharge and therefore I am more likely to be able to pick up signals of water flux into the stream. This section also has few tributaries because of the abundance of tile drainage, which means the chance of a flux being introduced through a tributary is greatly reduced. For ease of access, all sites are located where a road crosses or runs along the creek. In short, I examined all potential sites in a site selection trip and choose the final eight sampling locations based on accessibility, location in the watershed, and how evenly the site was spaced between other sites in the watershed (Fig. 3). The drainage area increases from 6.1 km^2 to 77.1 km^2 between the first site and final site, which is over an order of magnitude (Table 1). This ensures that there is a least one log-cycle and therefore an appropriate degree of scaling.

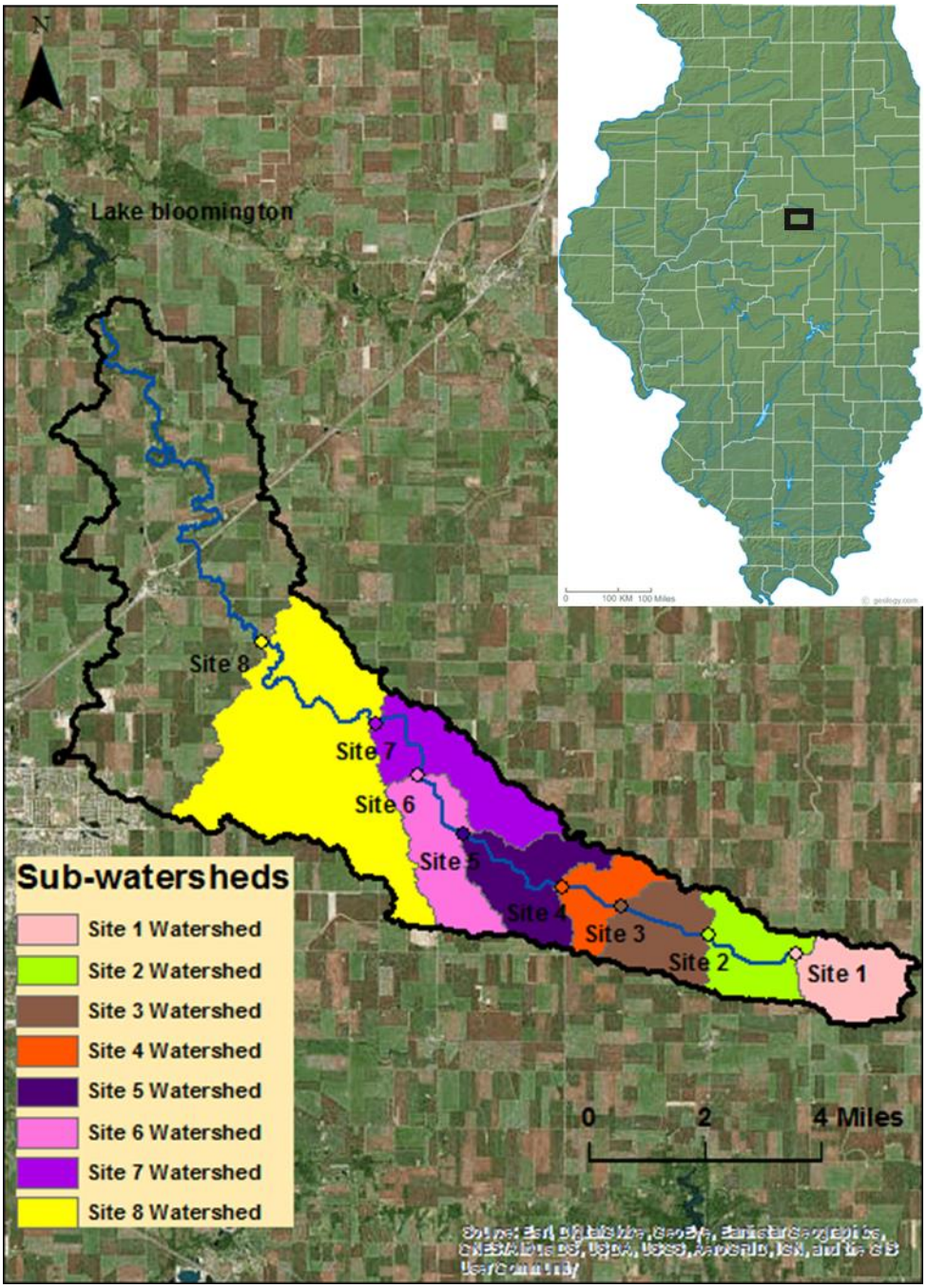

Figure 3. Study region with the eight sampling stream site locations and the Money Creek watershed outlined. Each site's watershed represents additional drainage that is not included the previous site's drainage area.

Table 1

Table Describing Site Locations

Site #	Drainage Area	Location	Township	Easting and Northing
Site 1	6.4 Km2	County Rd 1300 N and N 3000 East Rd Arrowsmith, IL	Dawson	356885, 4481438 m
Site 2	11.8 Km2	N 2850 East Rd Ellsworth, IL	Dawson	354471, 4482051 m
Site 3	18.9 Km2	N 2700 East Rd Ellsworth, IL	Dawson	352072, 4482899 m
Site 4	22.2 Km2	N 2600 East Rd Cooksville, IL	Blue Mound	350442, 4483458 m
Site 5	32.4 Km2	E 1500 North Rd Cooksville, IL	Blue Mound	347704, 4484951 m
Site 6	40.3 Km2	E 1600 North Rd Normal, IL	Towanda	346420, 4486620 m
Site 7	48.5 Km2	County Rd 2300 E Normal, IL	Towanda	345311, 4488065 m
Site 8	77.2 Km2	County Rd 1800 N Towanda, IL	Towanda	342219, 4490322 m

Note. Table showing the drainage area, location, township within McLean County, Illinois, and easting and northing of each site.

Site Descriptions

Site 1 is a drainage ditch that forms the beginning of Money Creek; Three large (0.75-1 meter diameter) tile drains enter this ditch which drains the uppermost 6.4 km^2 of the watershed (Fig. 4). Site 2 is in a channelized section of the stream. Despite this, the stream exhibits natural characteristics such as braided sections within the stream channel. Site 3 is similar to Site 2, except further downstream. Site 4 is the first area of the stream where the stream changes from multiple braided sections throughout the channel to a single channelized flow path. Site 5 is the first site where the stream becomes noticeably larger and wider than previous sections. Site 6 is

similar to Site 5 further downstream. Site 7 is a pooled section where the stream is deeper and has slower velocities than many other parts of the stream. Site 8 is the furthest downstream site and the only site that is not channelized, modified, or closely bordered by agricultural fields. This section has a natural meandering stream pattern and savanna and pasture surround it.

Once I selected sites, I completed work permits. Work permits were attained through different governmental entities based on who had jurisdiction for a particular road, and therefore the public right of way, where a study site was located. I received a work permit for Site 7 through IDOT, Sites 2 and 4 through the McLean County Highway department, Sites 1 and 3 through Tim Bane (Dawson Township Highway Road Commissioner), Site 5 through Joe Wissmiller (Blue Mound Township Highway Road Commissioner), and Sites 6 and 8 through Mike Fish (Towanda Township Highway Road Commissioner). The McLean County Soil and Water Conservation District helped identify landowners with property adjacent to the sampling locations and mailed a flyer that explained the project and included contact information. I signed a waiver for the property owner adjacent to Site 8.

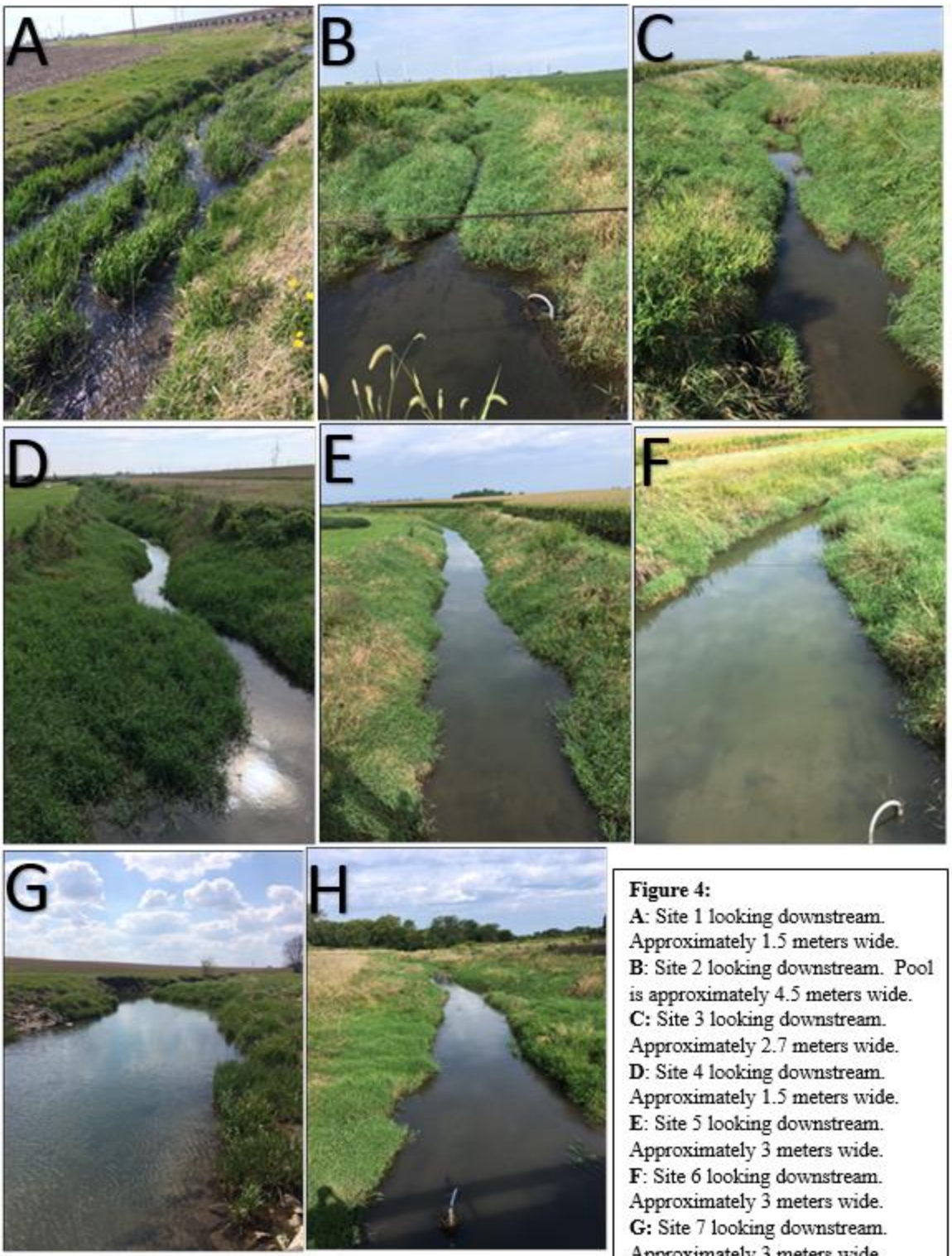

* All images are from August 26th, 2016, except for images **A** and **G** which are from April 17th, 2016.

Figure 4:
A: Site 1 looking downstream. Approximately 1.5 meters wide.
B: Site 2 looking downstream. Pool is approximately 4.5 meters wide.
C: Site 3 looking downstream. Approximately 2.7 meters wide.
D: Site 4 looking downstream. Approximately 1.5 meters wide.
E: Site 5 looking downstream. Approximately 3 meters wide.
F: Site 6 looking downstream. Approximately 3 meters wide.
G: Site 7 looking downstream. Approximately 3 meters wide.
H: Site 8 looking Downstream Approximately 15 feet wide.

I installed HOBO MX pressure transducers at the eight different sampling locations along Money Creek. At each site, the sensing end of the pressure transducer was secured in a PVC stilling well. The wiring was run through conduit to an onshore PVC unit that housed the logging end of the pressure transducer and protected the electronic components from the elements (Figs. 5 & 6).

Figure 5. The PVC Stilling well (in the stream) connected by conduit to the onshore PVC Unit. I secured both ends to metal posts.

Figure 6. The onshore PVC Unit that houses the logging end of the pressure transducer.

Data Collection

Automated Depth Sensors

The pressure transducers record stage and temperature measurements every 15 minutes (Fig. 7). Site 1 was installed and deployed on May 17th 2016, Sites 6-8 on May 18th 2016, while sites 2-5 on May 19th 2016. HOBO Rain gauges were installed at each station on September 23rd 2016. Staff gauges were installed at sites 3-8 on September 2nd , 2016, and at sites 1-2 on December 14th, 2016.

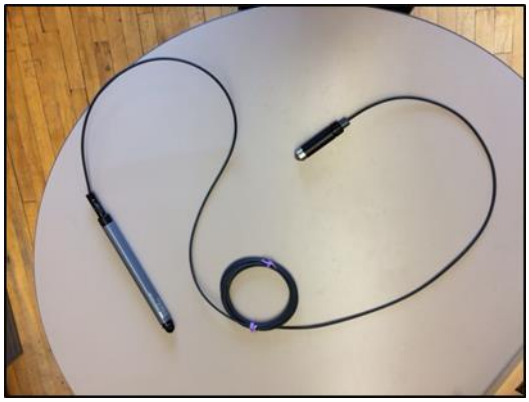

Figure 7. HOBO MX pressure transducer: Used to measure stream depth and temperature. The sensing end (right side) connected by wiring to the logging end (left side) of the pressure transducer.

Manual Discharge Measurements

I used a SonTek Flowtracker ADV to take discharge measurements approximately twice a week at my sampling locations from May 20th until August 26th, 2016, and approximately once a week from August 29th until November 4th (Fig. 8).

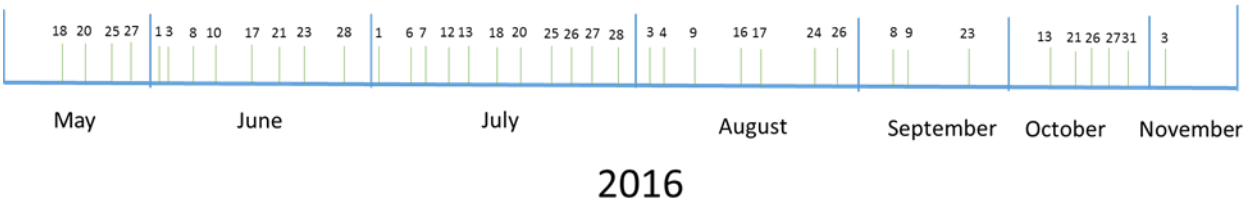

Figure 8. Timeline with sampling dates for discharge measurements. Timeline is not to scale.

Each stream site had a set number of points where discharge measurements were taken across the profile of the stream (Table 2). Sites that were further downstream had more discharge measurement points, because the stream channels themselves were wider and more

discharge measurement points were required to capture the range of velocities and depths through the stream cross-section (Fig. 4).

Table 2

Number of Discharge Measurement Points used at Each Site

Site 1	Site 2	Site 3	Site 4	Site 5	Site 6	Site 7	Site 8
5	5	5	5	8	8	10	10

Originally, Site 1 only had three discharge measurement points. This number was increased to five after I found that three discharge measurement points were not enough to provide an accurate discharge measurement; the data collected using the three discharge measurement points was not used in calculating the rating curves. Data from May 20th-June 17th at site 2 was not used in the rating curve because the section of stream that was used to take discharge measurements was overgrown with macrophytes, which caused inaccurate velocity measurements. After June 17th, a section of stream, approximately 15 meters downstream was used to take discharge measurements at site 2 because it contained fewer macrophytes.

During sampling, a measuring tape was stretched across the stream and the SonTek Flowtracker was used to take a depth and velocity measurement at each discharge measurement point across the stream. The velocity reading was a 30-second average taken at 6/10ths of the water column depth at each point. All measured values were recorded in a notebook. The Flowtracker electronically-calculated discharge was used in most cases, except in a few instances where Excel was used to manually calculate discharge based on the data from the notebook. The mid-section method was used to calculated discharge. Data was collect in an array of stream flow conditions, ranging from baseflow to stormflow, in order to produce an accurate rating

curve for each site. During excessively high flow events, when the stream was too deep to wade in, I used a bridgeboard and winch with a sigma portable velocity meter to collect discharge values. During high flow, discharge was taken at evenly spaced 1.8-meter intervals that correspond to steel posts along the side of each bridge guardrail.

Precipitation Data

I collected precipitation data from September 23, 2016 through January 21, 2017. I deployed Rainwise tipping-bucket rain gauges at each of the eight sites, but discarded the data from Site 3 because it only made measurements during installation and removal. I attached the rain gauges, approximately 1.2 meters above the ground to posts that house the logging end of the pressure transducer (Fig. 9). The rain gauge at site 5 was clogged with sediment on January 21, 2017, so measured precipitation values are likely artificially low in December and January. This study did not use publically available Bloomington airport precipitation data from before September 23, because that data does not provide the necessary spatial or temporal resolution needed for analysis of individual stream sites.

Figure 9. Rain gauge setup used at each site. I attached Rain gauge to the post that houses the logging end of the pressure transducer.

GIS Calculations

I used ArcGIS to calculate the drainage area of each stream site, which I later used in the scaling relationships. I used the hydrology tools in ArcGIS with a ten-meter digital elevation model (DEM) from the United States Geological Survey to calculate each site's drainage area. I projected a DEM of the study area to NAD_1983_stateplane_Illinois_East (Fig 10). Next, I used the fill tool to fill in erroneous basins within the DEM that could potentially cause errors when calculating watersheds. I computed a flow direction raster, which shows which way water would flow for each cell within the DEM. Afterwards, I used the flow accumulation tool to calculate how many cells (drainage area) drains into each unit cell.

I used the editor toolbar to digitize each of my stream sites as a point. With the flow accumulation raster and each stream site as inputs, I used the snap pour point tool to attach each stream station to a nearby cell that has the highest drainage area. This ensures that each station is

finding the drainage area of Money Creek at that location, rather than the drainage area of a nearby shoreline. I then input the flow direction raster and snap pour point raster into the watershed tool to find the subwatershed, of each stream site. Next, I converted the watershed to a Shapefile, and I used the calculate geometry option within the attribute table to calculate the drainage area of each stream site.

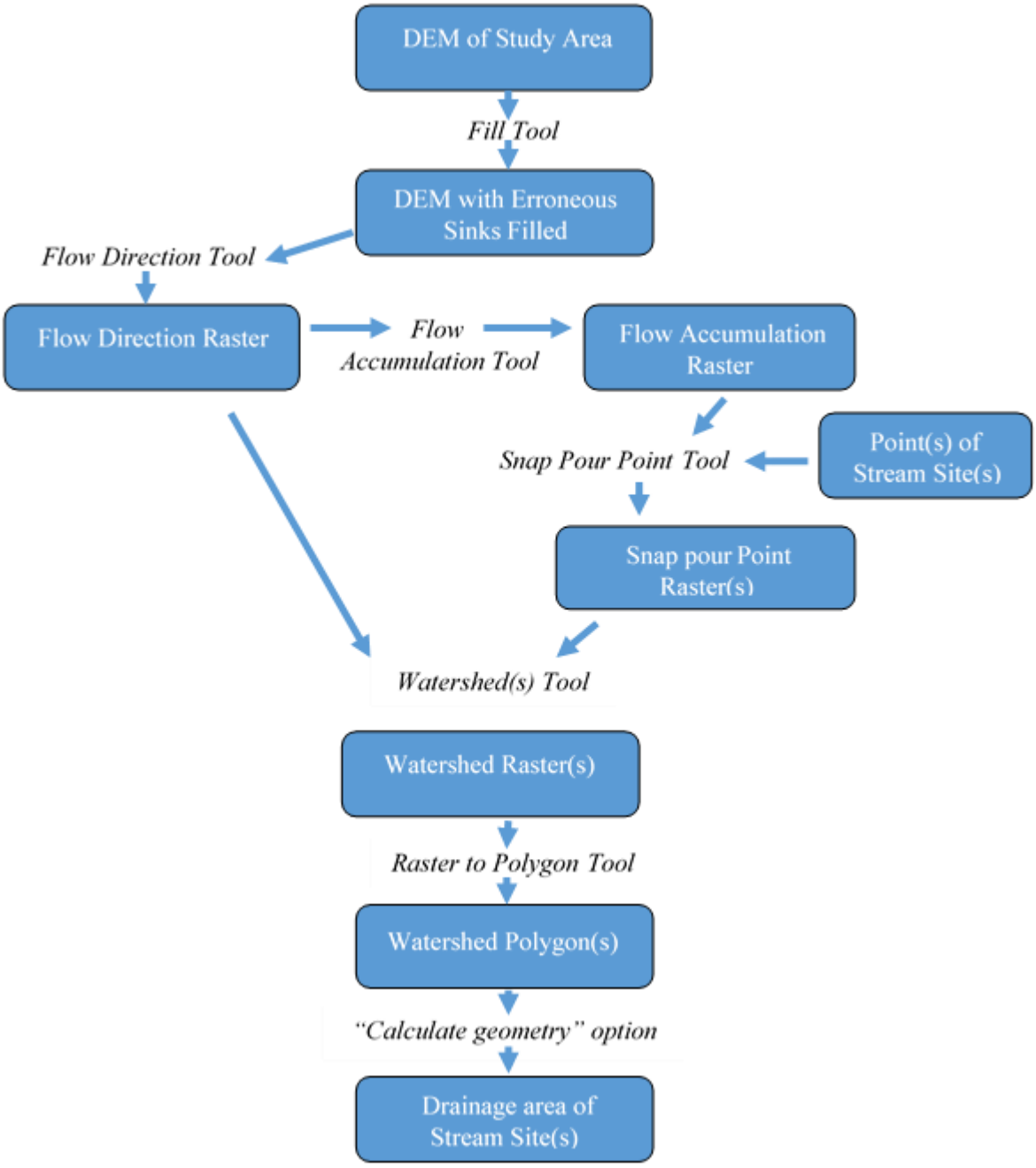

Figure 10. A flow chart that outlines the process taken in ArcGIS to calculate the drainage area of each stream site.

Data Analysis

Rating Curves

I plotted manual discharge measurements against their corresponding electronically collected stage value to produce a rating curve for each of the eight sites (Figs. 11-20). Sites 2 and 7 have multiple rating curves, one for before July 25th, 2016 and one for afterwards, due to a storm that changed the streambed cross-sections and invalidated the original rating curves for all measurements afterwards (Table 3). I log-transformed the data used in the linear regressions for Sites 1, 2 (July 25th - January 21st), 3, 5, 6, and 7 to be able to produce a linear model with an R^2 value. These model's slopes and y-intercepts were then transformed to produce the power functions seen in these site's rating curves. I did not manipulate the data for Sites 2 (May 19th - July 25), 4, and 8 because these data were naturally linear. I used these rating curves to calculate the discharge values used the hydrographs.

Table 3

Summary Table for Rating Curves

Site	Date Range	Measurements	Slope	Intercept	R^2	Transformation
1	May 17 - January 21	21	2.534	-0.053	0.946	logged
2	May 19 - July 24	10	0.459	-0.171	0.99	none
2	July 25 - January 21	20	2.257	-0.1	0.925	logged
3	May 19 - January 21	28	2.176	0.01	0.948	logged
4	May 19 - January 21	25	1.209	-0.488	0.961	none
5	May 19 - January 21	26	3.568	-0.055	0.961	logged
6	May 18 - January 21	24	2.32	0.203	0.982	logged
7	May 18 - July 24	17	1.564	0.129	0.97	logged
7	July 25 - January 21	10	1.469	0.373	0.947	logged
8	May 18 - January 21	25	2.734	-0.648	0.973	none

Note. The table displays the site, date range, number of measurements, slope, intercept, R^2 value, and data transformation type for each rating curve used.

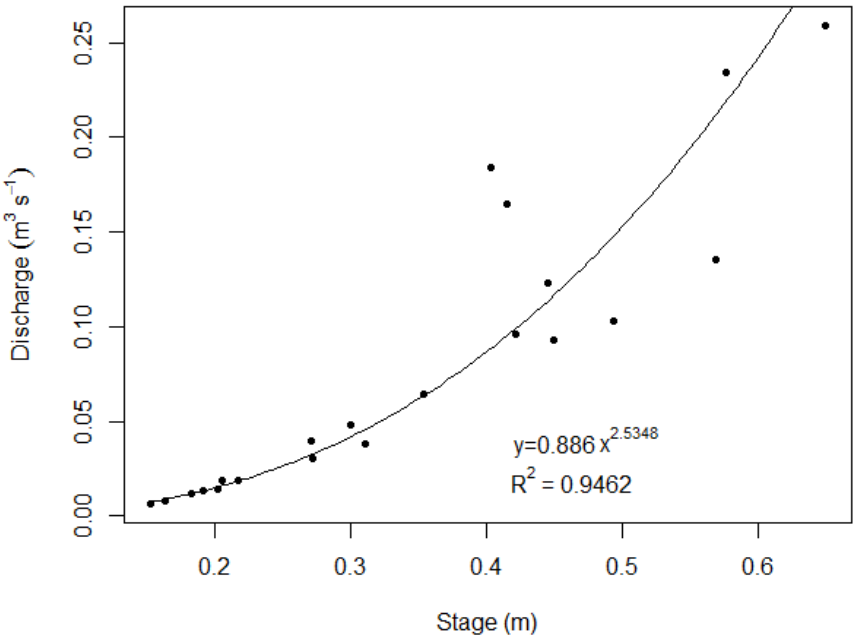

Figure 11. Rating Curve for Site 1.

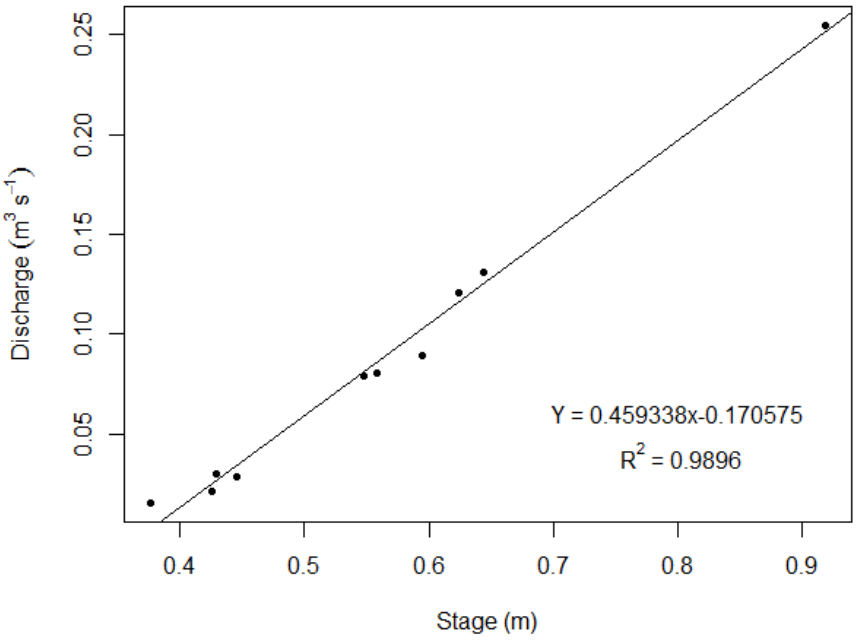

Figure 12. Rating Curve for Site 2. This rating curve applies from the beginning of the study until July 25.

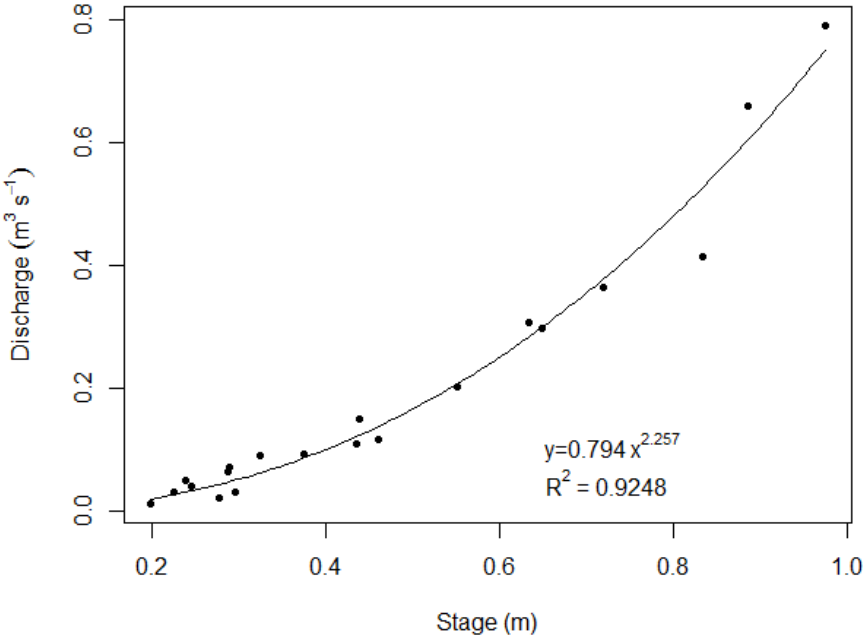

Figure 13. Rating Curve for Site 2. This rating curve applies from July 25 through the end of the study.

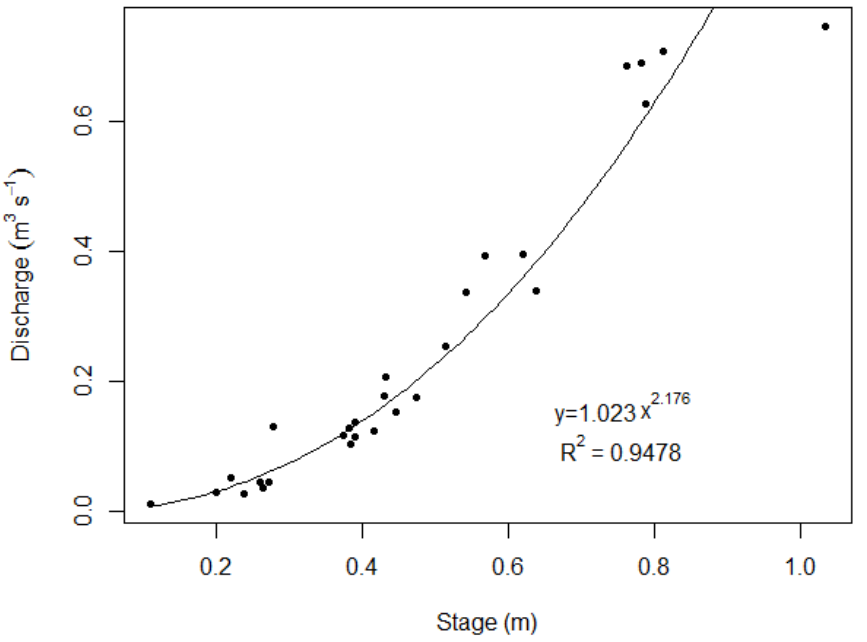

Figure 14. Rating Curve for Site 3.

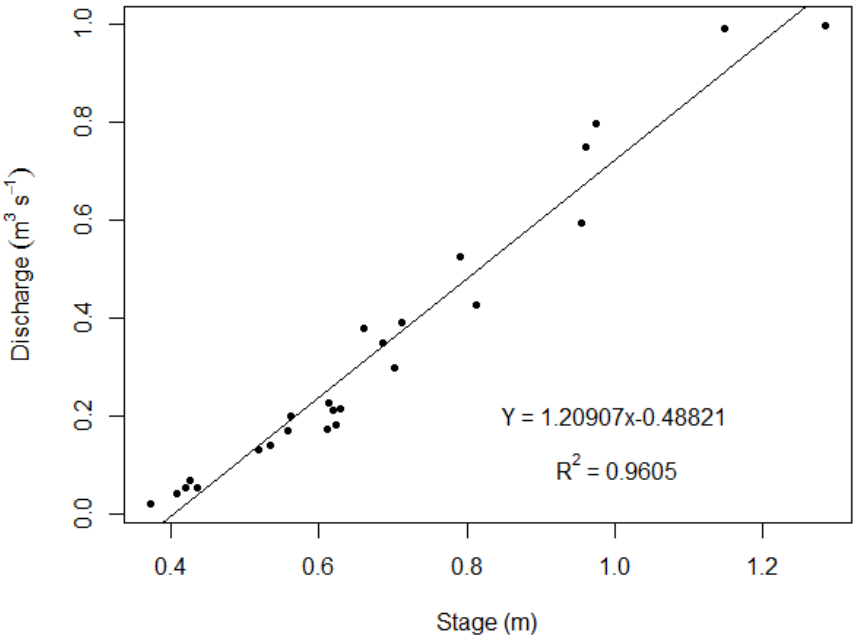

Figure 15. Rating Curve for Site 4.

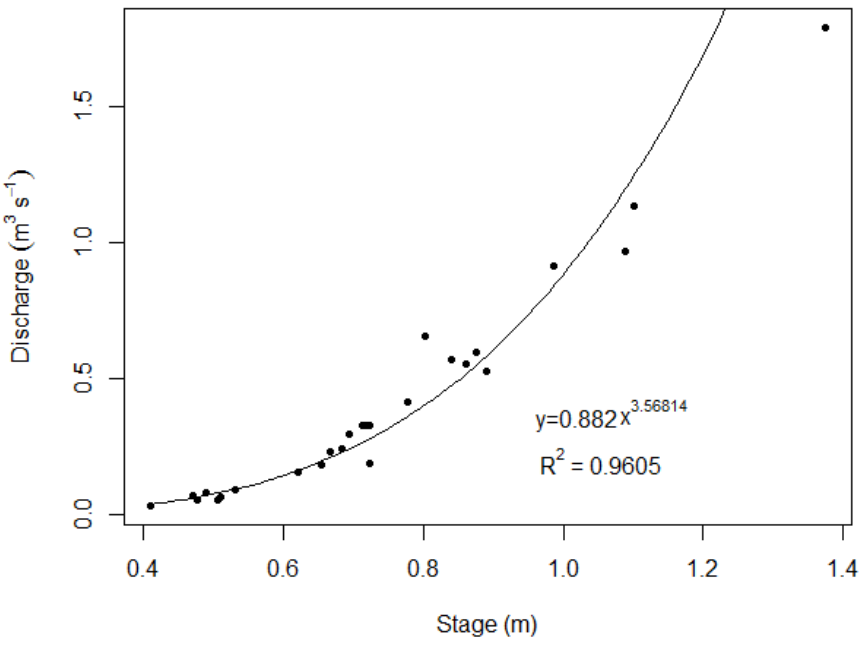

Figure 16. Rating Curve for Site 5.

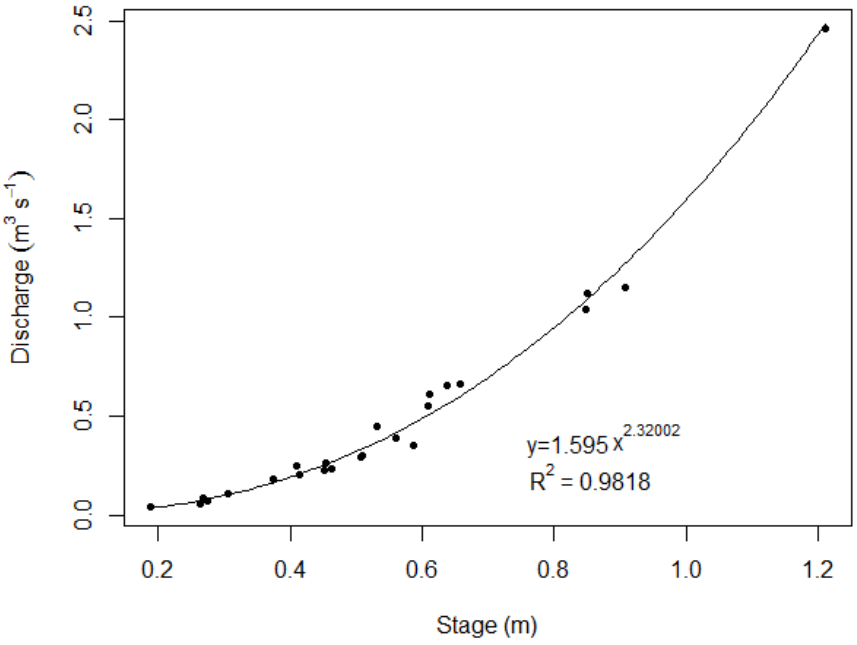

Figure 17. Rating Curve for Site 6.

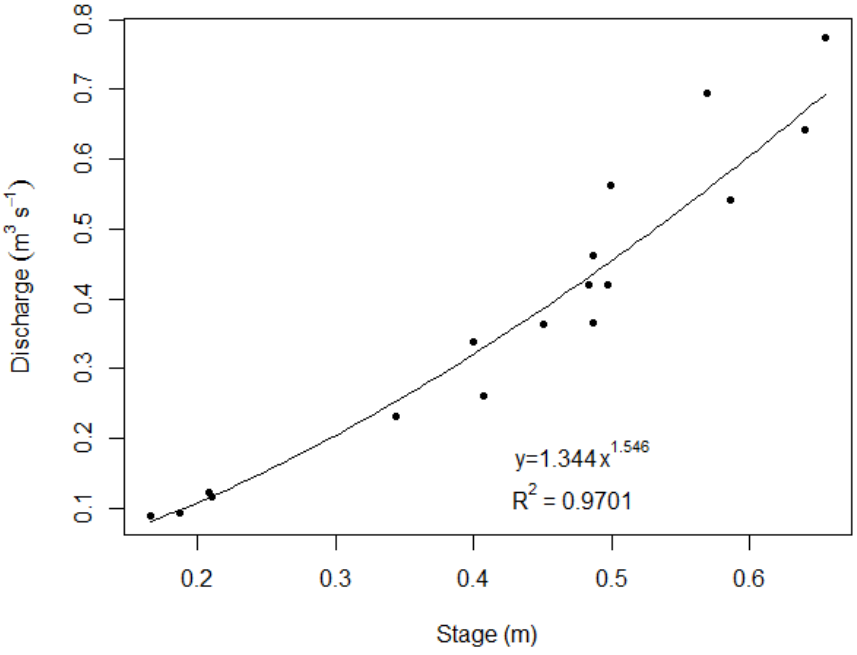

Figure 18. Rating Curve for Site 7.

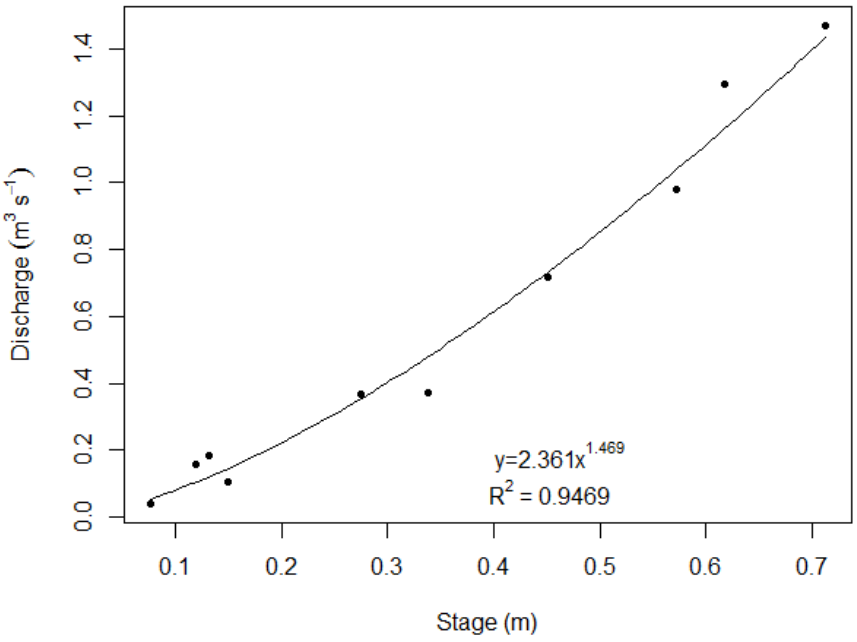

Figure 19. Rating Curve for Site 7. This rating curve applies from July 25 through the end of the study.

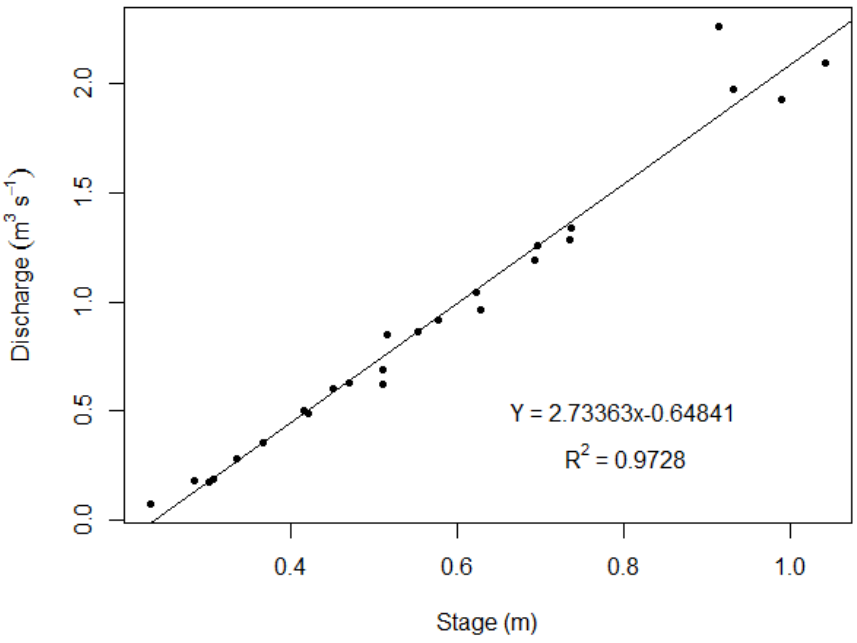

Figure 20. Rating Curve for Site 8.

Tileflow and No-tileflow Period Determination

I determined the no-tileflow period based on a combination of hydrograph and tile drain observation datasets from this study, as well as datasets from other researchers working in the same region. I used Ben Bruening's tile drain discharge datasets, and Luke Lampo's nitrate concentration dataset. The hydrograph datasets from this study showed a recession of baseflow during the end of June and beginning of July; baseflow remained low until after Storm 14 on September 14, where baseflow remained above levels seen in the previous few months. Ben's tile drain datasets, which were from the Money Creek watershed, showed a sudden drop in discharge during the beginning of July and appeared to remain low until September 15, when discharge increased again. Luke Lampo's data showed nitrate concentration data from the neighboring Six Mile Creek watershed. Initially, the concentration of nitrate was above 10 mg/l, until July 7 when the concentration dropped below 10 mg/l. The concentrations decreased, until September when they gradually began to increase again. There was a surprising amount of correspondence between these three separate datasets. By amalgamating information from all three, I determined a no-tileflow period of July 7 – September 15. I designated May 19th - July 7 the early summer tileflow period, and the period after September 15, the fall / winter tileflow period.

Mean Baseflow Scaling Relationship Calculations

I created three mean baseflow scaling relationships: early summer tileflow period (~May 18- July 7), summer no-tileflow period (July 7 – September 15), and fall / winter tileflow period (September 15 – January 21). For each respective period, I took the log of the mean discharge value of baseflow for each site over that period and plotted it against the log of that respective station's drainage area. I delineated between baseflow and stormflow by classifying the start of

the rising limb through the end of the storm period as stormflow; the remaining time was designated baseflow. To calculate the end of the stormflow period I used the equation, $T=D^{0.2}$, where T is time from peak discharge in days, and D is the drainage area in miles.

Double Peak Determination

I created storm event hydrographs that focused on each individual storm for every stream gauging station throughout the study to look for double or extended peaks in the hydrographs. Hydrographs with a bimodal pattern were considered a double peak, while hydrographs with a peak or falling limb that expectantly plateaus in its regression towards baseflow was considered an extend peak. Admittedly, observing extended peaks is a qualitative and somewhat subjective task, so I attempted to be uniform in applying my criteria for an extend peak across the entire span of the dataset. I plotted sites that had hydrographs with a double peak or an extended peak on a summary table to show patterns across the dataset.

CHAPTER III: RESULTS

Hydrographs

I used the measured stage data and rating curves to produce hydrographs for each of the eight sites in the watershed (Figs. 21-28). The hydrographs span the length of the stage measurements (May 17th – January 21st), except for Site 5, which only extends until November 23rd, when a storm caused the stream channel cross-section to change and invalidate the rating curve for all subsequent measurements.

Twenty-one storms occurred throughout the watershed, during the study period. There are other minor events, but they do not display a rising and falling limb across the entire watershed. For example, storm 2, between Storm 1 and 3, exists in the upper watershed, but does not extend throughout the entire watershed (Fig. 21). Storm 3 was the largest storm event of the study period for Sites 1,3,4,5, and 6. Storm 8 was the largest for Sites 2 and 7, while Storm 1 was the largest for Site 8. Storm 8 occurred during the no-tileflow period, while Storm 3 and 6 occurred during the tileflow period. While the magnitude of discharge of each storm event varies at each stream site, there is consistency in the fact that large discharge storm events often have high discharge across the entire watershed, and small discharge events often have low discharge across the entire watershed.

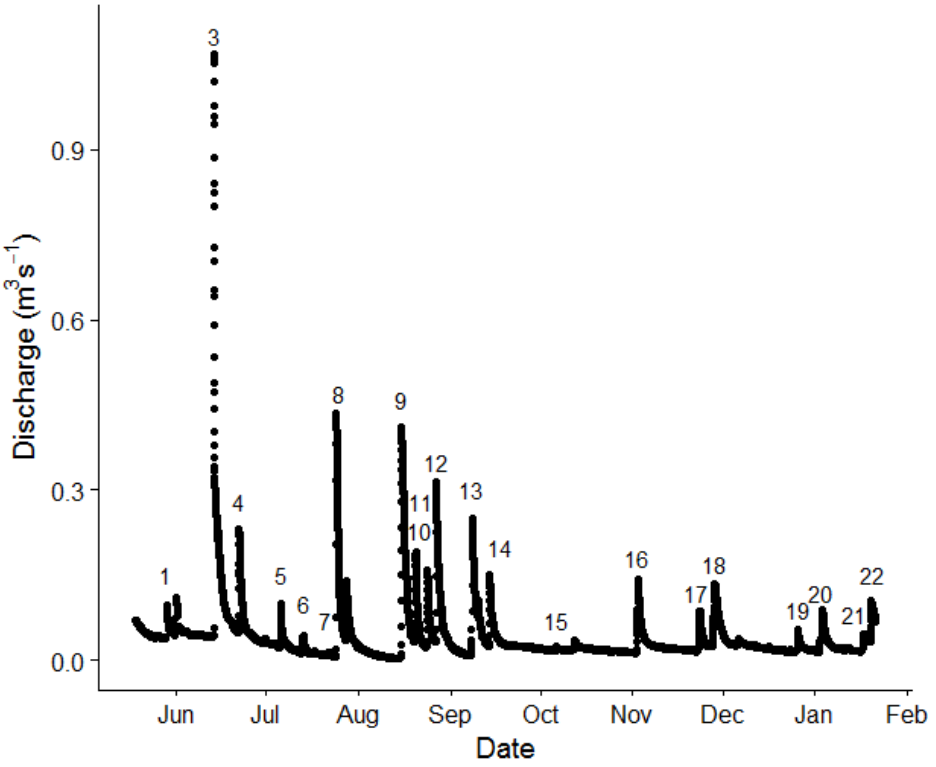

Figure 21. Hydrograph of Site 1. Numbers represent storm events.

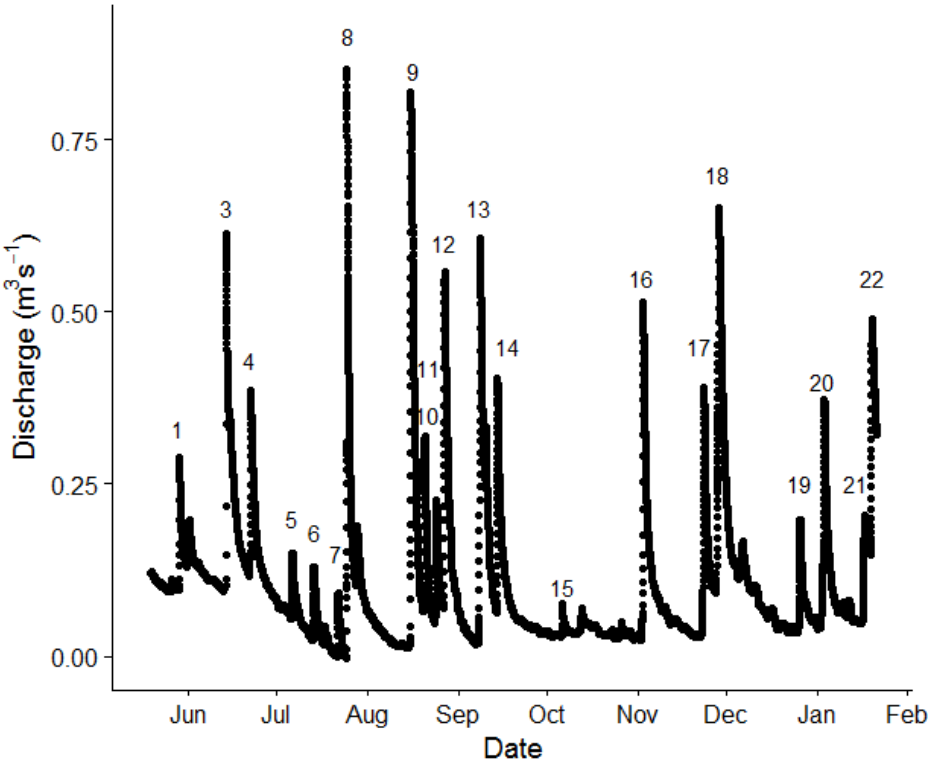

Figure 22. Hydrograph of Site 2. Numbers represent storm events.

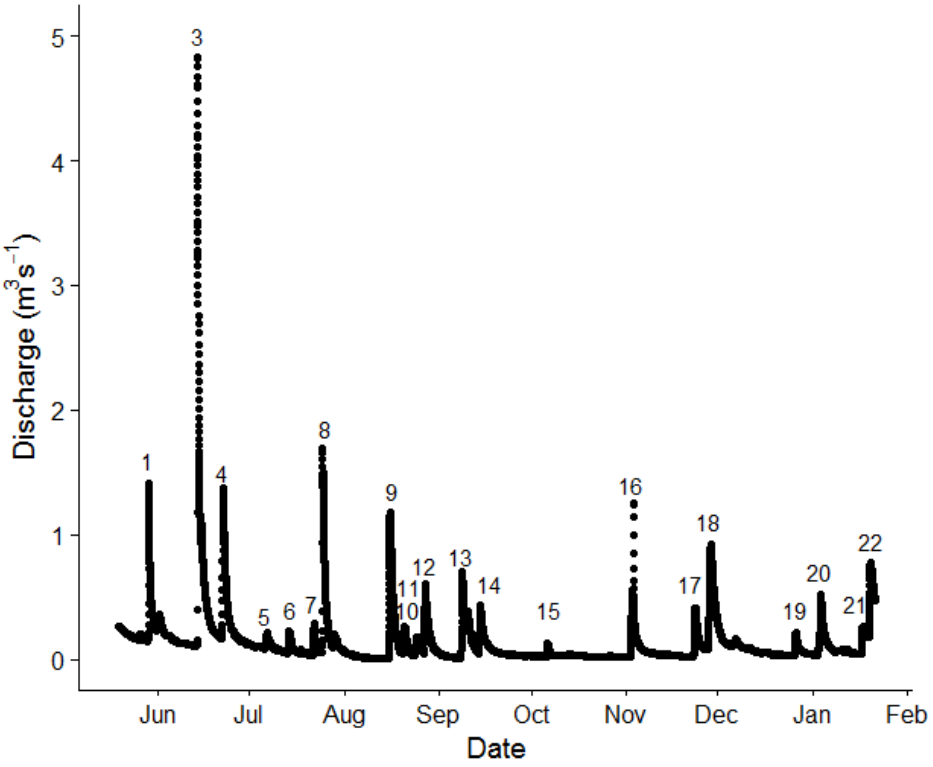

Figure 23. Hydrograph of Site 3. Numbers represent storm events.

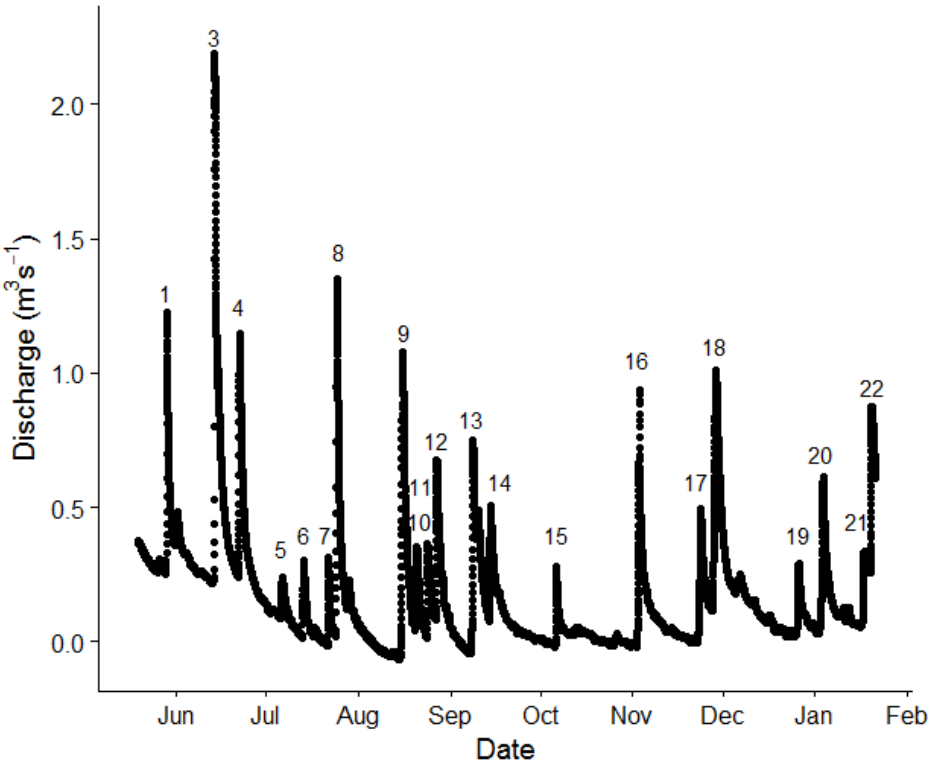

Figure 24. Hydrograph of Site 4. Numbers represent storm events.

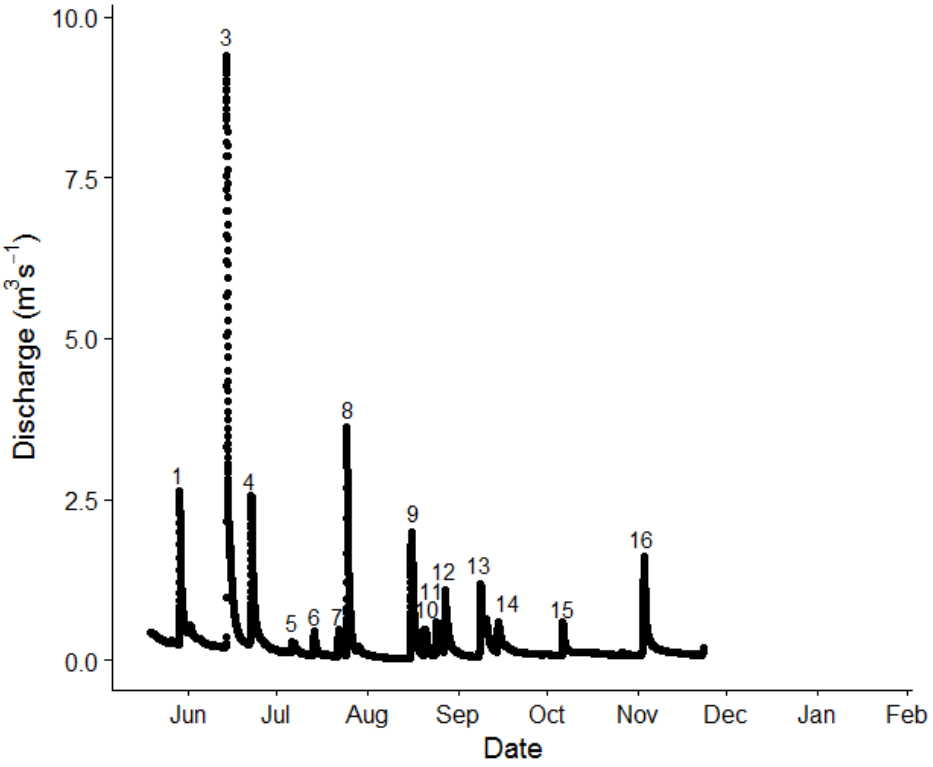

Figure 25. Hydrograph of Site 5. Numbers represent storm events. Limited data available.

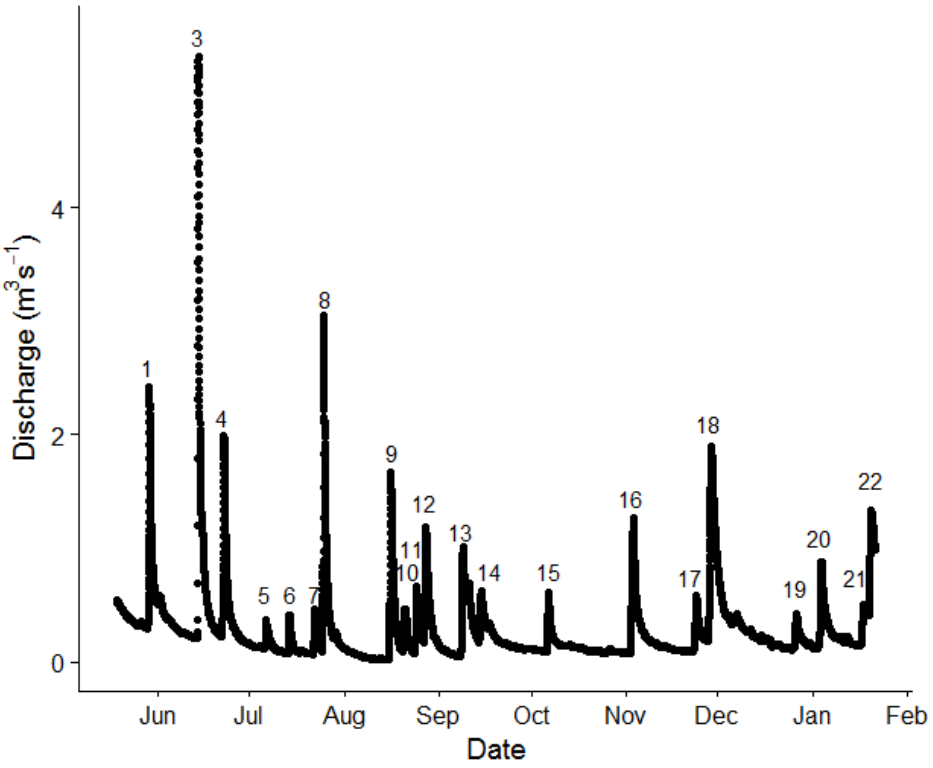

Figure 26. Hydrograph of Site 6. Numbers represent storm events.

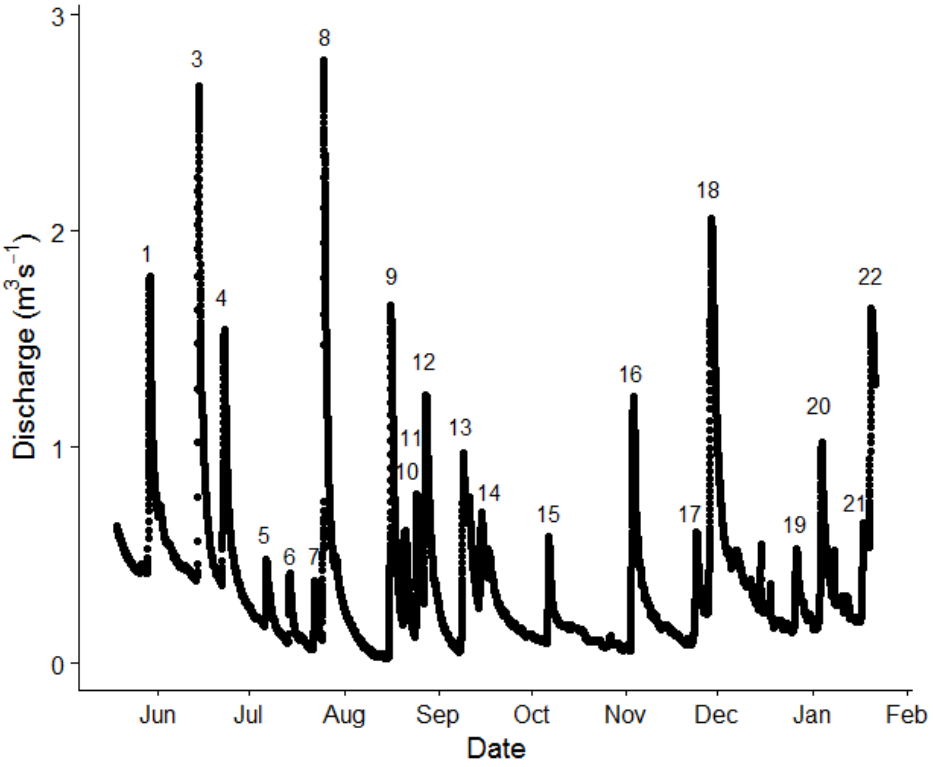

Figure 27. Hydrograph of Site 7. Numbers represent storm events.

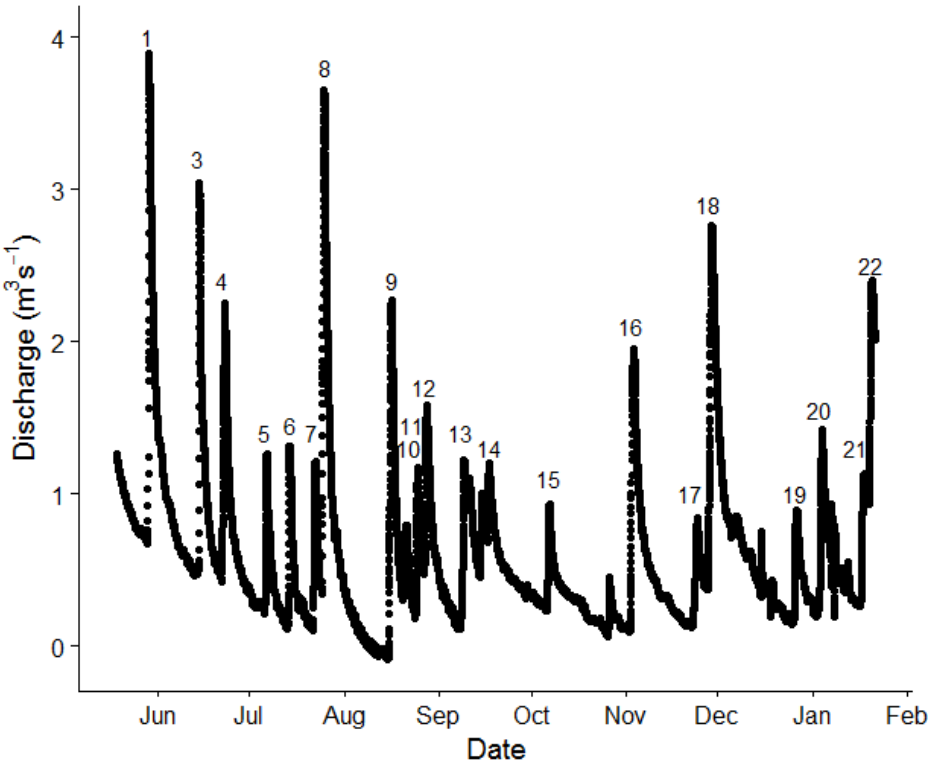

Figure 28. Hydrograph of Site 8. Numbers represent storm events.

Precipitation Data

Precipitation data is available from September 23 – January 21, for all sites except 3, which did not properly record data. I plotted the precipitation data as the daily sum of precipitation throughout the study period plotted on a bar graph (Figs. 29-35). The largest recorded rain event varied by site (Table 4). Storm 17 had the largest precipitation for Sites 1-2, Storm 18 was the largest precipitation for Sites 5 and 8, while Storm 16 had the largest precipitation for Site 5-6 and 8. The largest total recorded precipitation amount for any storm at an individual site was for Storm 16 at Site 5, which had 4.064 cm of precipitation. The smallest precipitation event was Storm 21, except for Site 5 where Storm 19 produced no measurable precipitation.

While some storms produced larger or smaller precipitation totals across the entire study area, the data does show spatial heterogeneity. For example, recorded precipitation nearly triples between Sites 1-4 for Storm 15. A final similarity seen in the data is that many of the storms spanned more than a single day.

Table 4

Rain Gauge Records for each Storm

	Storm 15	Storm 16	Storm 17	Storm 18	Storm 19	Storm 20	Storm 21	Storm 22
Date	10/6/16	10/7/16	10/8/16	10/9/16	10/10/16	10/11/16	10/12/16	10/13/16
Site 1	1.07	3.02	3.07	3.00	1.12	2.16	0.74	1.73
Site 2	1.96	2.72	3.94	3.05	1.02	2.24	0.71	2.06
Site 4	3.05	3.43	1.68	3.86	0.43	1.93	0.20	0.89
Site 5	1.80	4.06	1.47	1.17	0.00	0.03	0.23	0.20
Site 6	1.35	3.89	2.57	3.40	1.12	1.70	0.66	1.22
Site 7	1.22	3.12	2.21	3.66	0.99	1.63	0.79	0.99
Site 8	1.91	2.72	2.06	2.44	0.94	1.91	0.74	1.30

Note. Table includes the precipitation (in cm) for each storm. The storm date is the date the precipitation associated with the storm began. Rain gauge data are unavailable for storms before 9-23-16

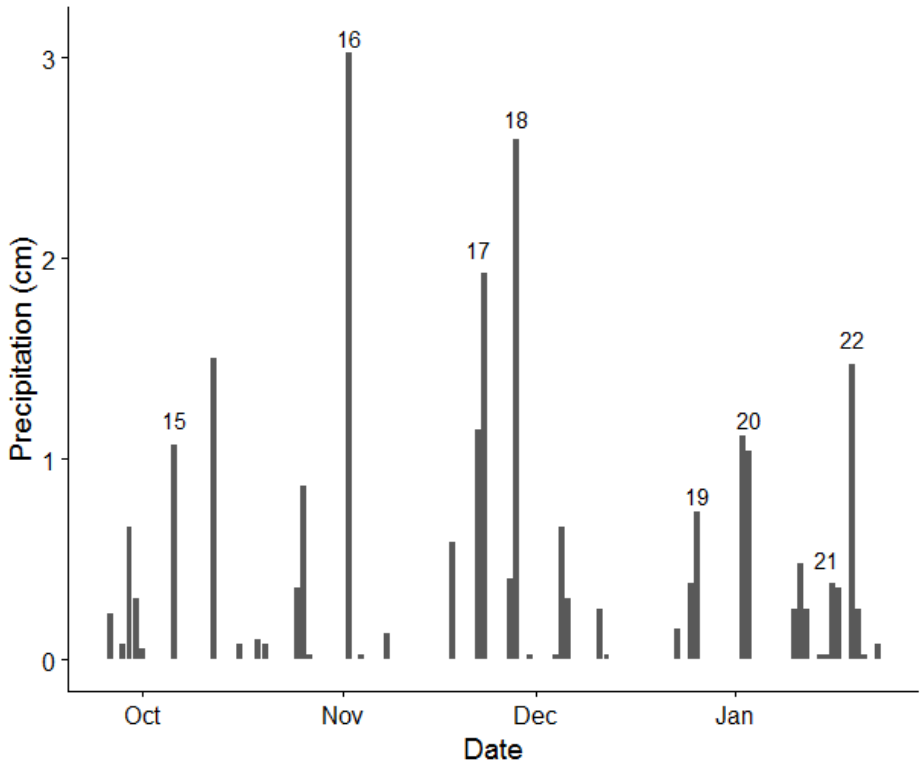

Figure 29. Precipitation data at Site 1. The numbers represent storm events during this period.

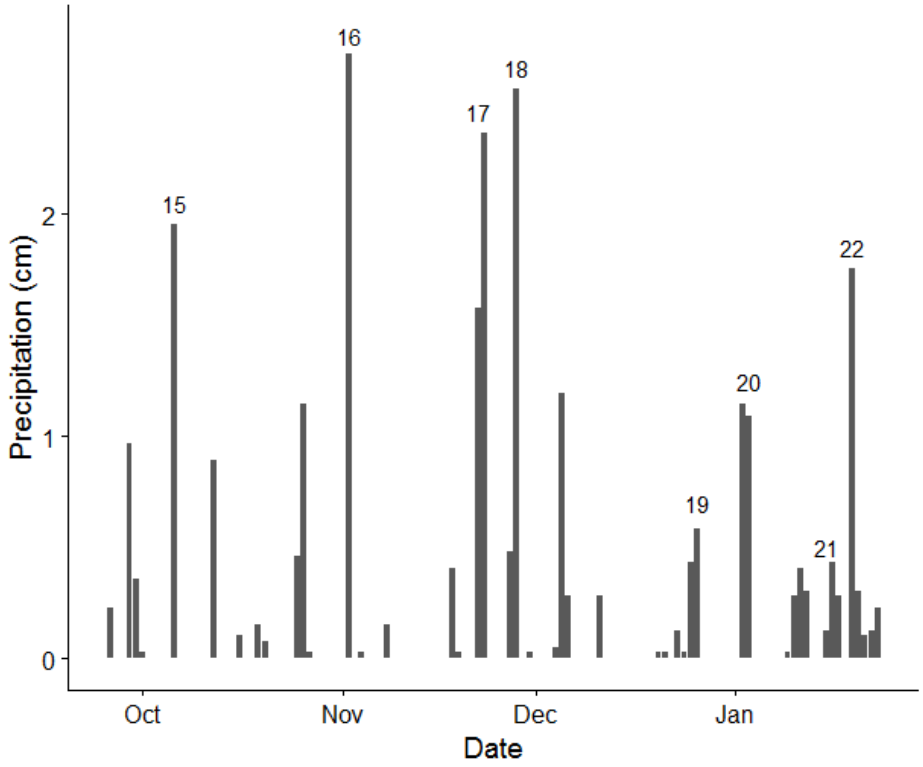

Figure 30. Precipitation data at Site 2. The numbers represent storm events during this period.

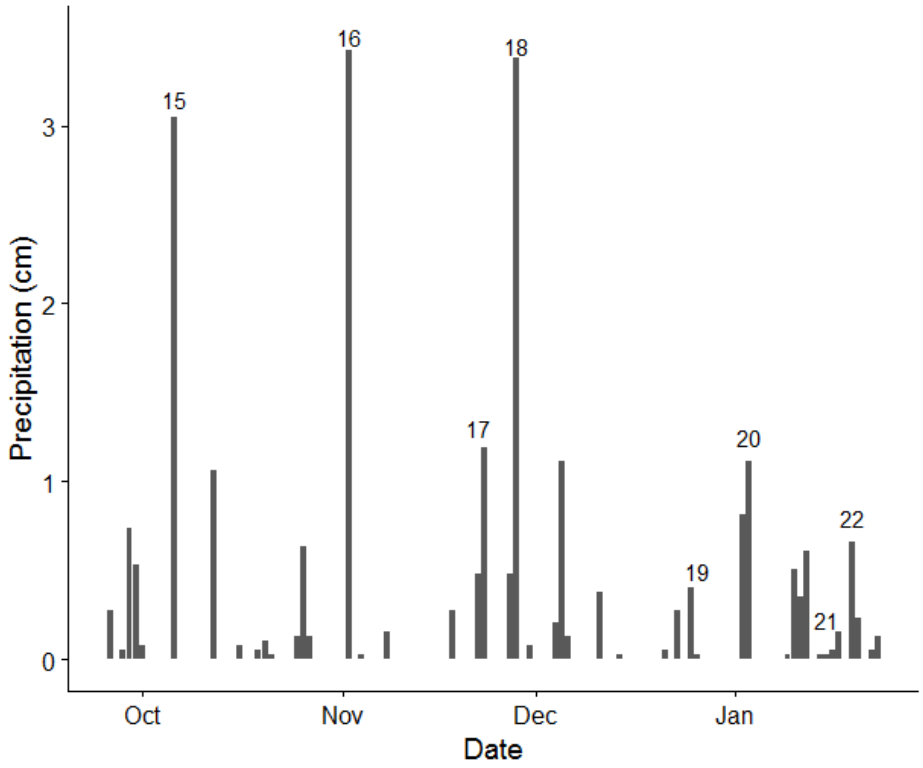

Figure 31. Precipitation data at Site 4. The numbers represent storm events during this period.

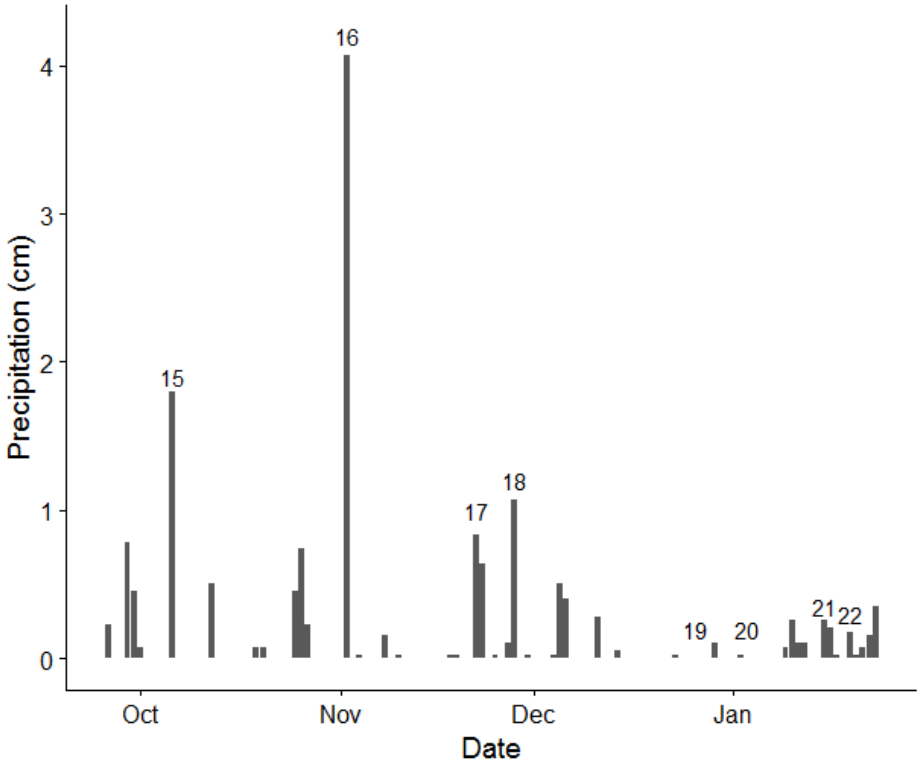

Figure 32. Precipitation data at Site 5. The numbers represent storm events during this period.

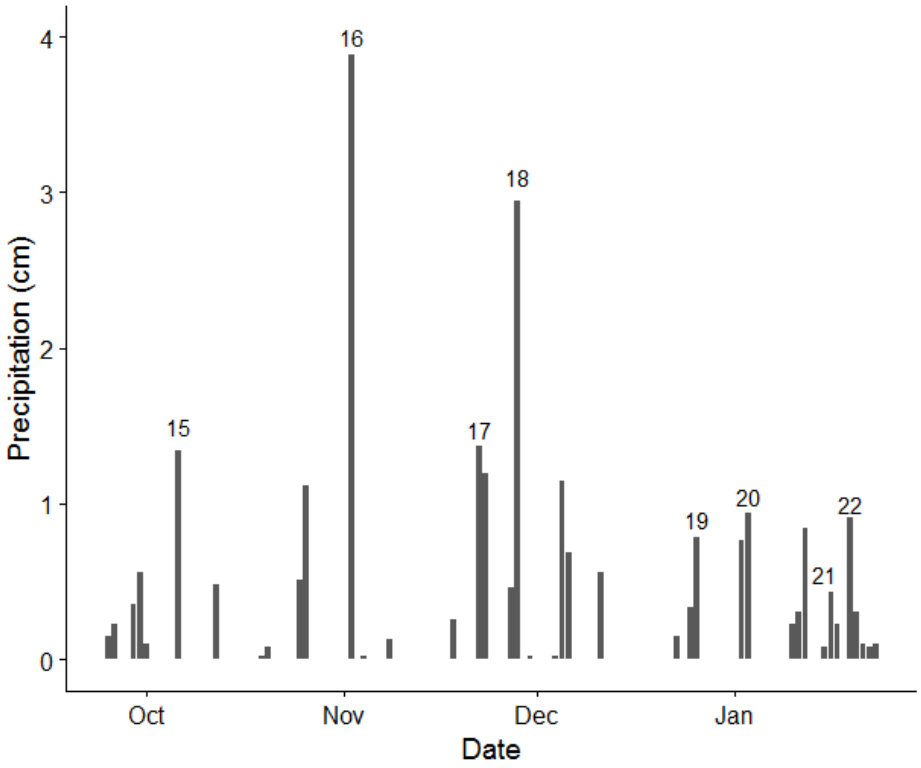

Figure 33. Precipitation data at Site 6. The numbers represent storm events during this period.

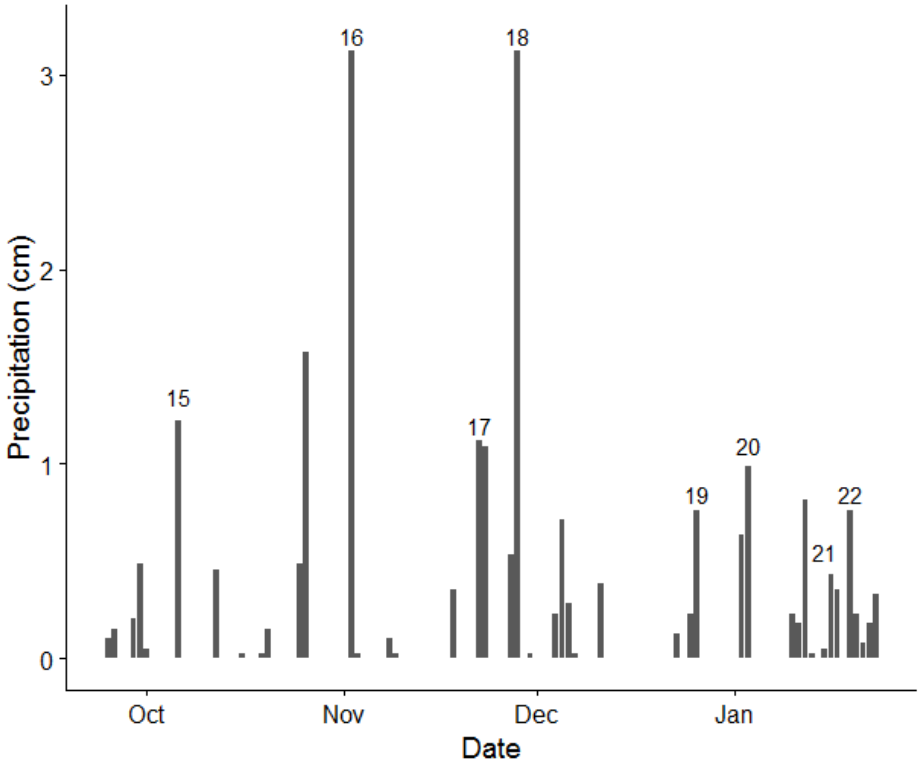

Figure 34. Precipitation data at Site 7. The numbers represent storm events during this period.

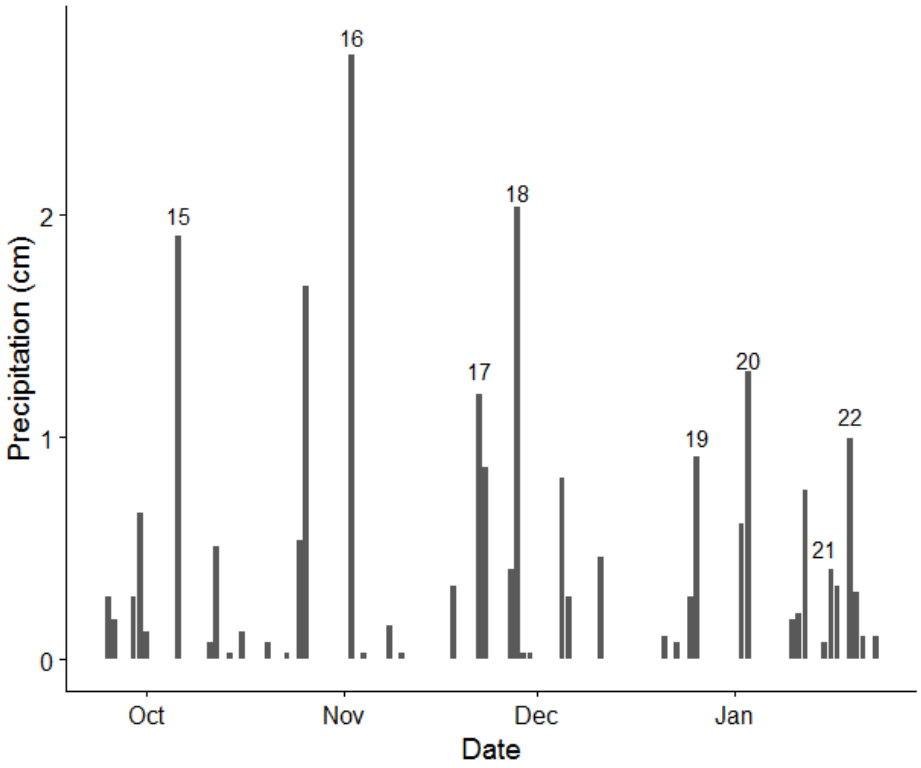

Figure 35. Precipitation data at Site 8. The numbers represent storm events during this period.

Peak Discharge Scaling Relationships

I created a peak discharge scaling relationship for each of the 21 storms that produced hydrograph runoff events at all eight sites (Figs. 36-56). Storm 2 does not have a scaling relationship because it did not produce rises in the hydrograph for every site. For each storm event, I applied a linear model between the log-transformed maximum discharge and the corresponding logged drainage area of each site.

Each scaling relationship graph displays its regression equation, R2 value, and scaling exponent (c-value) (Table 5). The average R2 value was 0.86. The maximum scaling exponent throughout the study was Storm 7 with a value of 1.576, while the minimum was Storm 10 with a value of 0.556. The mean scaling exponent of 11 storms from the tileflow period (both the early summer and fall/winter tileflow periods) was 1.109, while the mean from nine storms during no tileflow was 0.86 (Table 5). I excluded the scaling exponent from Storm 3 because the regression failed an F-test.

I conducted a Wilcoxon-Mann-Whitney Test to assess whether the means of the scaling exponent between tileflow and no-tileflow periods were statistically different. The no-tileflow scaling exponent group failed a Shapiro-Wilk test for normality (p-value= 0.040). Therefore, I conducted a Wilcoxon-Mann-Whitney test; this test is the equivalent of a t-test, but used for data that does not follow a normal distribution. The null hypothesis was rejected and the sample means between the tileflow and no-tileflow periods were deemed statistically different (p-value= 0.038).

Table 5

Summary Table for Parameters in the Peak Discharge Scaling Relationships

	C-value	Y-intercept	R^2
Storm 1	1.466	-6.407	0.872
Storm 3	0.647	-2.413	0.339
Storm 4	0.793	-4.221	0.971
Storm 5	0.932	-4.64	0.918
Storm 6	1.221	-5.92	0.955
Storm 7	1.576	-7.54	0.898
Storm 8	0.902	-3.717	0.875
Storm 9	0.668	-2.847	0.906
Storm 10	0.556	-2.843	0.923
Storm 11	0.874	-4.226	0.874
Storm 12	0.664	-3.012	0.959
Storm 13	0.6	-2.756	0.853
Storm 14	0.678	-3.29	0.93
Storm 15	1.553	-7.441	0.939
Storm 16	0.952	-4.233	0.809
Storm 17	0.761	-3.742	0.772
Storm 18	1.106	-4.9	0.849
Storm 19	1.009	-5.003	0.919
Storm 20	0.996	-4.67	0.846
Storm 21	1.134	-5.523	0.919
Storm 22	1.127	-5.084	0.862

Note. Table showing the C-value (slope), Y-intercept, and R^2 value for each peak discharge scaling relationship.

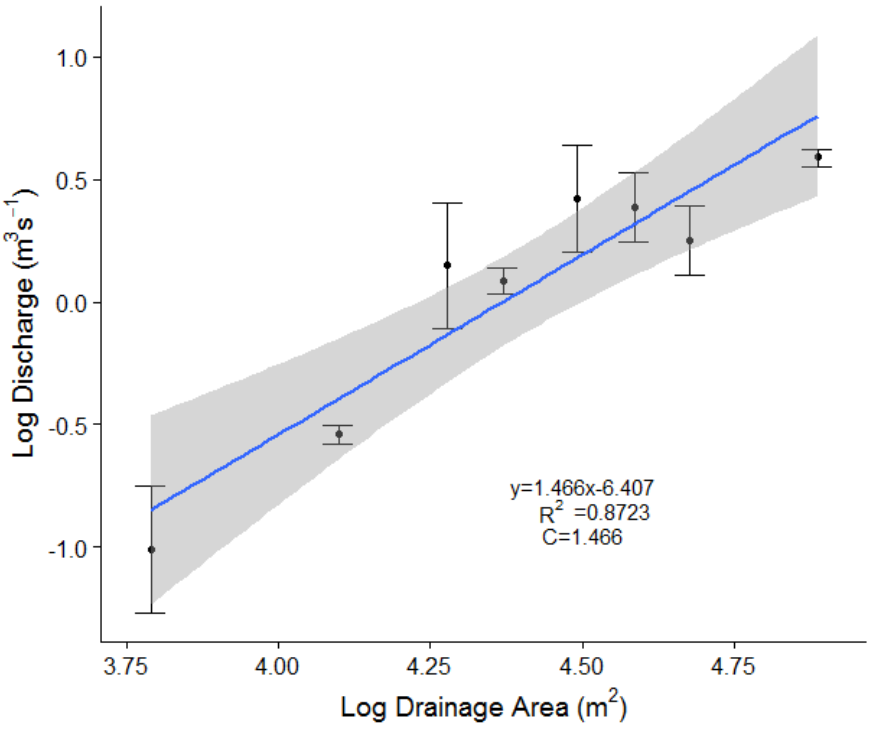

Figure 36. Peak discharge scaling relationship for Storm 1 (~ 5/29/16). Error bars represent the upper and lower limit of the 95% confidence interval for that point's calculated discharge value.

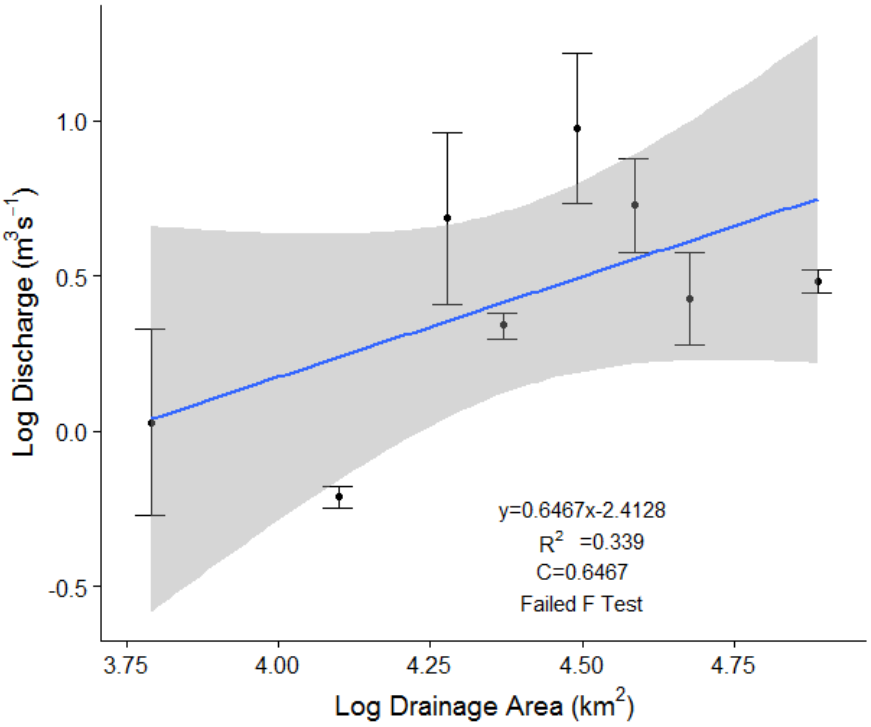

Figure 37. Peak discharge scaling relationship for Storm 3 (~ 6/14/16). Error bars represent the upper and lower limit of the 95% confidence interval for that point's calculated discharge value.

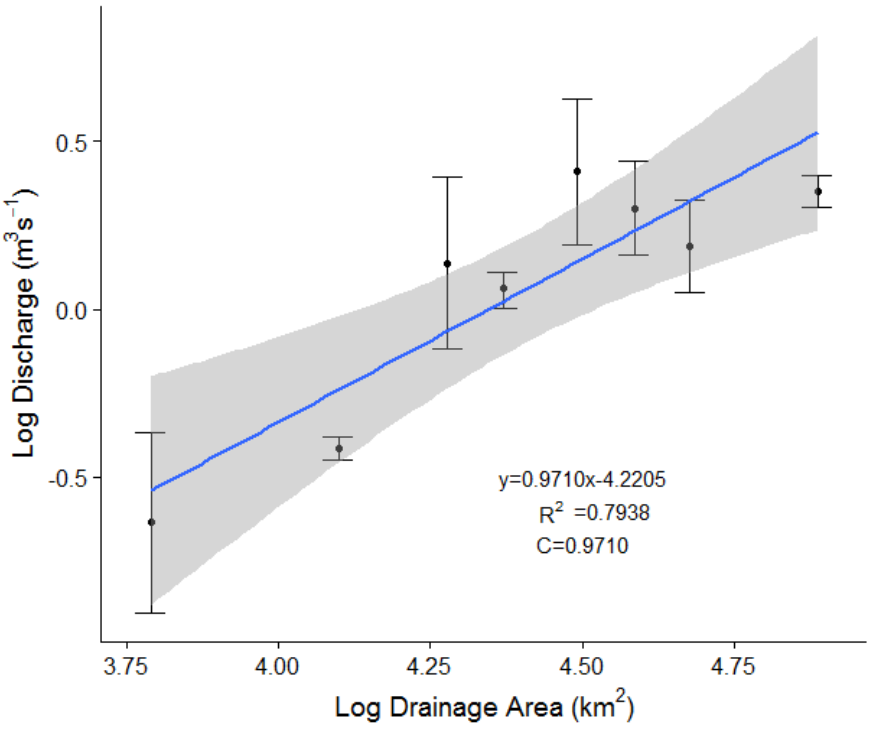

Figure 38. Peak discharge scaling relationship for Storm 4 (~ 6/22/16). Error bars represent the upper and lower limit of the 95% confidence interval for that point's calculated discharge value.

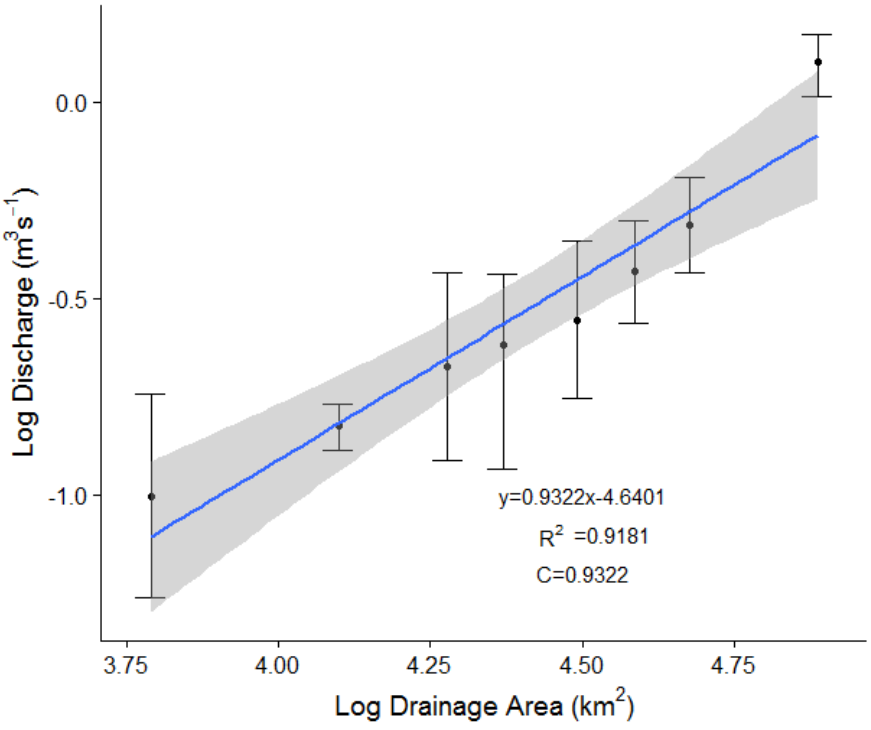

Figure 39. Peak discharge scaling relationship for Storm 5 (~ 7/6/16). Error bars represent the upper and lower limit of the 95% confidence interval for that point's calculated discharge value.

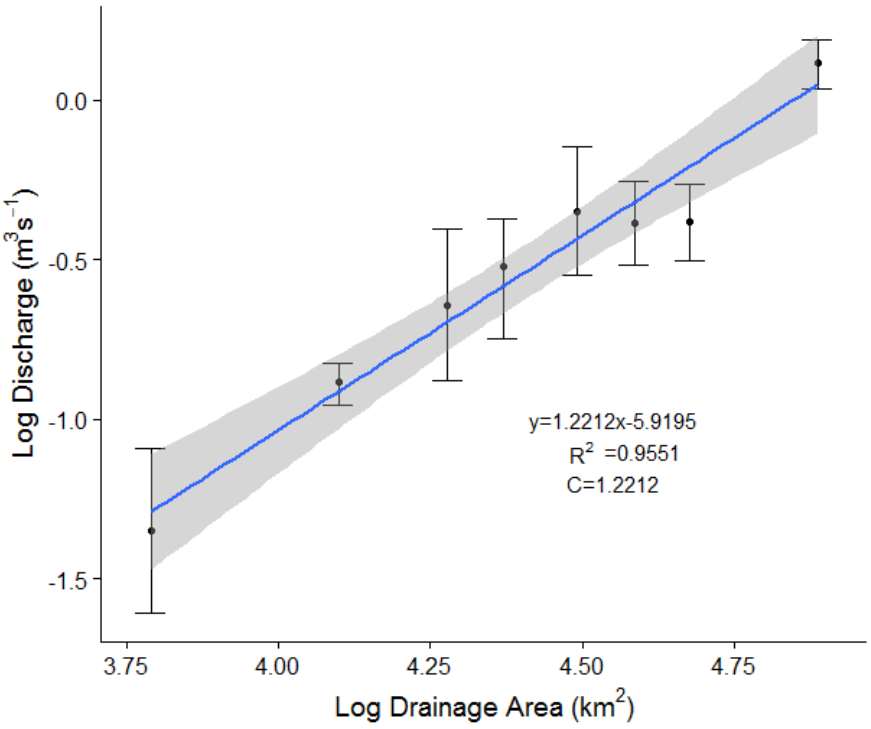

Figure 40. Peak discharge scaling relationship for Storm 6 (~ 7/14/16). Error bars represent the upper and lower limit of the 95% confidence interval for that point's calculated discharge value.

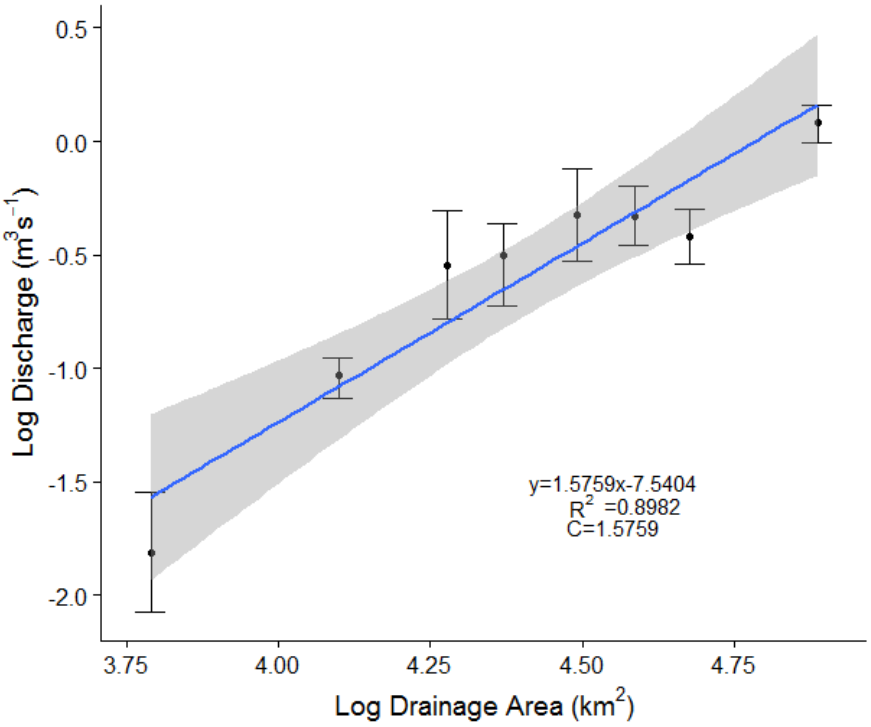

Figure 41. Peak discharge scaling relationship for Storm 7 (~ 7/14/16). Error bars represent the upper and lower limit of the 95% confidence interval for that point's calculated discharge value.

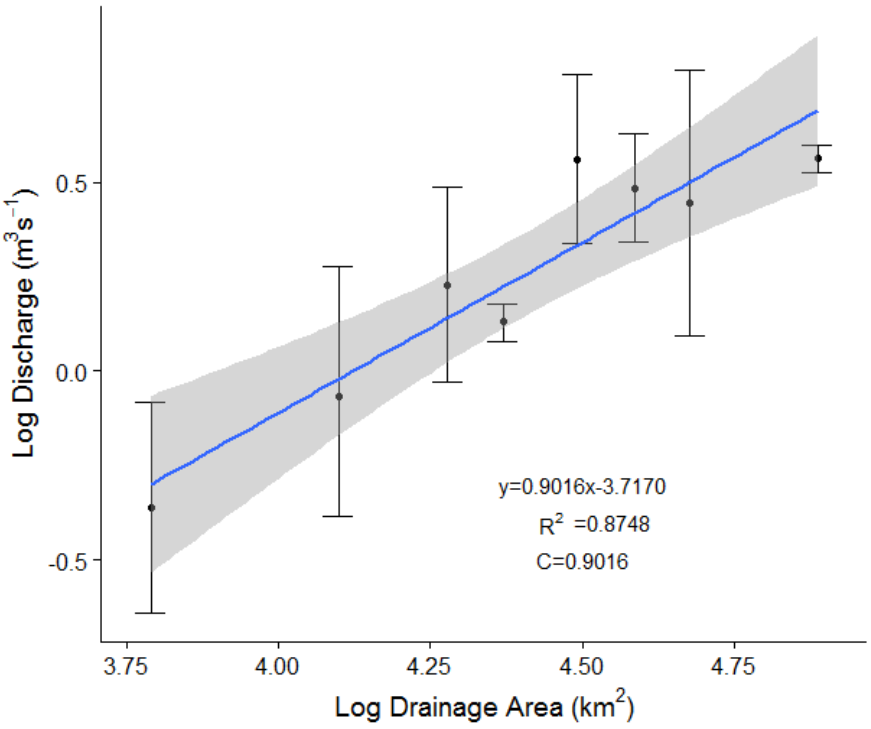

Figure 42. Peak discharge scaling relationship for Storm 8 (~ 7/25/16). Error bars represent the upper and lower limit of the 95% confidence interval for that point's calculated discharge value.

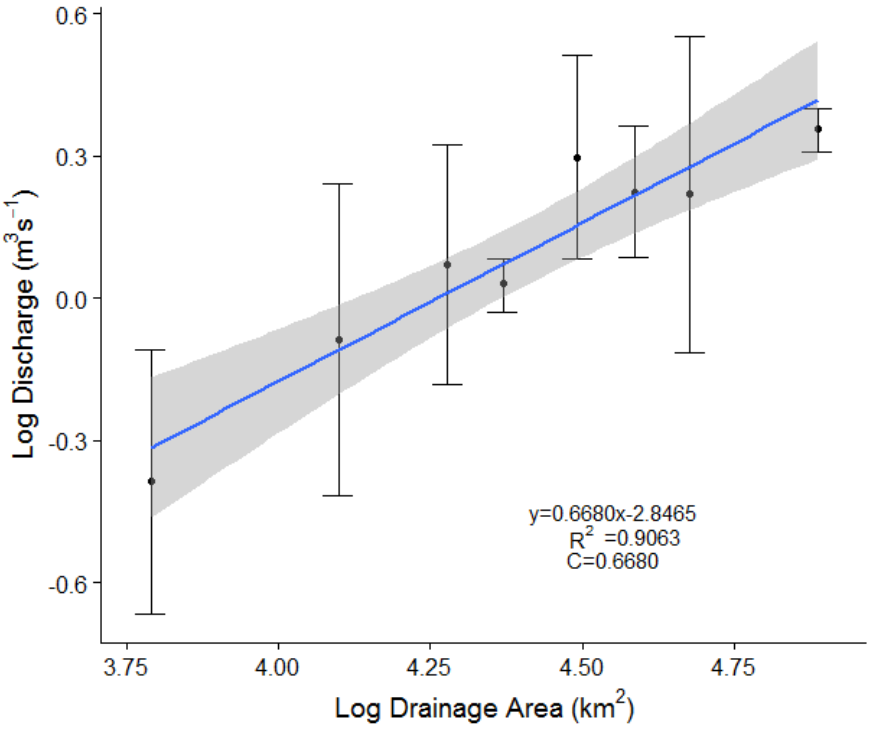

Figure 43. Peak discharge scaling relationship for Storm 9 (~ 8/16/16). Error bars represent the upper and lower limit of the 95% confidence interval for that point's calculated discharge value.

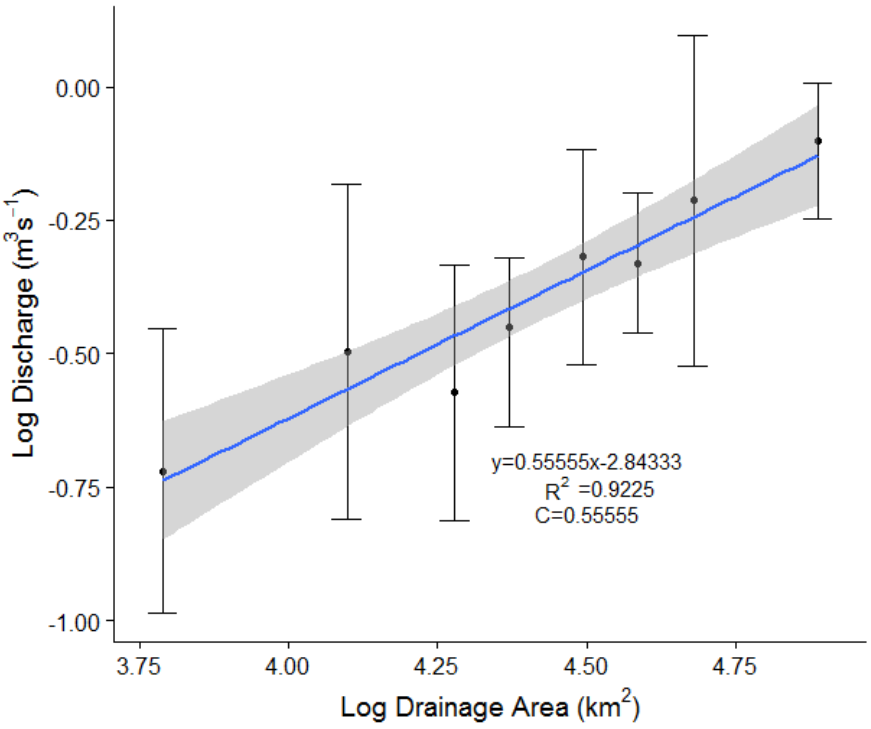

Figure 44. Peak discharge scaling relationship for Storm 10 (~ 8/21/16). Error bars represent upper and lower limit of the 95% confidence interval for that point's calculated discharge value.

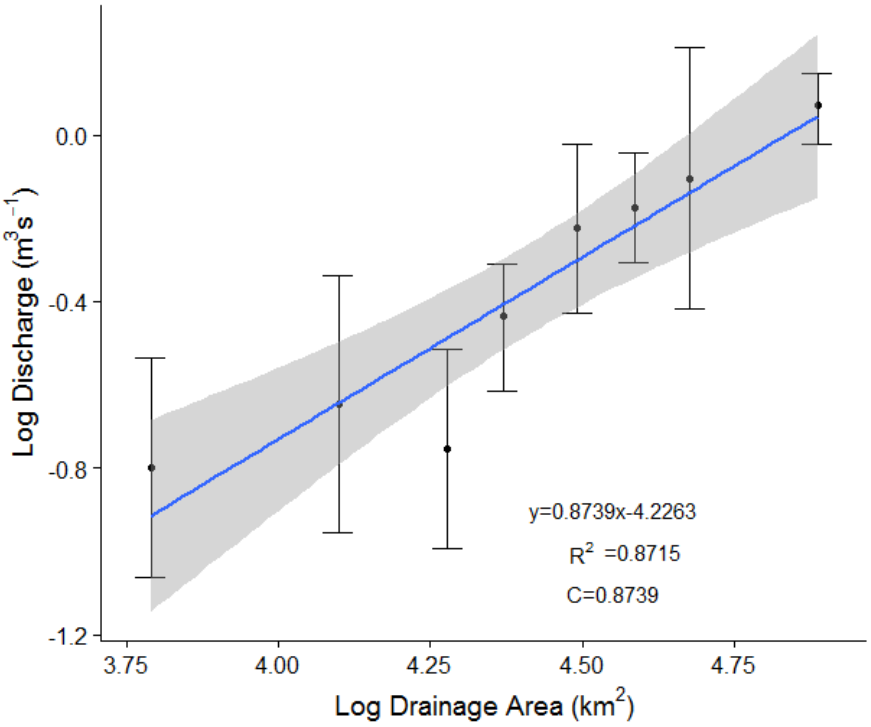

Figure 45. Peak discharge scaling relationship for Storm 11 (~ 8/24/16). Error bars represent upper and lower limit of the 95% confidence interval for that point's calculated discharge value.

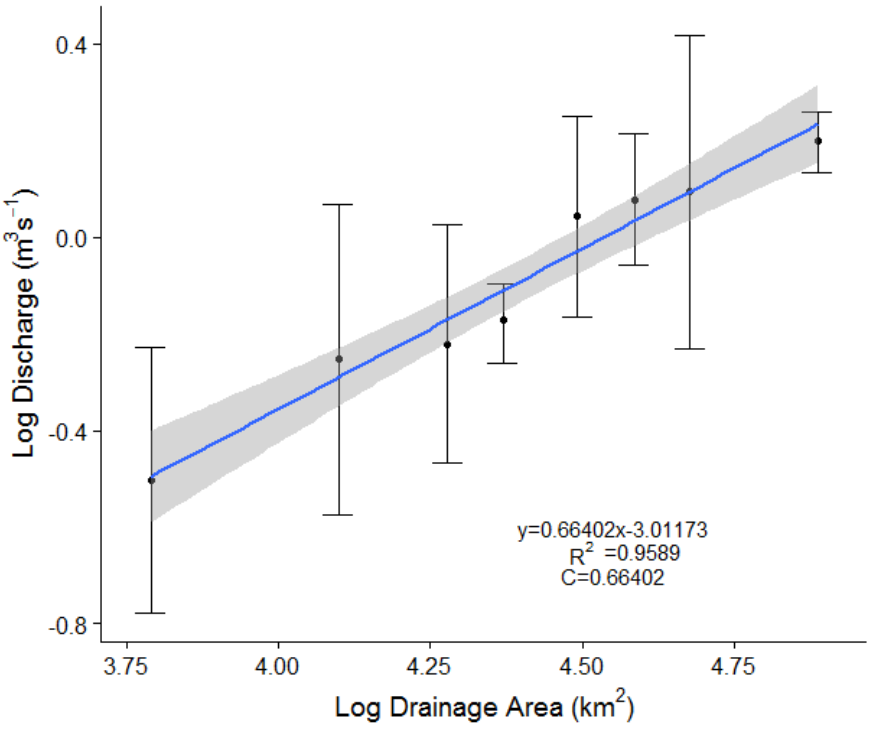

Figure 46. Peak discharge scaling relationship for Storm 12 (~ 8/27/16). Error bars represent upper and lower limit of the 95% confidence interval for that point's calculated discharge value.

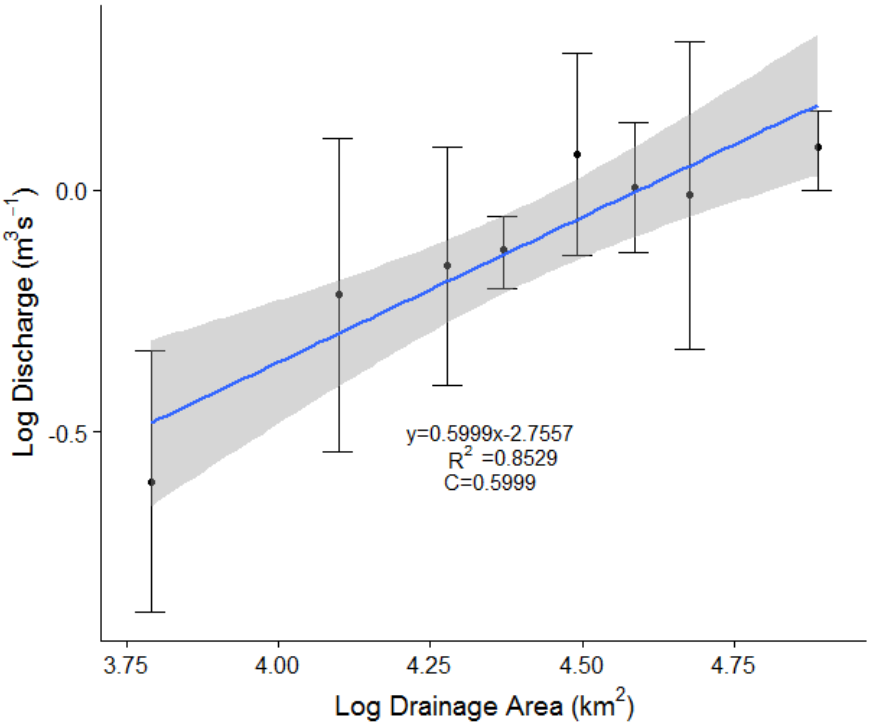

Figure 47. Peak discharge scaling relationship for Storm 13 (~ 9/8/16). Error bars represent the upper and lower limit of the 95% confidence interval for that point's calculated discharge value.

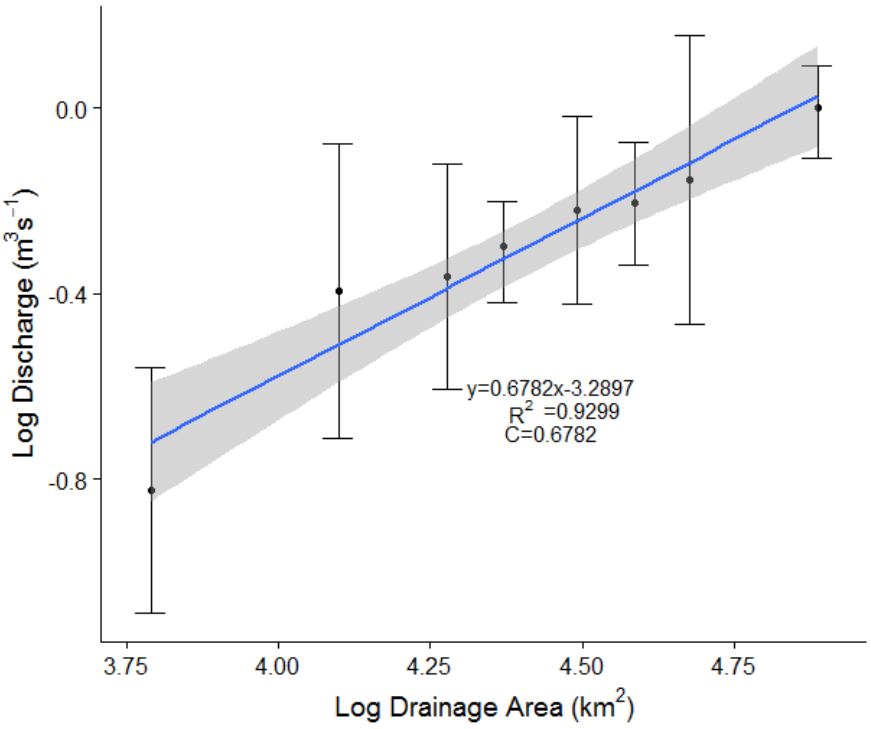

Figure 48. Peak discharge scaling relationship for Storm 14 (~ 9/14/16). Error bars represent upper and lower limit of the 95% confidence interval for that point's calculated discharge value.

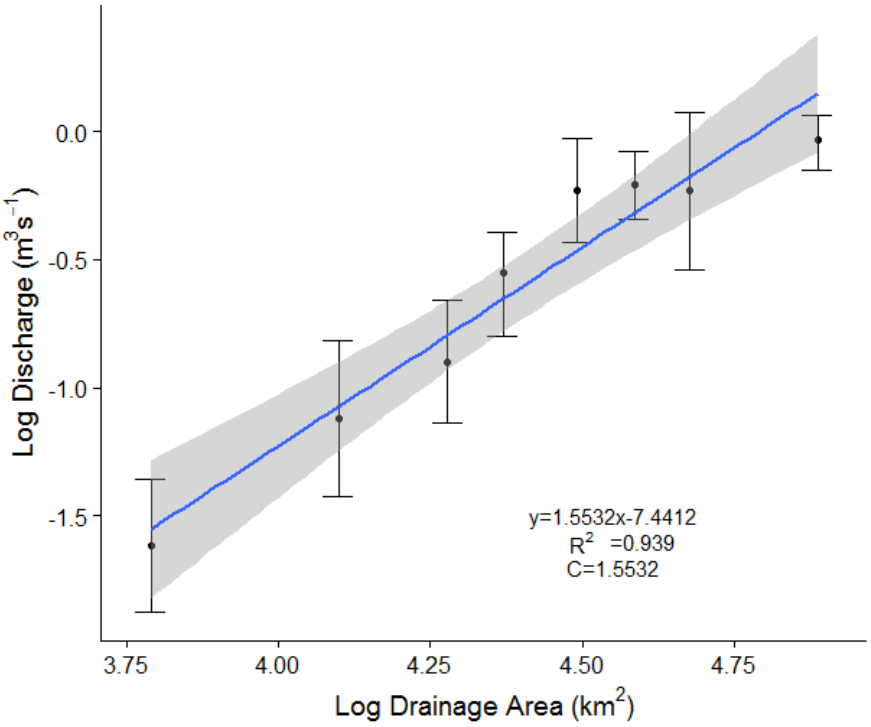

Figure 49. Peak discharge scaling relationship for Storm 15 (~ 10/6/16). Error bars represent upper and lower limit of the 95% confidence interval for that point's calculated discharge value.

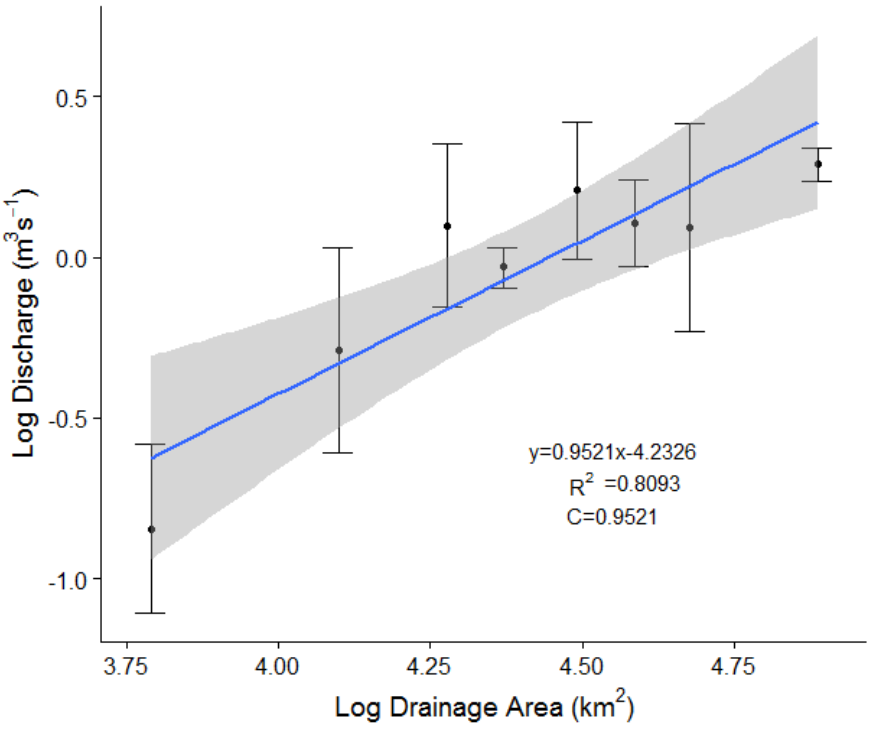

Figure 50. Peak discharge scaling relationship for Storm 16 (~11/3/16). Error bars represent the upper and lower limit of the 95% confidence interval for that point's calculated discharge value.

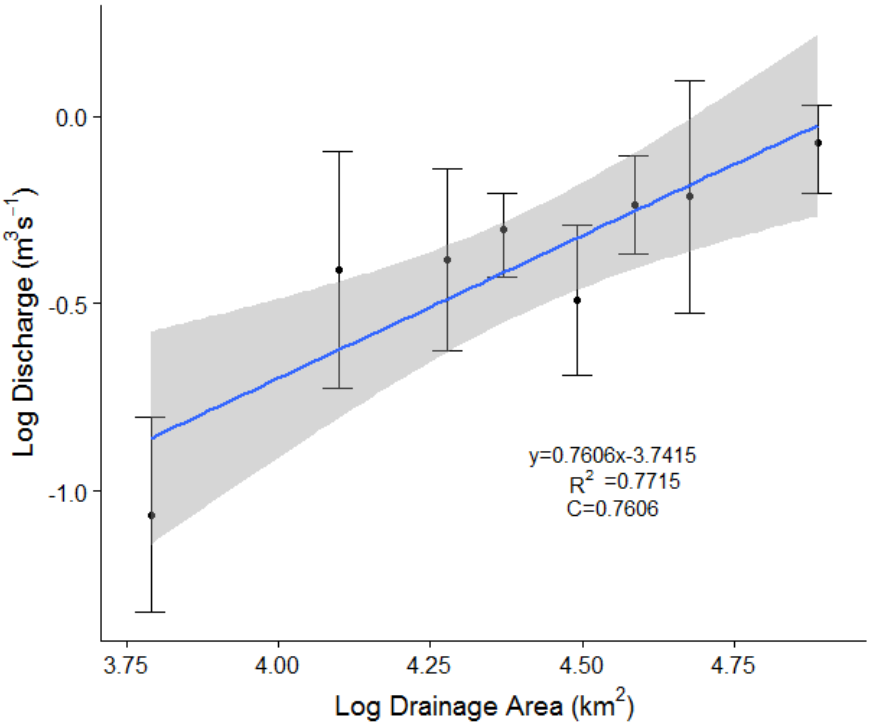

Figure 51. Peak discharge scaling relationship for Storm 17 (11/23/16). Error bars represent upper and lower limit of the 95% confidence interval for that point's calculated discharge value.

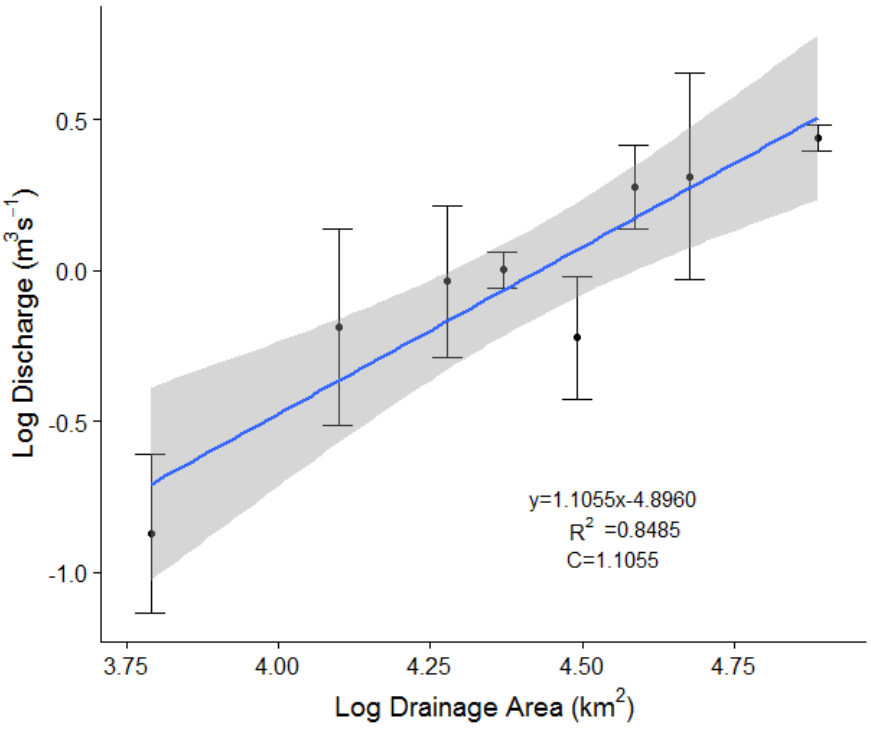

Figure 52. Peak discharge scaling relationship for Storm 18 (~ 11/28/16). Error bars represent upper and lower limit of the 95% confidence interval for that point's calculated discharge value.

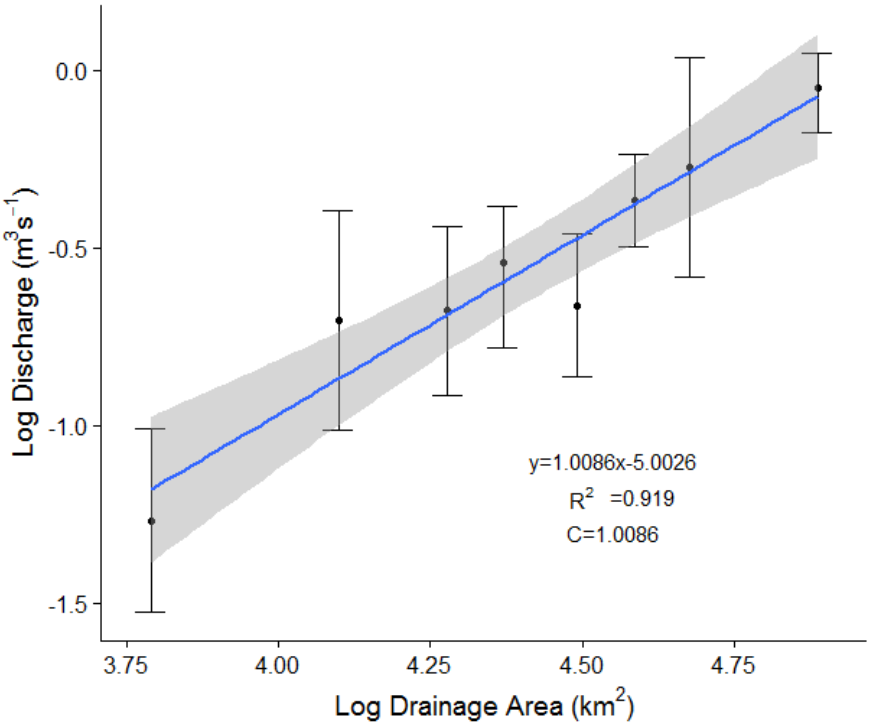

Figure 53. Peak discharge scaling relationship for Storm 19 (~ 12/26/16). Error bars represent upper and lower limit of the 95% confidence interval for that point's calculated discharge value.

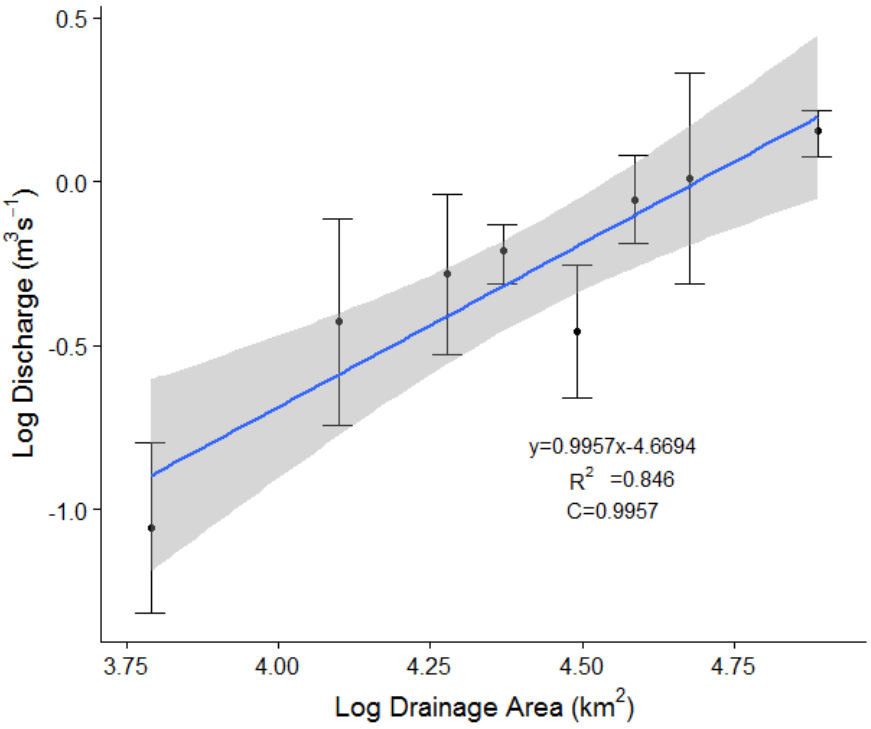

Figure 54. Peak discharge scaling relationship for Storm 20 (~ 1/3/17). Error bars represent the upper and lower limit of the 95% confidence interval for that point's calculated discharge value.

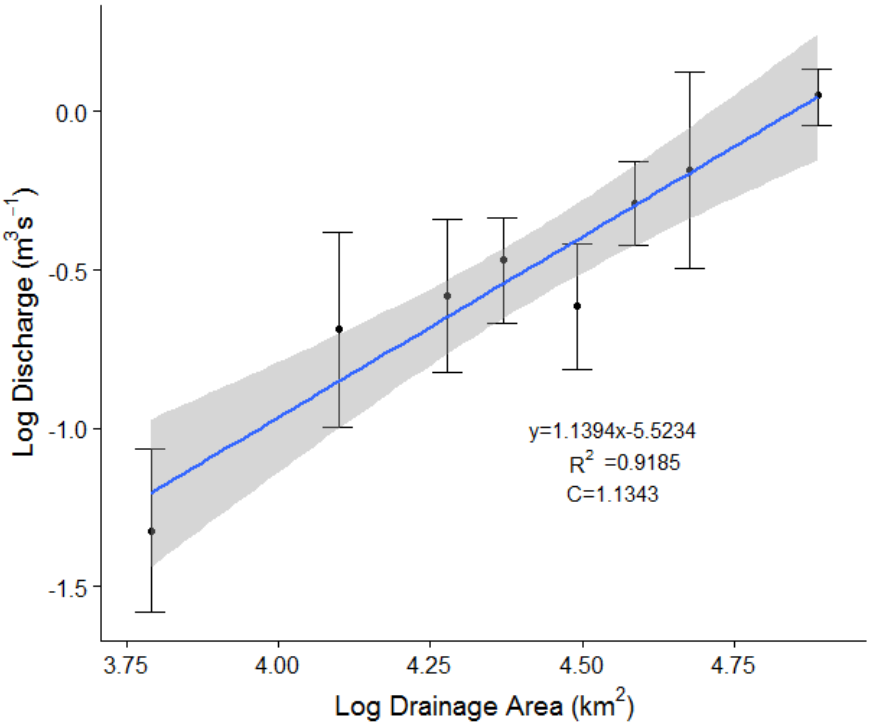

Figure 55. Peak discharge scaling relationship for Storm 21 (~ 1/17/17). Error bars represent upper and lower limit of the 95% confidence interval for that point's calculated discharge value.

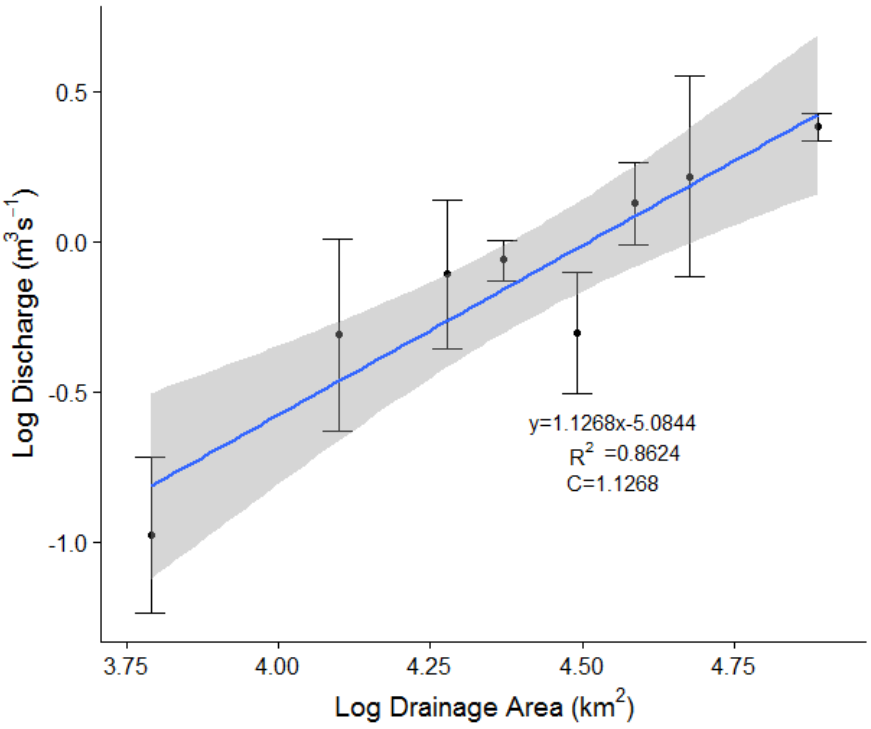

Figure 56. Peak discharge scaling relationship for Storm 22 (~ 1/20/17). Error bars represent upper and lower limit of the 95% confidence interval for that point's calculated discharge value.

Mean Baseflow Scaling Relationships

The C-values (slopes) for the mean baseflow scaling relationship ranged from 0.930 – 1.112 (Table 6). They were smaller than the C-values found during the peak discharge scaling relationships. The average R2 was 0.96. Overall, R2 values were larger than in the peak discharge scaling relationships (Figs. 57-59).

Table 6

Summary Table for Parameters in the Mean Baseflow Discharge Scaling Relationships

	Condition	Dates	C-value	Y-intercept	R^2
Early Summer	tileflow	May 17 - July 6	0.996	-4.997	0.978
Summer	no-tileflow	July 7 - September 14	0.93	-5.09	0.959
Fall and Winter	tileflow	September 15 - January 21	1.112	-5.87	0.954

Note. Table showing the tile condition, date range, C-value (slope), y-intercept, and R2 value associated with each mean baseflow scaling relationship.

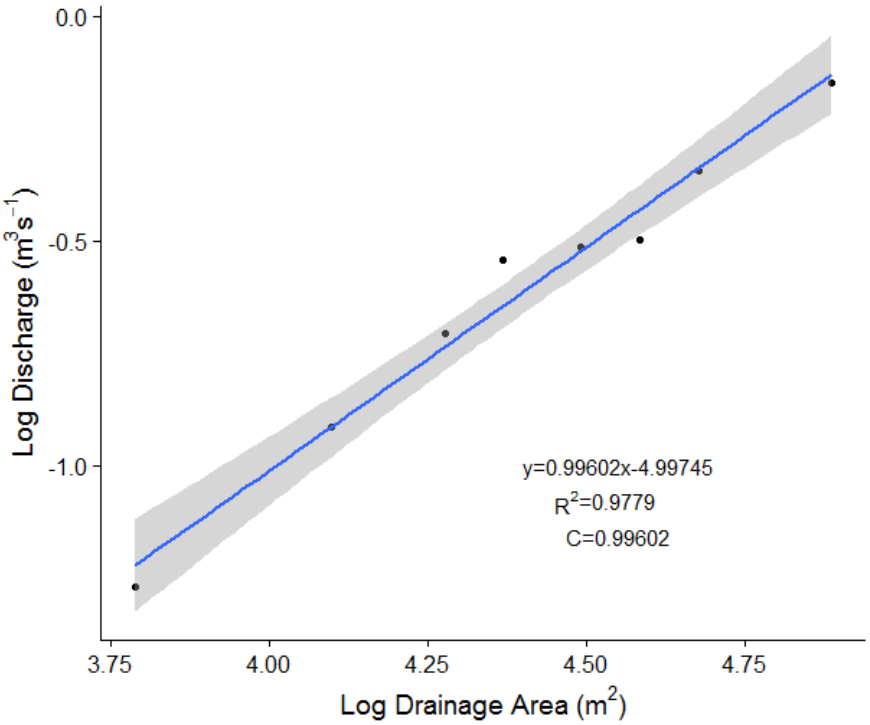

Figure 57. Mean Baseflow Scaling relationship for the early summer tileflow period (May 18 – July 7).

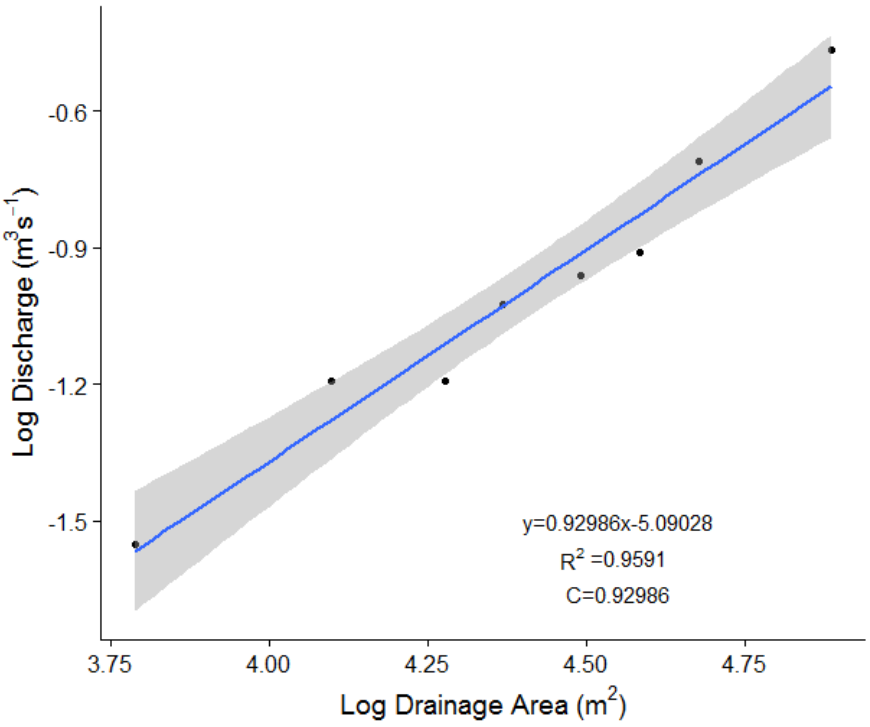

Figure 58. Mean Baseflow Scaling relationship for the no-tileflow period (July 7 – September 15).

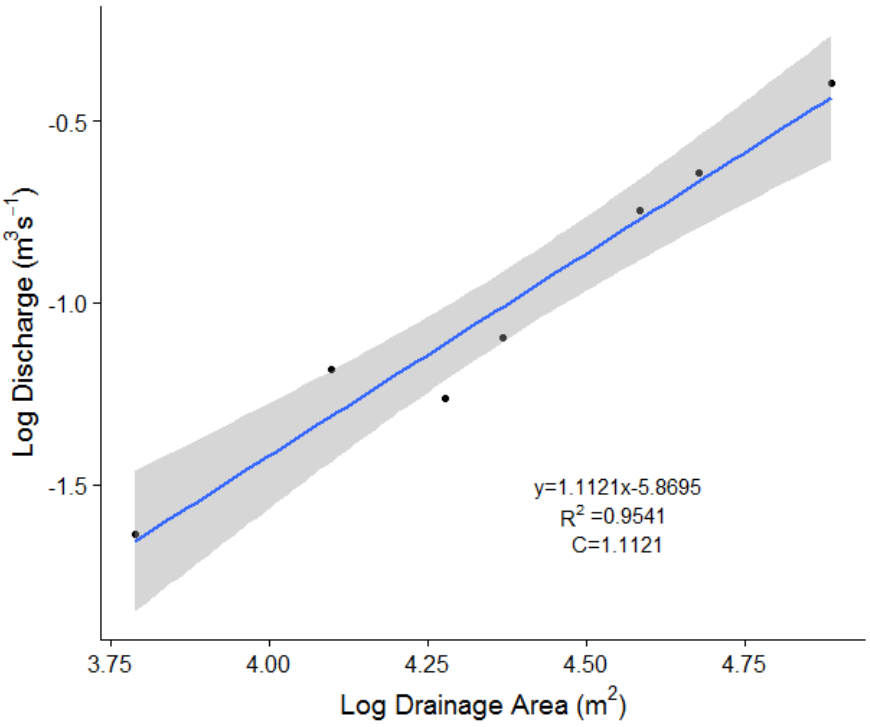

Figure 59. Mean Baseflow Scaling relationship for the fall and winter tileflow period (September 15 – January 21).

Scaling Relationship Summary Tables

I compiled Information from both the peak discharge scaling relationships and the mean baseflow scaling relationships on a summary table to look for patterns (Table 7-9). The first table represents the early summer tileflow period, the second represents the summer no-tileflow period, and the third represents the fall and winter tileflow period. Every storm has an outlier. There were a total of 42 outliers, 24 upper outliers and 18 lower outliers.

Overall, there did not appear to be a pattern where a site was often an outlier during tileflow and rarely an outlier during no-tileflow. However, Site 3 was occasionally an upper outlier during the tileflow period (five times) and somewhat frequently a lower outlier during the no-tileflow period (four times). Additionally, Site 5 was regularly an upper outlier for the majority of the study period, until Storm 17 when it was subsequently a lower outlier from then on. Finally, it is worth noting that there is limited overlap between outliers that occurred during baseflow conditions and outliers that occurred during storm events.

Table 7

Summary Table for Outliers to Scaling Relationships during the Early Summer Tileflow Period

	Baseflow	Storm 1	Storm 3	Storm 4	Storm 5
Site 1					
Site 2			-		
Site 3		+	+	+	
Site 4	+				
Site 5		+	+	+	-
Site 6	-				
Site 7					
Site 8					+

Note. Baseflow represents the mean baseflow scaling relationship, as opposed to a specific storm. Upper outliers are represented by a +, while lower outliers are represented by a -.

Table 8

Summary Table for Outliers to Scaling Relationships during the Summer No-tileflow Period

	Baseflow	Storm 6	Storm 7	Storm 8	Storm 9	Storm 10	Storm 11	Storm 12	Storm 13	Storm 14
Site 1										
Site 2	+									+
Site 3	-		+			-	-	-		
Site 4								-		
Site 5		+		+	+			+	+	
Site 6	-									
Site 7		-	-							
Site 8										

Note. Baseflow represents the mean baseflow scaling relationship, as opposed to a specific storm. Upper outliers are represented by a +, while lower outliers are represented by a -.

Table 9

Summary Table for Outliers to Scaling Relationships during the Summer No-tileflow Period

	Baseflow	Storm 15	Storm 16	Storm 17	Storm 18	Storm 19	Storm 20	Storm 21	Storm 22
Site 1									
Site 2	+			+		+		+	
Site 3	-		+						+
Site 4									
Site 5		+	+	-	-	-	-	-	-
Site 6									
Site 7									
Site 8									

Note. Baseflow represents the mean baseflow scaling relationship, as opposed to a specific storm. Upper outliers are represented by a +, while lower outliers are represented by a -.

Summary Table for Double and Extended Peaks

Double peaks on hydrographs were observed (Fig. 60). Throughout the study period 36.9%, or 62, of 168 site-specific storm hydrographs had double or extended peaks (Tables 10-12). Double and extended peaks were common throughout the entire study period and do not appear to be limited to one season. Eight occurred in the early summer tileflow period, 29 occurred in the summer no-tileflow period, and 25 occurred in the fall and winter tileflow period. All storms except 1, 12, 14, and 20 had at least one site with a double peak. Double and extend peaks occurred during both small and large storms. In summary, double peaks occurred throughout all seasons and storm sizes.

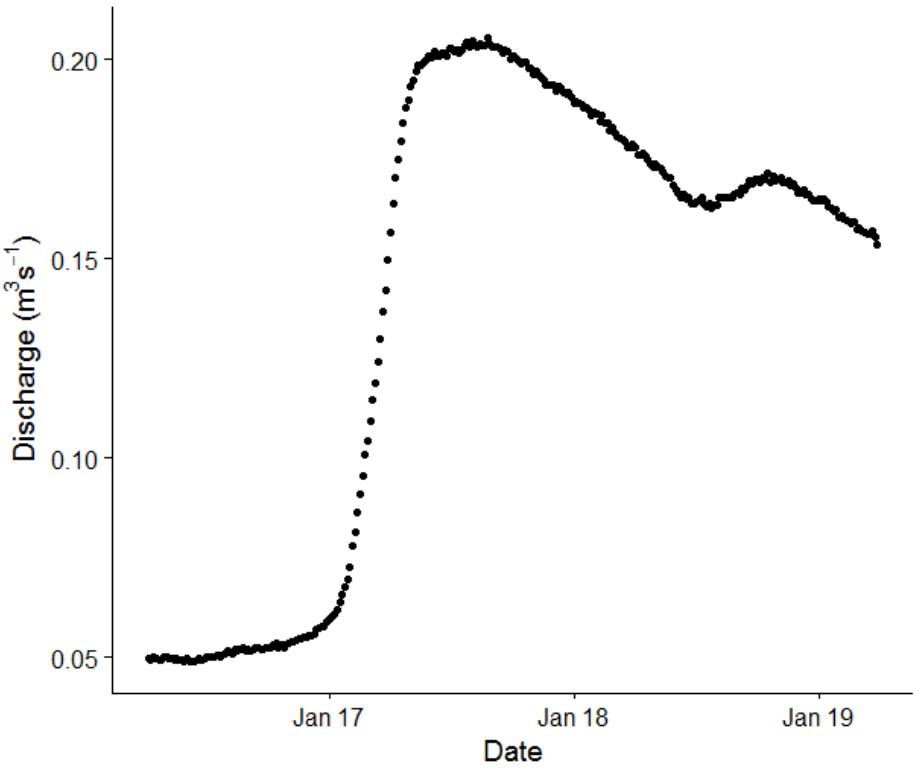

Figure 60. An example of a double peak at Site 2 during Storm 21.

Table 10

Summary Table for Double and Extended Peaks in the Early Summer Tileflow Period

	storm 1	storm 3	storm 4	storm 5
site 1		x	x	
site 2				
site 3		x		x
site 4		x		x
site 5				x
site 6				x
site 7				
site 8				

Note. Each column represents a different storm and each rows represent one of the eight sites. An X represents an observed double or extended peak.

Table 11

Summary Table for Double and Extended Peaks in the Summer No-tileflow Period

	storm 6	storm 7	storm 8	storm 9	storm 10	storm 11	storm 12	storm 13	storm 14
site 1		x		x				x	
site 2				x					
site 3	x	x	x			x		x	
site 4	x				x	x		x	
site 5	x				x			x	
site 6	x				x			x	
site 7	x	x			x	x		x	
site 8	x	x			x	x		x	

Note. Each column represents a different storm and each rows represent one of the eight sites. An X represents an observed double or extended peak.

Table 12

Summary Table for Double and Extended Peaks in the Fall and Winter Tileflow Period

	storm 15	storm 16	storm 17	storm 18	storm 19	storm 20	storm 21	storm 22
site 1	x	x	x				x	x
site 2				x			x	x
site 3		x		x			x	x
site 4		x					x	
site 5		x					x	
site 6		x					x	
site 7		x			x		x	
site 8	x	x			x		x	

Note. Each column represents a different storm and each rows represent one of the eight sites. An X represents an observed double or extended peak.

CHAPTER IV: DISCUSSION

Outliers in the Peak Discharge Scaling Relationships

An outlier that lies above the scaling relationship represents a site that is receiving proportionally more water than expected, based on that site's drainage area. A potential reason that a site could be receiving more water than expected in this system is that tile drains may be contributing water from crops fields that cross natural drainage divides. If a site is consistently an upper outlier during tileflow season, but not an upper outlier when this extra input of water stops during no-tileflow season, then the stream section just upstream of that site likely has a large input of discharge from tile drains.

Overall, there did not appear to be a pattern where a site was often an outlier during tileflow and rarely an outlier during no-tileflow (Tables 8-10). From these data, it was not clear if tile drain input affected Money Creek's hydrology. The method of looking at outliers within scaling relationships did not appear to be effective at detecting tile drain input. I suspect this is because the error associated with creating hydrographs is inherently too large to detect the amount of water that tile drains add to the stream. For example, despite the all of the rating curves having R^2 values of 0.92 or greater, the error bars on the scaling relationships still tend to be large (Figs. 36-56).

Additionally, this method relies on the assumption that the area directly upstream of an upper outlier has a very large input of discharge from tile drains, while the other sites have minimal discharge added from tile drains. In reality, tile drains are likely widely distributed throughout the watershed (an estimated 52%-82% of McLean County is tile drained) (Sugg, 2007), essentially negating the effective that tile drains have on any one individual site.

A remote sensing project, separate from this thesis, looked at tile drainage within the Money Creek Watershed (Appendix A). The project used shortwave bands (Band 5) of Landsat-5 and Landsat-7 satellite imagery to look at how effectively soil in the watershed was drained after a series of storms from April 3rd-7th, 2003, with the implication that soils that were well drained represent farm fields with tile drainage. The figure is the result of image differencing, comparing an image on April 11th to an image before the storms on April 2nd. Red areas on the image represent locations that likely have tile drainage, blue represents poor drainage or areas without tile drainage, and white / gray represents areas with moderate drainage. The image shows red throughout the entire watershed, reinforcing the idea that tile drainage is widely distributed throughout the entire watershed and not focused in a small region or individual stream site.

A final factor that likely contributed to this method not detecting tile drainage, was that there was no control for precipitation in the scaling relationships. The results showed that there was spatial heterogeneity in precipitation (Table 4). Though precipitation events typically cover the entire study area, the precipitation totals vary by site, despite the fact that many sites are less than ten kilometers from each other. For example, recorded precipitation nearly triples between Sites 1-4 for Storm 15 (Table 4). Spatial variation in precipitation totals likely have an effect on peak discharge. If a site receives more precipitation than other nearby sites did, it would likely produce a larger peak discharge, thus producing a misleading upper outlier. The same is possible for sites that receive less precipitation and produce a misleading lower outlier.

Despite there not being any patterns within the outliers suggesting tile drain input, there did appear to be a few separate patterns within the summary tables of data. Site 3 appears to be an upper outlier repeatedly during tileflow conditions; it was an upper outlier three times during

early summer tileflow and twice during fall tileflow conditions (Table 7-9). During the no tileflow period, it was only above the scaling relationship once, during Storm 7. In the other storms during no-tileflow, the site was either not an outlier or an outlier that plotted below the scaling relationship.

It is not clear that tile drain inputs from outside the watershed are discharging into Money Creek and contributing to Site 3's outlier status. One possible explanation for this is the originally speculated conceptual pattern, that a large input of discharge from tile drains was entering the creek just upstream of Site 3. I explored this using ArcGIS to view satellite imagery of the area upstream of Site 3 overlain with the watershed boundaries. Very few fields within this section of the watershed extend outside of the watershed, and the area of the sections that extend outside the watershed is small in comparison to the size of the rest of the watershed (Fig. 61). It is possible that multiple fields could be draining into one large tile main, but I am not able to accept or reject this possibility based on the available data. Field observations during the winter when vegetation does not obstruct the view of tile drains, suggests that the area just upstream of Site 3 does not have an excessive amount of tile drains as compared to other areas of the watershed. Therefore, a large input of discharge from tile drains directly upstream of Site 3 is an unlikely explanation for the pattern of outliers that Site 3 displays.

Figure 61. An Aerial image showing the site 3 subwatershed and the western border of the Site 2 subwatershed. The creek flows from east to west. Notice that the total area of fields that exist both within and outside of the Site 3 watershed is limited.

It is unlikely that bias in the rating curve is the reason for the pattern of outliers that Site 3 displayed. Another possible explanation for the pattern of outliers at Site 3 is that the Storm 3 rating curve could potentially overestimate high discharge periods. However, not all high discharge events were associated with outliers at Site 3.

The outlier patterns of Site 3 could also be from spatial variation in precipitation totals across the watershed. One study in New Mexico found that partial storm coverage of the

watershed and rainfall variability resulted in the watershed's runoff response becoming more nonlinear (Goodrich et al, 1997). An additional study of a small 21.2 km^2 watershed in Mississippi found that peak discharges and drainage area scaled linearly because precipitation on the watershed was relatively uniform and the entire watershed contributed to runoff (Ogden et al, 2003). The Money Creek watershed is much larger at 77.1 km^2 and has heterogeneous precipitation totals associated with each storm across the watershed (Table 4). Because of this heterogeneity, an outlier in the scaling relationship may exist simply because that area of the watershed received more or less precipitation, and thus discharge, than other areas.

Another pattern noticed was that Site 5 was regularly an upper outlier for the majority of the year, until Storm 17 (Tables 8-10). Beginning on Storm 17, Site 5 is always a lower outlier for every subsequent storm. For this site, error and bias in the rating curve is a possible reason that Site 5 was an upper outlier for the majority of the year. The Site 5 rating curve overestimates discharge for its three highest measured discharge events. The measured discharge values are lower than what the rating curve model predicts them to be, so it would be reasonable to predict that storms with higher discharge than the highest measured value would also be overestimated (Fig. 16). All of the storms at Site 5 that had a stage of greater than one meter (eight storms) were upper outliers, while only two storms with stage less than one meter were an upper outlier (Storms 6 and 15). This reinforces the idea that Site 5 overestimates large discharge events. The Site 5 rating curve's inability to accurately predict high discharge events was the most likely reason that Site 5 was commonly an upper outlier.

A stream morphology change that occurred during Storm 17 appears to be the reason that Site 5 is a lower outlier for Storm 17, and every subsequent event. The late November storm, which produced 1.4 cm of rain at Site 5, but 3.0cm and 3.9cm at Sites 1 and 2, respectively,

appears to have caused a sudden drop in measured stage (Fig. 62). Signs of beavers have been observed in this watershed. This sudden drop in stage could have been the result of a beaver dam that burst downstream during the storm, thus suddenly lowering stage. Upon visual examination, there appeared to be a change in channel morphology from this drop in stage. The pressure transducer, which originally was at the streambed, was now around six inches above the surface of the streambed due to scouring. Originally, the streambed had a mixture of sediment near the bottom, now the streambed is just bare clay (Fig. 63 & 64). Storm 17 converted the area just downstream of the recording station from a straight stretch of stream into a ripple section with large cobbles and boulders, much of which appears to be from limestone blocks that were used to fill the area beneath the bridge during construction (Figs. 64 & 65).

I compared cross sections of where I measure discharge at Site 5 from before and after Storm 17. The cross-sectional area after Storm 17 had a substantially shallower depth due to cobbles and boulders filling in the stream channel. When the cross-sectional area was measured after Storm 17 it had an average depth of 0.2 meters, while at a similar stage before Storm 17 the cross section had an average depth of 0.9 meters. The scoured area just upstream at the pressure transducer, likely had an increase in cross-sectional area, which invalidated the rating curve. All subsequent measurements underestimated Site 5's discharge and caused Site 5 to be a lower outlier in all of the peak discharge scaling relationships. This sudden shift in discharge was obvious on all subsequent scaling relationships for this site after the streambed cross-sectional change. It should be noted that the stream banks, and possibly the streambed, just downstream of site five was regraded with an excavator to a consistent slope during this period (winter of 2016 / 2017). This could have caused this section of stream to be out of morphologic equilibrium, thus making it more vulnerable to rapid morphologic changes. This example

demonstrates that hydrologists can use scaling relationships as a supplemental tool to check for rating curve shifts due to changes in streambed morphology. In addition to Site 5, Sites 7 and 2 also experienced changes in their stream cross-sections during the study. This displays that stream cross-sections changes and scouring occur frequently in this watershed.

In summary, the method of looking at outliers within scaling relationships did not appear to be effective at detecting tile drain input. This was likely due to a number of separate underlying technicalities and theoretical flaws within the methodology. Despite not observing the expected pattern with the outlier data, there were a couple of patterns within the data (Sites 3 and 7) as the result of various phenomena.

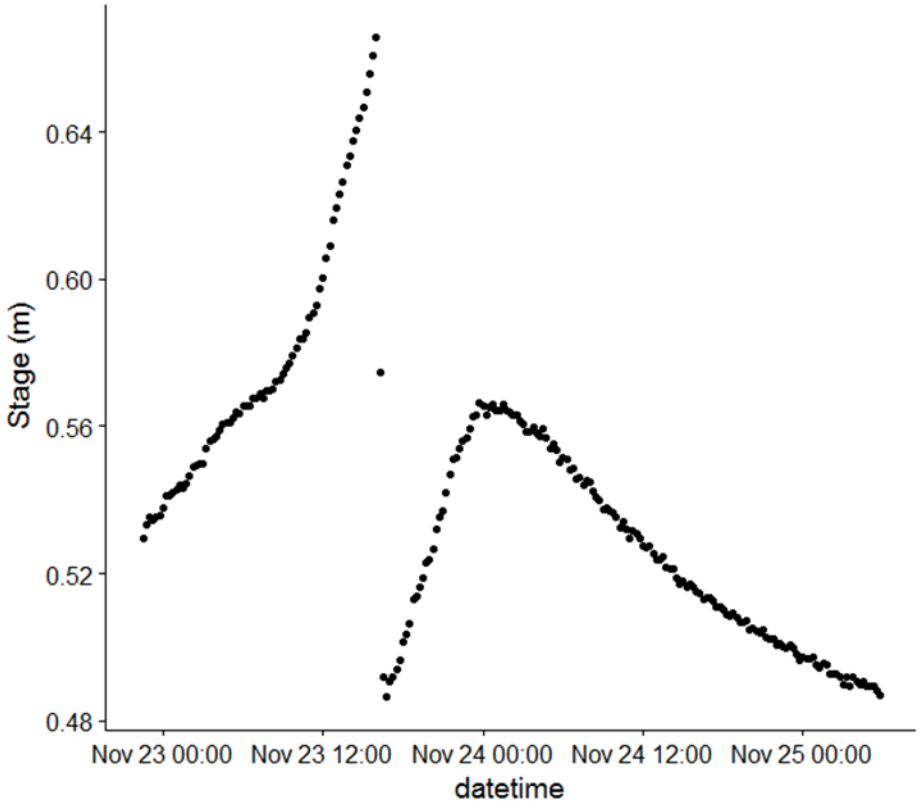

Figure 62. Stage hydrograph of Site 5 during Storm 17. The sudden drop in stage is possibly the result of a beaver dam that burst downstream during the storm.

Figure 63. Picture of site 5 before storm 17. Notice the ripple section is not present.

Figure 64. Streambed scouring and bare clay beneath the pressure transducer at Site 5 after Storm 17. Note the transition from the scoured pool section of the stream to the run with larger cobbles and boulders.

Figure 65. The streambed morphology changed after Storm 17. The storm moved cobbles and boulders, from near the pressure transducer and bridge, downstream to the area with ripples. This invalidated the rating curve at Site 5 for any measurement after the morphologic change.

Outliers in the Mean Baseflow Scaling Relationships

I created three scaling relationships that plotted the drainage area against the mean baseflow. The first scaling relationship is from tileflow conditions during the early summer, the second is from no tileflow conditions, and the third is from tileflow conditions during the fall and winter (Tables 8-10). Interestingly, there seems to be limited overlap between outliers that occurred during baseflow conditions with outliers that occurred during storm events. For example, the outliers during the early summer tileflow period were Sites 4 and 6. Neither of these were outliers during any of the storm events during that same period. The two examples of overlap between outliers during baseflow conditions and outliers during storm events, is Site 3 in the no-tileflow period and Site 3 in the fall / winter tileflow period. Rating curve bias could be a factor in this, but it is difficult to conclude on a reason for why any particular site would be an outlier.

Additionally, the early summer and fall / winter baseflow scaling relationships both have more common outliers with the no-tileflow period than they do with each other (Tables 8-10). Site 6 is a lower outlier during the early summer tileflow and no-tileflow periods, and Sites 2 and 3 are outliers during the no-tileflow and fall/winter tileflow season. The two tileflow periods share no common outliers. A potential explanation for this is that the no-tileflow period may be representing a transition zone between separate seasons in the watershed, which appear to bear particular outliers.

Coefficients of the Scaling Relationships

A scaling exponent of one implies that runoff is evenly distributed into a stream throughout the watershed. A scaling exponent of less than one signifies that proportionally less runoff is entering the stream in the lower watershed than in the upper watershed, while a scaling

exponent greater than one signifies that more runoff is entering the stream in the lower watershed than in the upper watershed (Galster, 2007). The scaling exponent means at Money Creek were statistically different between tileflow and no-tileflow, 1.109 and 0.86, respectively. This indicates that proportionately less runoff was contributed by the downstream watershed drainage area during no-tileflow period storms; while proportionally more discharge was contributed by the downstream watershed drainage area during tileflow period storms.

Overall, these means were both larger than what the literature would suggest. One study found a nationwide range of regional averages to be 0.4 – 0.9, and the region that Money Creek exists in was found to have an average of 0.63 (Winton and Criss, 2016). However, other national studies have found wider ranges, such as 0.3 – 1.6 (Kroll et al, 2014). Though the scaling exponent means at Money Creek were surprisingly high, it is important to remember that it is just from an individual stream, rather than an average taken across many streams in this region. Studies have shown individual streams to have a widely varying scaling exponent for each individual storm event (Lee et al, 2009; Galster et al, 2006).

These high means could potentially be an indication of anthropogenic influence in the Money Creek watershed. Studies have found that it is rare for watersheds to naturally have scaling exponents greater than one. For example, a study of the little Lehigh Creek watershed, a 254 Km^2 watershed in Pennsylvania, had an average scaling exponent of 1.81 (Galster, 2006). The scaling exponent was greater than one because the upper part to the watershed was a forested region, while the lower part of the watershed was an urban region. Impervious surfaces in the urban region allowed for greater runoff in the lower section of the watershed than the forest allowed in the upper region of the watershed, allowing the scaling exponent to become larger than one. The Money Creek watershed used in this study has an almost entirely

agricultural land cover, though agricultural land use or tile drainage, could potentially be increasing runoff in the lower section of the watershed.

The Image from a remote sensing project shows that, qualitatively, the lower section of the watershed has a greater concentration of red shading, while the upper watershed part of the watershed has a greater concentration of blue or white / grey shading (Appendix A). This suggests that the lower section of the watershed has more tile drainage, while the upper watershed is more poorly drained. More tile drainage in the lower watershed would have the effect of increasing the scaling exponent value, which corresponds the high scaling exponent values seen in this watershed. The high scaling exponents in the Money Creek Watershed may simply be the result of spatial variation of tile drainage throughout the watershed.

The pattern of scaling exponents seen during storm scaling relationship was similar to the mean baseflow scaling relationships as well. The scaling exponent during tile flow in early summer and fall / winter, were 0.996 and 1.112, respectively. The no tileflow scaling exponent was 0.93. These values are more consistent with the literature, as a study found the regional average for mean discharge to be 0.98 in Money Creek's physiographic region (Winton and Criss, 2016).

In summary, the scaling relationship coefficients in Money Creek are higher than expected. This may be the result of a higher concentration of tile drainage in the downstream section of the watershed that allows better drainage and more runoff to be transported to the stream.

Patterns in Coefficients during Tileflow and No-tileflow

A nationwide study of scaling exponents in United States' rivers, ranging in drainage area of 1 km^2 - 100,000 km^2, found that higher scaling exponents tended to occur in regions with

limited sunshine and low evapotranspiration, while lower scaling exponents tend to occur in regions with abundant sunshine, and high evapotranspiration (Winton and Criss, 2016). The tileflow period at Money Creek occurs during times of the year where sunshine and evapotranspiration are lower. The no-tileflow season occurs during the middle of the summer, a time of the year that has relatively high sunshine and evapotranspiration, consistent with the lower scaling coefficient during this period.

An additional study of 9,322 gauging stations across the United States showed that the scaling exponent is lower when precipitation is lost to soil moisture storage and evapotranspiration (Medhi and Tripathi, 2015). During the no-tileflow period at Money Creek, evapotranspiration is higher than precipitation and there is a net loss of soil moisture. This means that precipitation often is evapotranspired or stored in soil before it can reach Money Creek, which leads to a lower scaling exponent. Ultimately, conditions that cause lower scaling exponents and no-tileflow conditions likely coincide with the summer, rather than there being a causal relationship between no-tileflow periods and lower scaling exponents. The same factors that the literature has shown to cause regional differences in scaling relationships also appear to cause seasonal differences in scaling relationships in the Money Creek watershed. A larger dataset with more scaling exponents would be beneficial to provide more confidence in interpretations and to gain more insight into the phenomenon that the means between tileflow and no-tileflow are statistically different.

Peak Discharges during Tileflow and No-tileflow

Peak discharges have the potential to be higher during the tileflow period because baseflow is higher during the tileflow period than during the no-tileflow period. If a section of stream has the same magnitude storm event during tileflow as during a no tileflow period, all

other variables aside, the tileflow event would have a larger peak discharge, because the starting baseflow is larger than during no-tileflow. The majority of the largest discharge events did occur during tileflow periods, but this does not mean that tileflow events unequivocally have higher discharge than no tileflow events. For example, Storm 8 at Site 7, 2.79 m^3s^{-1}, occurred during the no-tileflow period, yet is the largest discharge event at Site 7 (Fig. 27). Storm 9, 1.66 m^3s^{-1}, occurred during the no-tileflow period and was also a large storm event. If this same magnitude of storm occurred in June during the tileflow period, it would have likely exceeded the discharge of Storm 1, 1.79 m^3s^{-1}, and have been an even larger event. However, because baseflow is so low during the no tileflow period, it is a smaller event than Storm 1.

There was a shift in baseflow by season in the hydrographs. This shift particularly stands out at Site 7 (Fig. 27). During the early summer tileflow period, late May and June, baseflow was much higher than it was for the rest of the year - around 0.5 m^3s^{-1}. By the end of June, baseflow began to rapidly decrease to around 0.2 m^3s^{-1}, and the stream quickly entered the no-tileflow period by July 7. By the beginning of August, baseflow went to its lowest of the year and approached a discharge of zero. Around September 15, Money Creek re-entered into a tileflow period. Though baseflow was never as high as it was in early June, baseflow remained above levels seen in August, despite lengthy periods between storm events. Additionally, recession curves after storms were much less steep than those in the no-tileflow period. Ultimately, the shift in baseflow throughout the seasons influences the peak discharge of a storm event. Higher baseflow promotes higher peak discharge events.

Hydrologic Conditions during Tileflow and No-tileflow

I hypothesized that double or extended peaks would exist during tileflow season due to the differences in timing between when overland flow and tile drainage enters the stream. Additionally, I expected that the double and extended peaks would disappear during the no-tileflow period. There are many dual peaks and extended peaks throughout the study period (36.9%), but these peaks did not appear to be restricted to tileflow conditions (Tables 10-12). Besides tile drainage, an additional cause for double peaks in a hydrograph is precipitation patterns. One mechanism for this would be if there were a storm with multiple bouts of rain, with a period between the rounds that had no, or much lower intensity of, rain. Additionally, variation in precipitation between different areas in the watershed could cause double peaks or extended peaks in a hydrograph. For example, if an upstream site received very heavy rainfall and a downstream site received a much lesser amount of rainfall, the sudden pulse of water from the upstream site could create a double peak or extended peak in the hydrograph.

It is not possible to completely answer this research question due to the lack of precipitation data in the watershed. I did not deploy rain gauges at each site until September 23, so it is not possible to determine whether double peaks before that time are precipitation or tile drain induced. Regional precipitation data do not provide the necessary precision needed to evaluate site-specific double peaks. I examined data from these rain gauges to try to identify if double or extended peaks from Storms 16 - 22 were from tile drainage or variation in precipitation. The summary table shows that for the period where rain gauge monitoring occurred, there were double and extended peaks seen in all storms, except Storm 20 (Table 13). Intermittent precipitation and tile drains can explain these double peaks, while some have an unknown cause.

Intermittent precipitation is one possible explanation for many of the double or extended peaks seen. An example of a double peak caused by intermittent precipitation is the double peak seen at Site 1 during Storm 17 (Fig. 66). The hydrograph shows an initial peak on the morning of the 23rd of November. Afterwards, the discharge starts to decrease slowly. Six hours later the discharge starts to increase and eventually reaches to a second peak. The pattern seen in the hydrograph matches the pattern seen in the precipitation gauges. The precipitation gauge shows an initial event during the night of the 22nd and the early morning of the 23rd (Fig. 67). There is a six-hour gap with minimal precipitation. A second wave of precipitation begins at 7 am on November 23rd. These two rounds of precipitation correspond to the peaks seen in the hydrograph. This leads me to conclude that the double peak seen at Site 1 during Storm 17 was the result of an intermittent participation pattern. Many of the other storm events across all sites that have double or extended peaks show a similar correspondence between the hydrograph and precipitation data.

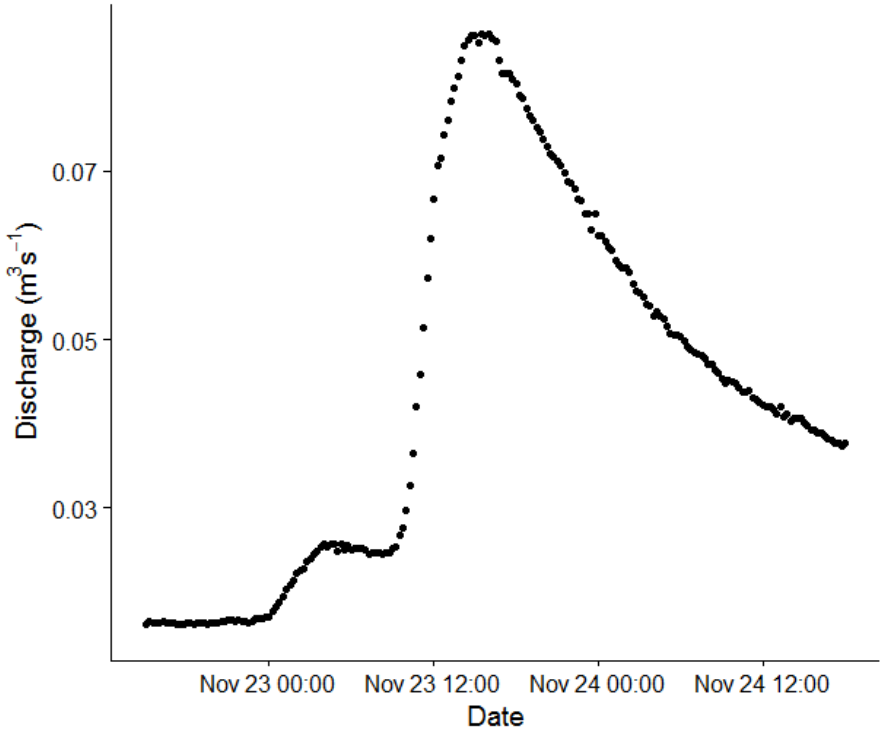

Figure 66. Hydrograph of Site 1 during Storm 17.

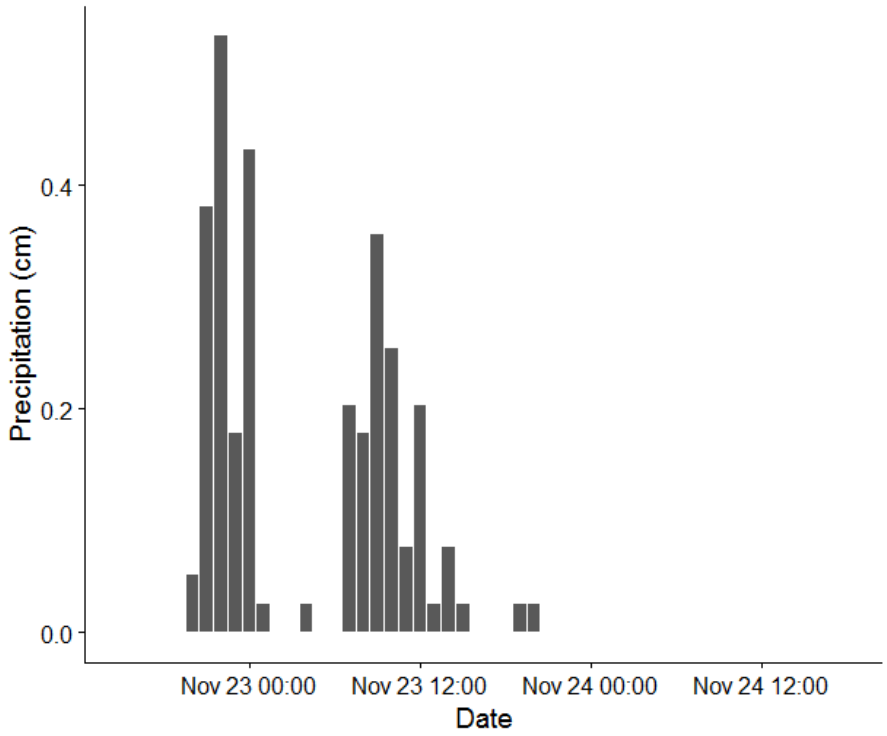

Figure 67. Hourly Precipitation data for Site 1 during Storm 17.

A fascinating phenomenon was observed during this two round storm event. Despite getting a similar amount of precipitation during the first and second rounds of precipitation (1.6 cm and 1.4 cm, respectively) the second round of precipitation caused a much greater increase in the hydrograph. This supports the idea that precipitation that occurs when soil is saturated will cause a greater spike in the hydrograph than a similar event that occurs when the soil is unsaturated. The first storm caused a small spike in the hydrograph, but occurred on what was presumably unsaturated soil. The previous major storm event occurred twenty days earlier on the 3rd of November. The unsaturated soil likely collected much of the water and was able to dampen the effect that the precipitation had on the hydrograph. Despite the second precipitation event being a similar quantity to the first round, it produced a much larger spike in the hydrograph, because the previous round of precipitation that occurred six hours earlier had saturated the soil. This meant that most of the precipitation from the second storm was runoff that went directly into the stream and caused a much larger spike in the hydrograph.

During Storm 21 in January, Sites 1-8 exhibited a second small peak or an extended peak during the falling limb of the hydrograph. All eight sites had this same affect and none displayed any precipitation that could contribute this second or extended peak. For example, in the hydrograph of Site 2, during the falling limb of the storm on January 18th, there was a small sudden increase in discharge until around January 19th, when the falling curve continues to decrease (Fig. 68). The rain gauge data showed the initial precipitation associated with the storm, but there was no precipitation on January 18th during the time of the second peak that could have caused this increase in discharge (Fig. 69). This small second peak is probably the result of tile drains in the stream. After the initial surge of water, the hydrograph started to recede. By January 18th precipitation from the storm on January 16th and 17th could have

percolated through the glacial till, allowed through unseasonably warm temperatures, and raised the head of the groundwater table. This would causes a sudden increase in the discharge flowing through tile drains into the creek. As the hydrograph recedes to a certain stage the influx of discharge from the tile drains cause the discharge in the stream to have a small second peak or to flat-line for a period of time. Though baseflow could also be playing a factor in this, it is more likely that hydraulic conductivity in the surrounding soil is too low to solely manifest an extended peak, and almost certainly not a second peak. The tile drains act as hydrologic "superhighways" that allow groundwater to quickly travel through fields and enter the stream, thus causing a double or extended peak.

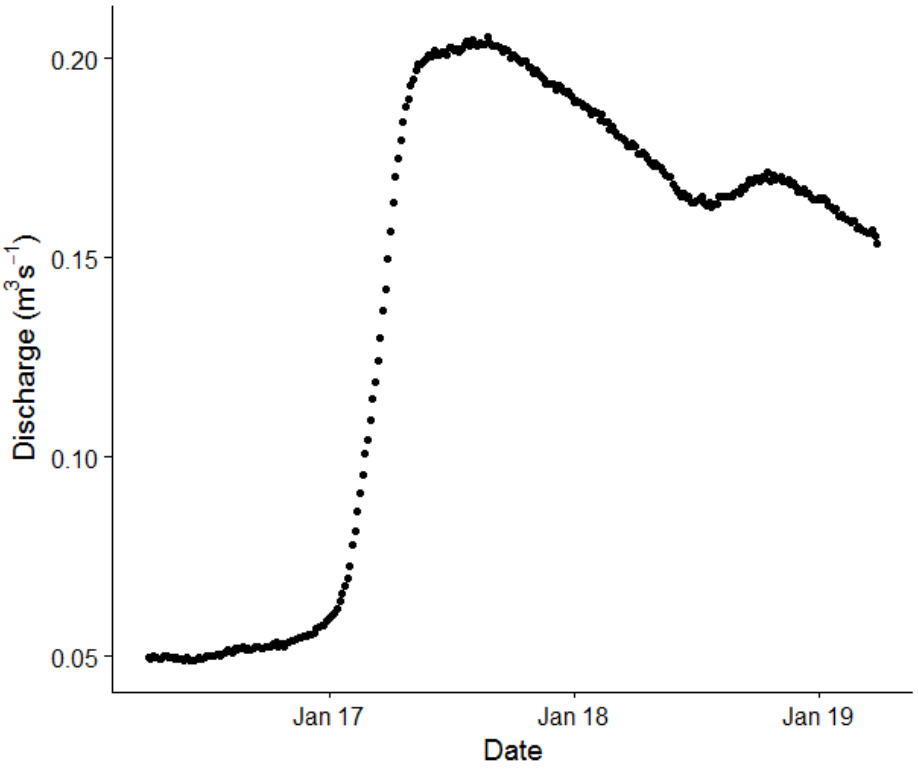

Figure 68. Hydrograph of Site 2 during Storm 21.

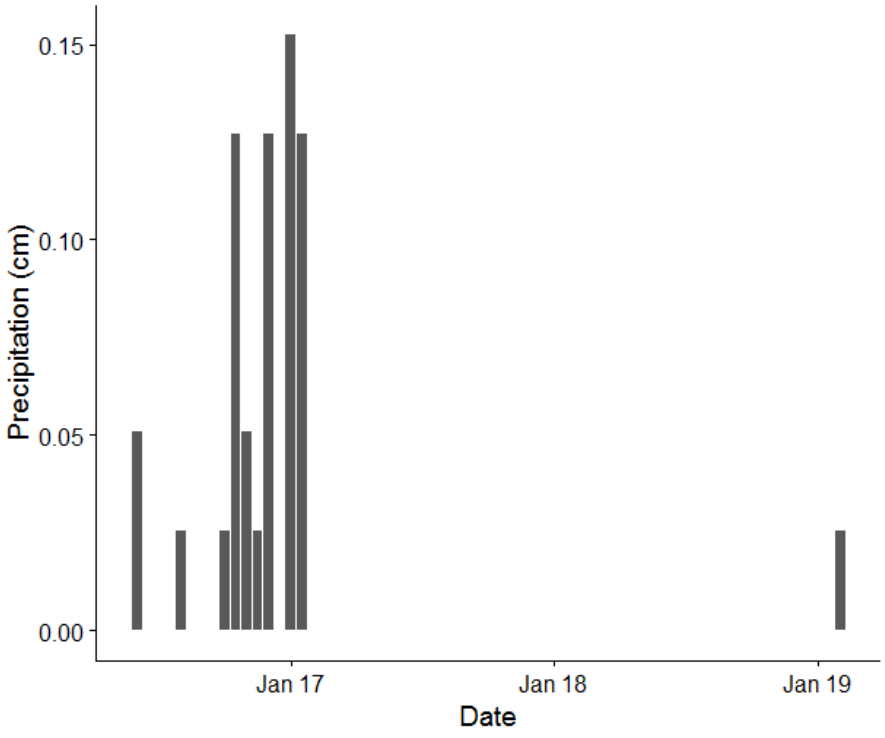

Figure 69. Hourly Precipitation data for Site 2 during Storm 21.

Double peaks caused by intermittent precipitation often occur during the raising limb of the storm, while double peaks caused by tile drains often occur during the falling limb. This is likely related to the fact that a second round of precipitation will often cause a larger peak discharge than the first round, due to soil being saturated from the first round of precipitation. Conversely, water that enters a stream from tile drains will likely enter the stream during the falling limb, because tile drain water is slower to enter the stream because it first needs to infiltrate the soil (Birkinshaw, 2008). These properties are why there is the pattern of dual peaks from intermittent precipitation often occurring on the rising limb, while dual peaks caused from tile drains often occur during the falling limb.

While most double peaks were explained by intermittent precipitation or tile drains, there are five sites during Storm 16 that have a large double peak, and no obvious cause. The falling limb of the hydrograph during Storm 16, on November 3rd at 11 a.m., shows a sudden spike in the hydrograph and the discharge at Site 4 goes from 0.55 m3s-1 to 0.93 m3s-1 in an hour and a half (Fig. 70). This double peak first appears at Site 3 and translates down through the rest of the stream sites. The last precipitation during this storm event occurs during the evening of November 2nd and there is a subsequent 18-hour period without precipitation (Fig. 71), so the double peak on Sites 3-8 have no corresponding precipitation. Tile drains are not likely the cause of this double peak, because this peak is so sudden and dramatic, while a double or extended peak caused by tile drains would likely be more subtle and would likely not have the necessary input of water to cause discharge to increase so drastically and to such large magnitude. Thus, it is possible that there was some large and instantaneous input of water between Sites 2 and 3 around 11am on November 3rd, because the double peak does not manifest at Site 2 and first occurs at Site 3. It could possibly be from a dammed drainage ditch

that was suddenly overtopped and released into the stream. As the drainage area between Sites 2 and 3 is entirely agricultural, the sudden pulse of water could have an anthropogenic origin. Ultimately, this sudden rise in the hydrograph is not seen during any other storm events, and the reason is unclear.

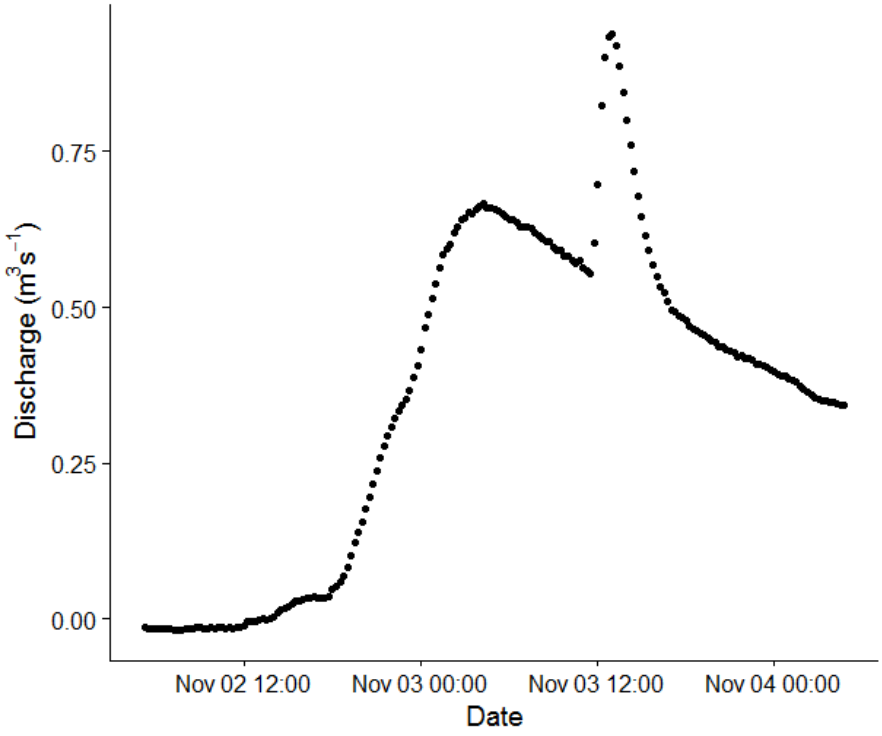

Figure 70. Hydrograph of Site 4 during Storm 16.

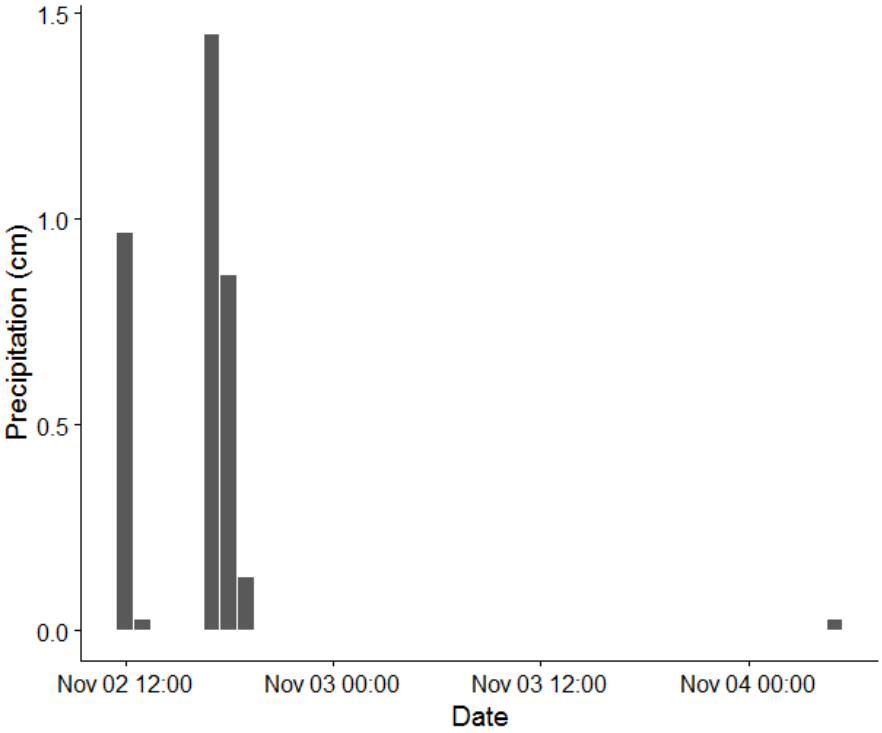

Figure 71. Hourly Precipitation data for Site 4 during Storm 16.

In Short, double and extended peaks occurred during 36.9% of storms and throughout the entire study period. It was interpreted that the two primary origins of them were intermittent precipitation and the lag time of water input associated with the difference in timing between overland flow and tile drainage.

Scaling Relationships in Small Human-modified Streams with Tile Drainage

This study is unique in that it is the first study to apply scaling relationships to a small human-modified stream with tile drainage. Previous hydrologic studies have primarily focused on larger streams, and those that focused on smaller streams were located in forested or arid regions, rather than an agricultural region. Despite the uniqueness of this study, Money Creek is typical in many regards. In the Midwest, most rivers are fed through a series of tributaries much like Money Creek. These tributaries are small, often modified by humans, and located in agricultural regions that employ tile drainage. Because of the uniqueness of this research, this study brought to forefront a number of unique challenges and characteristics of this system.

Though Money Creek is located in a rural area, it would be misguided to think that it is natural or unmodified by humans. Humans have modified much of the upper section of Money Creek into a channelized stream with a trapezoidal cross-section. This stream channelization in conjunction with tile drainage keeps the water table from becoming too high and allows excess precipitation to be quickly removed from the system, allowing for optimal crop production.

An important result of this research was the high frequency of stream scouring and changing cross-sections within the stream channel (Sites 2, 5, and 7). Though this presents a challenge in creating robust rating curves, it also highlights an important and surprising phenomenon. General wisdom supports the idea that Money Creek would not have frequent

channel scouring or changing stream cross-sections; because it is a small stream within a region with little topographic relief, and thus does not have the potential energy required to cause frequent scouring or cross-sectional changes. Human modification through tile drainage and stream channelization has produced a very flashy stream because runoff is quickly transported to the stream and rapidly moved downstream, thus producing high discharge runoff events that can be multiple orders of magnitude larger than baseflow (Figs 21-28). These large discharge events provide the energy necessary to cause scouring and cross-sectional changes in the stream. Additionally, a study at Little Kickapoo Creek, a similar stream in the same county as Money Creek, found that the streambed was dominated by fine grained sediment, which allowed for a more mobile streambed than seen within mountain streams (Peterson et al, 2008). A final aspect to consider is that a channelized stream may be out of morphologic equilibrium, and more prone to erosion or scouring. Ultimately, scouring and cross-sectional changes to Money Creek are largely the result of human modification.

Human modification is also responsible for the double peaks from tile drainage observed in this study. Lag-time between overland flow and tile drainage caused these double peaks. Ultimately, the origin of this lag time was human modification, thus creating a system that can have lag time between overland flow and tileflow, rather than the natural system with would have had unimodal runoff.

The primary focus of this study was looking at peak discharge scaling relationships. The results of the study, such as the double peaks caused from tile drainage, suggest that tile drains are most dominant on the recessional limb of the hydrograph. Therefore, future studies that want to examine how tile drains affect stream hydrology should focus on the recessional limb of the hydrograph

CHAPTER V: CONCLUSION

I created scaling relationships, of discharge and drainage area, for each storm event and the mean baseflow of the different tileflow periods during the study. Overall, this method was not effective for detecting tile drain input into Money Creek, because there were not major differences in the outliers of the scaling relationships between the tileflow and no-tileflow periods. Patterns in the data suggest that outliers may exist due to heterogeneous precipitation patterns. Additionally, the study shows that streambed morphology in the study region is dynamic, as three of eight sites had cross-sectional changes caused from storm events during this study. The scaling relationships proved an effective supplementary tool to detect changes in stream-cross sections.

The scaling exponent means between the tileflow and no-tileflow period were statistically different. This is likely because, factors that studies have shown to cause regional differences in scaling exponents (evapotranspiration, soil moisture storage, and sunshine) are causing seasonal differences in the scaling exponent within the Money Creek watershed. Analysis of the hydrograph showed that peak discharges have the potential to be higher during the tileflow period, because baseflow is higher.

36.9% of storms had double or extended peaks. Though a comparison between tileflow and no-tileflow was not possible due to limited precipitation data, I observed examples of double peaks from intermittent precipitation and tile-drains from available data.

REFERENCES

Alexander, G.N., 1972, Effect of catchment area on flood magnitude: Journal of Hydrology, v. 16, no. 3, p. 225-240, doi: 10.1016/0022-1694(72)90054-6.

Billy, C., Birgand, F., Sebilo, M., Billen, G., and Tournebize, J., 2011, Nitrate dynamics in artificially drained nested watersheds: Physics and Chemistry of the Earth, v. 36, no. 12, p. 506-514, doi: 10.1016/j.pce.2008.09.007.

Birkinshaw, S., 2008, Physically-based modelling of double-peak discharge responses at Slapton Wood catchment: Hydrological Processes, no. 10 v. 22, p. 1419-1430, doi: 10.1002/hyp.6694.

Blann, K., Anderson, J., Sands, G., and Vondracek, B., 2009, Effects of Agricultural Drainage on Aquatic Ecosystems: A Review: Critical Reviews in Environmental Science and Technology, v. 39, no. 11, p. 909-1001, doi: 10.1080/10643380801977966.

Breitburg, D., 2002, Effects of hypoxia, and the balance between hypoxia and enrichment, on coastal fishes and fisheries: Estuaries, v. 25, no. 4b, p. 767-781, doi: 10.1007/BF02804904.

Brown, T., and Froemke, P., 2012, Nationwide Assessment of Nonpoint Source Threats to Water Quality: Bioscience, v. 62, no. 2, p. 136-146, doi: 10.1525/bio.2012.62.2.7.

Christianson, L.E., and Harmel, R.D., 2015, The MANAGE Drain Load database: Review and compilation of more than fifty years of North American drainage nutrient studies: Agricultural Water Management, v. 159, p. 277-289, doi: 10.1016/j.agwat.2015.06.021.

David, M., Drinkwater, L., Mclsaac, G., and McIsaac, G., 2010, Sources of nitrate yields in the Mississippi River Basin: Journal of Environmental Quality, v. 39, no. 5, p. 1657-1667, doi: 10.2134/jeq2010.0115.

David, M., Gentry, L., Kovacic, D., and Smith, K., 1997, Nitrogen balance in and export from an agricultural watershed: Journal of Environmental Quality, v. 26, no. 4, p. 1038-1048, doi: 10.2134/jeq1997.00472425002600040015x.

Furey, P., and Gupta, V., 2005, Effects of excess rainfall on the temporal variability of observed peak-discharge power laws: Advances in Water Resources, v. 28, no. 11, p. 1240-1253, doi: 10.1016/j.advwatres.2005.03.014.

Galster, J., Pazzaglia, F., Hargreaves, B., Morris, D., and Peters, S., 2006, Effects of urbanization on watershed hydrology: The scaling of discharge with drainage area: Geology, v. 34, no. 9, p. 713-716, doi: 10.1130/G22633.1.

Galster, J., 2007, Natural and anthropogenic influences on the scaling of discharge with drainage area for multiple watersheds: Geosphere, v. 3, no. 4, p. 260-271, doi: 10.1130/GES00065.1.

Goodrich, D., Lane, L., Shillito, R., Miller, S., and Syed, K., 1997, Linearity of basin response as a function of scale in a semiarid watershed: Water Resources Research, v. 33, no. 12, p. 2951-2965, doi: 10.1029/97WR01422.

Gupta, V.K. and Waymire, E.C., 1998, Spatial variability and scale invariance in hydrologic regionalization: in Sposito, G., ed., Scale dependence and scale invariance in hydrology: p. 88-135.

Hatfield, J., and Follett, R., 2008, Nitrogen in the Environment: Sources, Problems, and Management, 2nd Edition: San Diego, Elsevier Academic Press Inc., p. 1-702, doi: 10.1100/tsw.2001.269.

Hirose T, Onda Y, Matsukura Y., 1994, Runoff characteristics and solute concentration on four small catchments with different bedrocks in the Abukuma mountains Japan: Transactions Japanese Geomorphological Union 15A: 31-48.

Ikenberry, C., Soupir, M., Schilling, K., Jones, C., and Seeman, A., 2014, Nitrate-nitrogen export: magnitude and patterns from drainage districts to downstream river basins: Journal of Environmental Quality, v. 43, no. 6, p. 2024-33, doi: 10.2134/jeq2014.05.0242.

Kladivko, E.J., Frankenberger, J.R., Jaynes, D.B., Meek, D.W., Jenkinson, B.J., and Fausey, N.R., 2004, Nitrate leaching to subsurface drains as affected by drain spacing and changes in crop production system: Journal of Environmental Quality, v. 33, no. 5, p. 1803-13, doi: 10.2134/jeq2004.1803.

Kroll, C.N., Rapant, D.F., and Vogel, R.M, 2014, The prediction of hydrologic statistics in nested watersheds across the United States: Water Environmental and Water Resources Congress (ASCE, Portland, Oregon), p. 2326-2335.

Lakey, B., and Krothe, N., 1996, Stable isotopic variation of storm discharge from a perennial karst spring, Indiana: Water Resources Research, v. 32, no. 4, p. 721-731, doi: 10.1029/95WR01951.

Lee, K., Chen, N., and Gartsman, B., 2009, Impact of stream network structure on the transition break of peak flows: Journal of Hydrology, v. 367, no. 3, p. 283-292, doi: 10.1016/j.jhydrol.2009.01.021.

Lemke, A.M., Kirkham, K.G., Lindenbaum, T.T., Herbert, M.E., Tear, T.H., Perry, W.L., and Herkert, J.R., 2011, Evaluating agricultural best management practices in tile-drained subwatersheds of the Mackinaw River, Illinois: Journal of Environmental Quality, v. 40, no. 4, p. 1215-1228, doi: 10.2134/jeq2010.0119.

Medhi, H., and Tripathi, S., 2015, On identifying relationships between the flood scaling exponent and basin attributes: Chaos, v. 25, no. 7, p. 075405-075405, doi: 10.1063/1.4916378.

Ogden, F., and Dawdy, D., 2003, Peak discharge scaling in small hortonian watershed: Journal of Hydrologic Engineering, v. 8, no. 2, p. 64-73, doi: 10.1061/(ASCE)1084-0699(2003)8:2(64).

Onda, Y., Komatsu, Y., Tsujimura, M., and Fujihara, J., 2001, The role of subsurface runoff through bedrock on storm flow generation: Hydrological Processes, v. 15, no. 10, p. 1693-1706, doi: 10.1002/hyp.234.

Patterson, C.J., Hansel, A.K., Mickelson, D.M., Quade, D.J., Bettis III, E.A., Colgan, P.M., McKay, E.D., Stumpf, A.J., 2003, Contrasting glacial landscapes created by ice lobes of the southern Laurentide Ice Sheet: in Easterbrook, D.J., ed., Quaternary Geology of the United States, INQUA 2003 Field Guide Volume, Desert Research Institute, Reno, NV, p. 135-153.

Peterson, E. W., Sickbert, T. B., and Moore, S. L., 2008, High frequency stream bed mobility of a low-gradient agricultural stream with implications on the hyporheic zone: Hydrological Processes, v. 22, no. 21, p. 4239-4248, doi:10.1002/hyp.7031.

Powlson, D., Addisott, T., Benjamin, N., Cassman, K., de Kok, T., Addiscott, T., van Grinsven, H., L'Hirondel, J., Avery, A., and van Kessel, C., 2008, When does nitrate become a risk for humans?: Journal of Environmental Quality, v. 37, no. 2, p. 291-5, doi: 10.2134/jeq2007.0177.

Randall, G.W., Goss, M.J., Follett, R.F., and Hatfield, J.L., 2008, Nitrate Losses to Surface Water Through Subsurface, Tile Drainage: in Nitrogen in the Environment: Sources, Problems, and Management, 2nd Edition: San Diego, Academic Press, p. 145-175, 10.1016/B978-0-12-374347-3.00006-8.

Skaggs, R., Breve, M., and Gilliam, J., 1994, Hydrologic and Water-Qualtiy Impacts of Agricultural Drainage: Critical Reviews in Environmental Science and Technology, v. 24, no. 1, p. 1-32, doi: 10.1080/10643389409388459.

Stewart, W., Dibb, D., Johnston, A., and Smyth, T., 2005, The contribution of commercial fertilizer nutrients to food production: Agronomy Journal, v. 97, no. 1, p. 1-6, doi: 10.2134/agronj2005.0001.

Sugg, Z., 2007, Assessing U.S. Farm Drainage: Can GIS Lead to Better Estimates of Subsurface Drainage Extent?: World Resources Institiute, p. 1-8.

Tiemeyer, B., Kahle, P., and Lennartz, B., 2010, Designing Monitoring Programs for Artificially Drained Catchments: Vadose Zone Journal, v. 9, no. 1, p. 14-24, doi: 10.2136/vzj2008.0181.

Williams, M.R., King, K.W., and Fausey, N.R., 2015, Contribution of tile drains to basin discharge and nitrogen export in a headwater agricultural watershed: Agricultural Water Management, v. 158, p. 42-50, doi: 10.1016/j.agwat.2015.04.009.

Winston, W., and Criss, R., 2016, Dependence of mean and peak streamflow on basin area in the conterminous United States: Journal of Earth Science, v. 27, no. 1, p. 83-88, doi: 10.1007/s12583-016-0631-6.

Yang, Y., Endreny, T., and Nowak, D., 2015, Simulating Double-Peak Hydrographs from Single Storms over Mixed-Use Watersheds: Journal of Hydrologic Engineering, v. 20, no. 11, doi: 10.1061/(ASCE)HE.1943-5584.0001225.

APPENDIX A: ADDITIONAL IMAGES

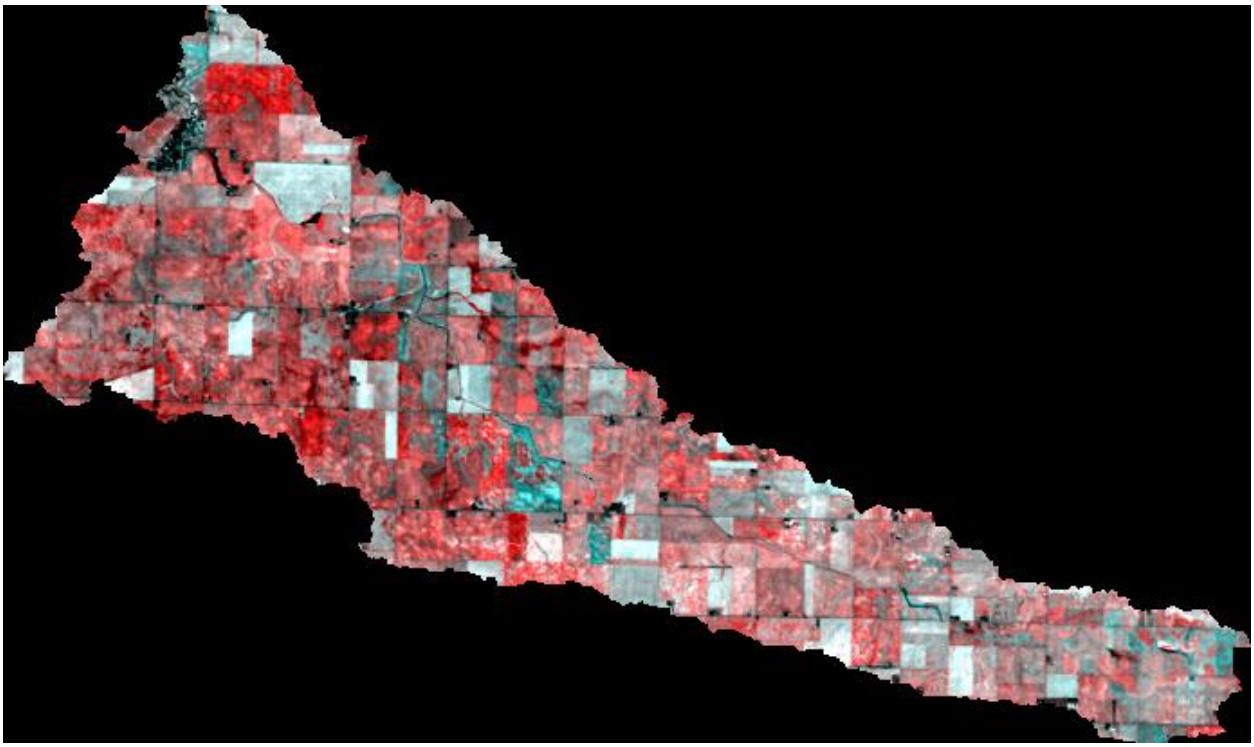

Figure A – 1. Map produced through remote sensing project.

APPENDIX B: REMOTE SENSING POWER POINT PRESENTATION

Using Remote Sensing to Find Tile Drained Fields in Money Creek Watershed

AUDREY HAPPEL
RYAN PLATH
ROMEO AKARA
ANDREW JENNINGS

Introduction

- Central Illinois is a region that has extensive agricultural land use
- Many of these fields are tiled in order to lower water table and prevent plants from being flooded
- These tiles drain water contaminated with agricultural runoff
- This runoff effects water supplies locally and internationally

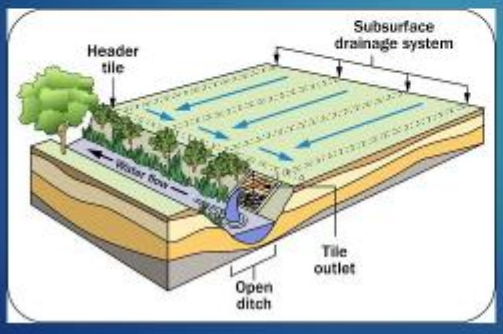

Water Quality

- Water quality improvements have been made since the passing of the Clean Water Act
- Non-point source pollution reduction has lagged behind point source pollution reduction (Brown and Froemke, 2012)
- There is now much focus on water quality improvement in agricultural areas

Regional and international Impacts

- Nitrate Loads eventually drain through the Mississippi River to the Gulf of Mexico and result in a hypoxic zone
- These hypoxic zones exist in many areas where major river systems enter an ocean, such as the Baltic and Adriatic seas (Tiemeyer et al., 2010)

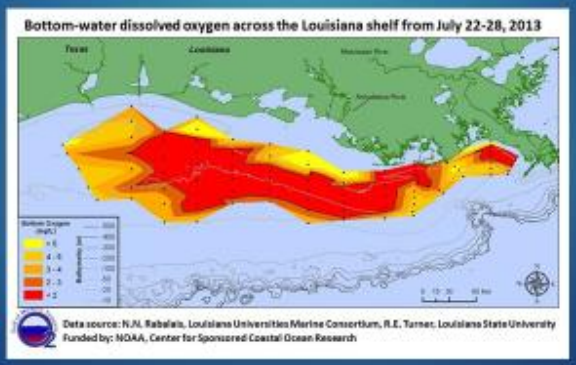

Local Impacts

- Agricultural regions often struggle to keep surface drinking water below the EPA drinking water standard of 10 mg/L (Hatfield and Follett)
  - This standard is set due to "blue baby syndrome", in which hemoglobin does not does circulate enough oxygen through newborns (Powlson et al., 2008)
  - Long term effects are not fully understood, but recent studies seem to show a link with bladder and gastric cancer (Oregon DEQ)

Purpose of study

- Attempt to determine fields that are tile drained, with the use of remote sensing

How

- Look at shortwave bands (**Band 5**) of images before and after a rain event
- Soil has:
  - Higher band 5 reflectance when dry
  - Lower band 5 reflectance when wet
- Dry fields after a storm are more likely to have tile drainage

Data Sources

- Landsat-5 and Landsat-7
  - Row 23 Path 32
- Dates used were April 2, 2003 and April 11, 2003
  - Intermittent precipitation from April 3-7

Study Location

- Upper Money Creek watershed ~40 mi^2 (~ 12 miles of creek that cover ~ 60% of the watershed)
- Land cover: agricultural
- Geology : Wisconsin age glacial till

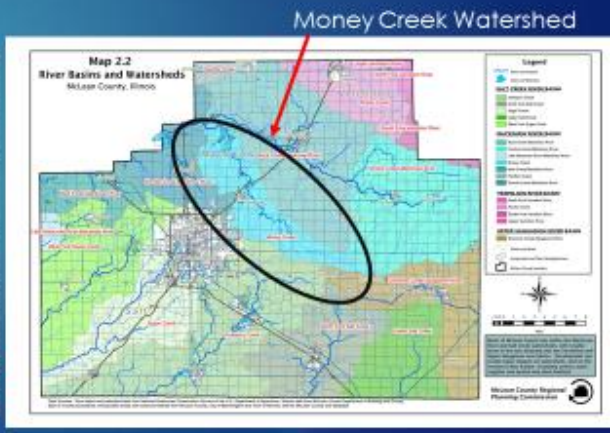

Methods

- Step 1- Dark Object Subtraction
- Step 2- Spatial subset for Money Creek Watershed
- Step 3- Mixed raster image for band 5 of the two images
- Step 4- Image differencing, Landsat 5 image first, Landsat 7 image second
- Step 5- Built mask of watershed
- Step 6- Data Analysis

Step 1

- Dark Object Subtraction
- Image is stretched to linear 1%

Step 2

- Spatial subset of Money Creek Watershed
  - Removed unnecessary Landsat data

Step 3

- Mixed Raster image for **band 5** of the two selected images
  - Image 1 = red
  - Image 2 = Green and blue

Step 4

- Image Differencing

Step 5

- Built mask of watershed

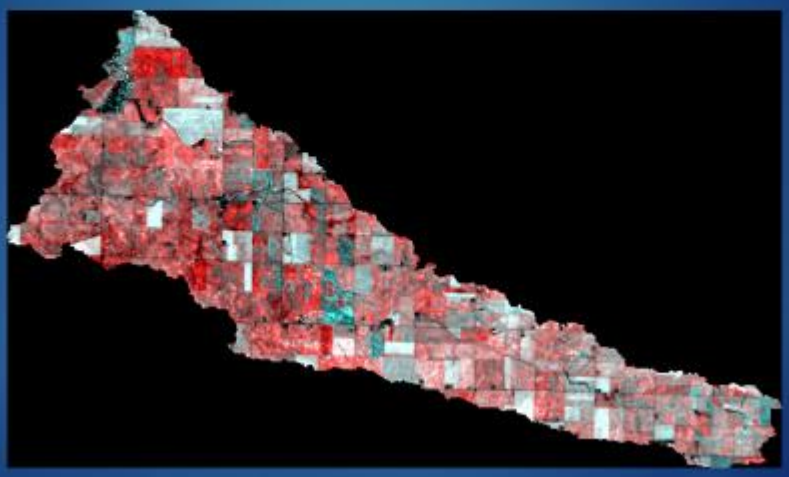

Results and Discussion

- Pink Circles represent well drained fields
- Green Circles represent poorly drained fields
- Grays/pale colors represent little to no change

Conclusions

- No validation assessment was conducted
- Method is sufficient for mapping entire fields not individual tile drains.
  - Due to the resolution (30 m) of image (Landsat)
  - Ideal methodology would be aerial imagery, however not cost effective
- Problems:
  - Timing: finding the correct images before and after a rain event
  - Seasonal: crop cover, snow, till residue
  - Resolution: Only good for entire fields, cannot determine individual tiles
  - Temporal: Landsat orbits every 16 days
- Further studies
  - Create a mask to filter out land that is not agricultural
  - Use aerial imagery
  - Accuracy Assessment

References

- Ale, S., Naz, B.S., and Bowling, L.C., Mapping of tile drains in Hoagland watershed for simulating the effects of drainage water management, in 2007 ASAE Annual Meeting, , American Society of Agricultural and Biological Engineers, p. 1.
- Johansen, R.A., 2015, An Automated Approach to Agricultural Tile Drain Detection and Extraction Utilizing High Resolution Aerial Imagery and Object-Based Image Analysis, .
- Naz, B., Ale, S., Bowling, L., and Johannsen, C., Question and Answers: Automated identification of tile drainage from remotely sensed data: .
- Naz, B., and Bowling, L., 2008, Automated identification of tile lines from remotely sensed data: Transactions of the ASABE, v. 51, p. 1937-1950.
- NAZ, B., 2009, Detecting subsurface drainage systems and estimating drain spacing in intensively managed agricultural landscapes: Agricultural Water Management, v. 96, p. 627-637, doi: 10.1016/j.agwat.2008.10.002.
- Northcott, W.J., Verma, A.K., and Cooke, R.A., 2000, Mapping subsurface drainage systems using remote sensing and GIS: 2000 ASAE Annual International Meeting, Milwaukee, Wisconsin, USA, 9-12 July 2000, p. 1-10.
- Reynolds, E.P., 2014, An Automated Method of Identifying the Location of Agricultural Field Drainage Tiles in Northwest Ohio [Ph.D. thesis]: University of Toledo, .